DESIGNING FOR UNCERTAINTY
Material-based Fabrication Processes for Indeterminate Outcomes

Joseph Henry Kennedy Jr.
Bachelor of Architecture,
Cornell University, 2015

Submitted to the Program in Media Arts and Sciences,
School of Architecture and Planning,
in partial fulfilment of the requirements for the degree of
Master of Science in Media Arts and Sciences

at the
Massachusetts Institute of Technology
May 2020

Author:
……
Joseph Henry Kennedy Jr.
Program in Media Arts and Sciences
May 7, 2020

Certified by:
……
Neri Oxman
Associate Professor of Media Arts and Sciences
Thesis Advisor

Accepted by:
……
Tod Machover
Academic Head
Program in Media Arts and Sciences

DESIGNING FOR UNCERTAINTY
Material-based Fabrication Processes for Indeterminate Outcomes

Joseph Henry Kennedy Jr.

Submitted to the Program in Media Arts and Sciences,
School of Architecture and Planning,
in partial fulfilment of the requirements for the degree of
Master of Science in Media Arts and Sciences

ABSTRACT

Recent advances in digital fabrication tools have enabled designers to create physical objects and structures with greater degrees of precision and efficiency. These forms of contemporary manufacturing prioritize consistency in order to create identical products whose form and behavior are easily predictable. As a result, the modern expectation for reliable uniformity at the end of a production cycle has led both creators and consumers to place value in maintaining a high standard of perfection. Rather than constraining external factors that contribute to behavioral uncertainty, manufacturing tolerances can be expanded to benefit both the design and function of products made from organic materials. Although unstable material properties may traditionally be considered weaknesses, it is possible to utilize aesthetic imperfection and operational temporality in a performative manner.

With the adoption of environmentally reactive biodegradable materials, designers must accept higher levels of unpredictability to accommodate the unknown. This thesis considers methods to leverage high precision robotic fabrication to functionalize unpredictable material behavior by generating tools and workflows that can accommodate variable conditions and create value out of indeterminacy.

Thesis Supervisor: Neri Oxman
Title: Associate Professor of Media Arts and Sciences

DESIGNING FOR UNCERTAINTY
Material-based Fabrication Processes for Indeterminate Outcomes

Joseph Henry Kennedy Jr.

This thesis has been reviewed and approved by the following committee members.

Thesis Advisor:

……

Neri Oxman
Associate Professor of Media Arts and Sciences, MIT Media Lab
Program in Media Arts and Sciences

Thesis Reader:

……

Kent Larson
Professor of Media Arts and Sciences, MIT Media Lab
Program in Media Arts and Sciences

Thesis Reader:

……

James C. Weaver
Senior Research Scientist, Harvard University
Wyss Institute for Biologically Inspired Engineering

ACKNOWLEDGEMENTS

I am immensely grateful for this truly once in a lifetime opportunity to have worked among such a diverse group of talented and compassionate people at the Media Lab. It would never have been possible without Professor Neri Oxman, whose mentorship and inspiration has unlocked so many different ways of thinking and paths forward for me. Thank you James Weaver, Kent Larson, and Hiroshi Ishii for all the advice and encouragement during my time at MIT.

Thank you to all my colleagues in the Mediated Matter family for supporting my artistic and intellectual pursuits both inside and outside of the lab: Jorge Duro-Royo, Josh Van Zak, Nicolas Lee, Ramon Weber, Felix Kraemer, Ren Ri, Rachel Smith, João Costa, Christoph Bader, Sunanda Sharma, Susan Williams and Jean Disset. Thank you to those who came before and first introduced me to the research group and have continued to encourage me: Timothy Tai, Sara Falcone, Andrea Ling and Levi Cai. Thank you to all of the team's amazing admins Becca Bly, Natalia Casas and Kelly Egorova for arranging of every material purchase, group lunch, and last-minute travel.

Thank you to my family and friends for your love and support throughout the years.

INDEX

LIST OF FIGURES

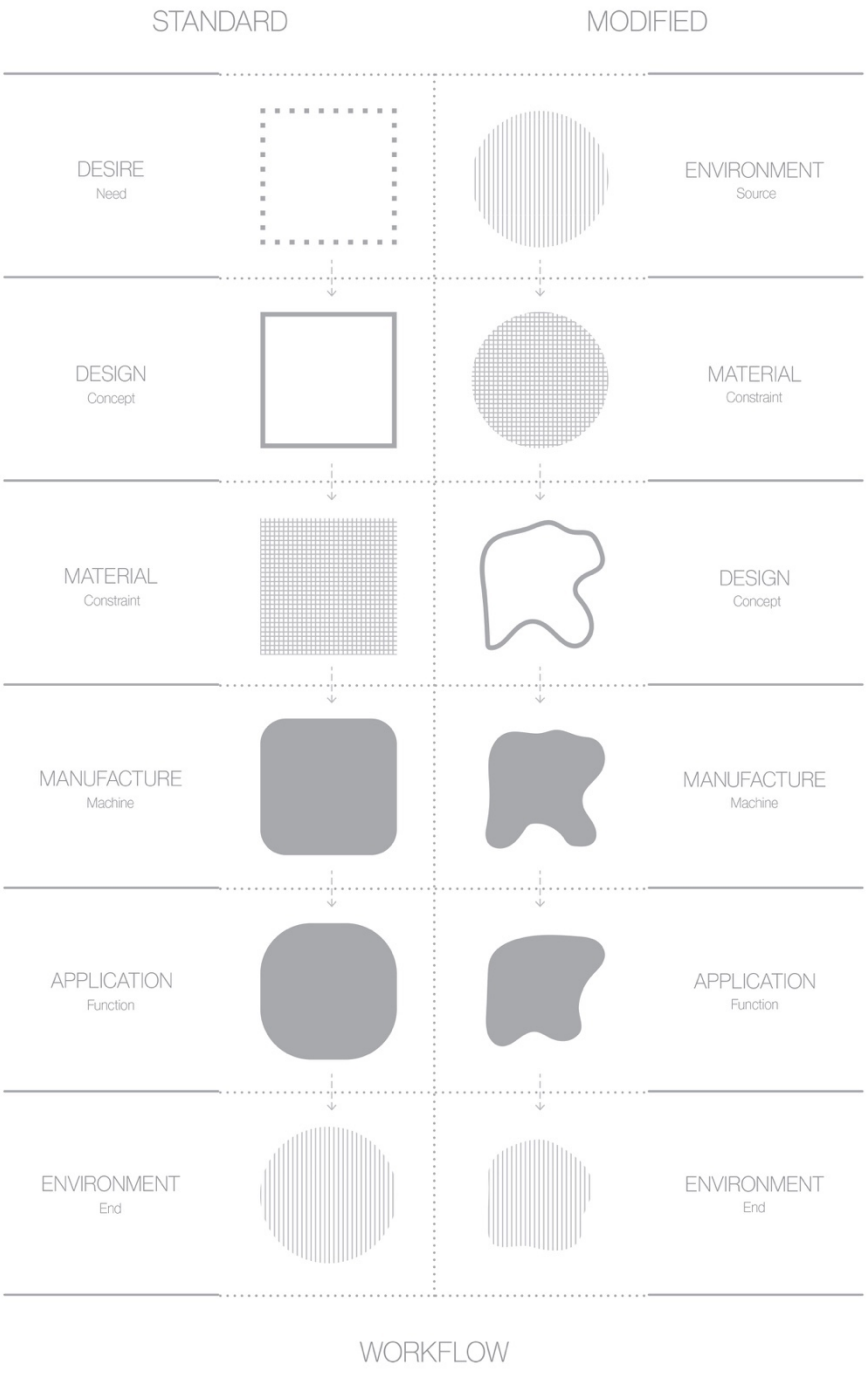

Figure 1: Diagram comparing standard workflows that use inert synthetic materials to prioritize consistency with environmentally aware workflows that use reactive organic materials to accommodate inconsistency.

1 INTRODUCTION

The modern expectation for permanence requires vast amounts of money, resources, and time devoted to maintenance. Made from mostly inert materials and conceived to cater to human convenience and comfort, most objects and structures are unable to participate in ecological systems that are inherently complex and dynamic. This thesis explores design and fabrication methods that integrate organic materials with reactive properties in order to challenge the dependence of traditional manufacturing on processed synthetic materials and high standards of uniformity. From sourcing, to production, to decay, we will consider the perception, use, and application of biodegradable materials as alternatives to existing industrial workflows.

Current manufacturing processes depend on vast amounts of materials and components that are shipped across the world. As a result, the financial and environmental cost of extricating and transporting materials from source to factory to site can be rather high, especially for rural areas that lack a robust infrastructural network. (Ofori, 2000) Today, a building might be made of steel from Brazil, marble from Italy, wood from Canada, and composites manufactured in China. Instead of relying on an international supply chain, materials such as chitin, pectin, and cellulose can be extracted from biomass grown adjacent to a construction site in a variety of climates and locations. (Keating, 2016) These materials have the potential to be locally farmed with limited resources and modify the standard workflow of design in relationship to materials and production as outlined in figure 1.

Biopolymers are a sustainable and renewable resource with potential applications in both buildings and products. As their name would suggest, biopolymers are polymers made by living organisms. Pectin is found in the skins of most fruit. (Baker, 1997) Chitin is found in mycelium growing in the earth or in the shells of insects and

crustaceans. (Peniche, Argüell, & Goycoolea, 2008) Cellulose is found in nearly all plant matter. The majority of the commercially available chitin is a byproduct of the shrimp industry that is then chemically converted to chitosan. (Islam, Khan, & Alam, 2017) Pectin is typically refined from the peels of apples that have been used to make cider. (May, 1990)

Chitosan, pectin, and cellulose are biodegradable and thus susceptible to small changes in the environment. These biopolymers can be highly responsive to variations in temperature and humidity both before and after production. (Mogas-Soldevila, 2015) The reactive quality of biopolymers adds uncertainty to the manufacture and lifecycle of products that incorporate these materials.

By better understanding the inherent structural and mechanical instabilities of biopolymers we can harness their behavior to produce environmentally responsive objects and structures. (Duro-Royo, 2015) Biopolymer hydrogels of various mixtures are extruded using a custom-built 3D printer to track visual and physical changes of objects throughout an entire year. Different material formulas, printing methods, toolpaths, and geometries are tested to determine how manufacturing and design parameters affect product behaviors over time. These insights provide design guidelines for how to allow greater control over characteristics such as shape deformation and color change in reactive biopolymer materials.

In order to accommodate the natural material behaviors of biopolymers, this thesis will reevaluate the creative aspirations, design processes, and industrial standards that surround both the aesthetics and performance in product and architectural design.

How can designers embrace the inherent uncertainty in materials and fabrication processes to produce physical objects that compensate for indeterminacy? How can we expand the acceptance of indeterminacy to leverage inconsistency in the manufacturing process and product lifecycle?

The traditional approach to manage uncertainty is to constrain the unknown so that it matches a preconceived design by developing tools that can predict or control the end result. (Morse, et al., 2018) However, another broader approach is to allow the unknown to influence the result of the original design intent by defining a range of acceptable outcomes and establishing parameters that will ensure the result will fall within that domain. By expanding manufacturing tolerances and encouraging a general acceptance of higher degrees of inconsistency, we can better design with and for the unknown to use uncertainty and imperfection to add value to the design process.

Before exploring the implications of uncertainty with biopolymers, we will better understand contemporary and historical attitudes towards uncertainty in the fields of design, craftsmanship, manufacture, and culture.

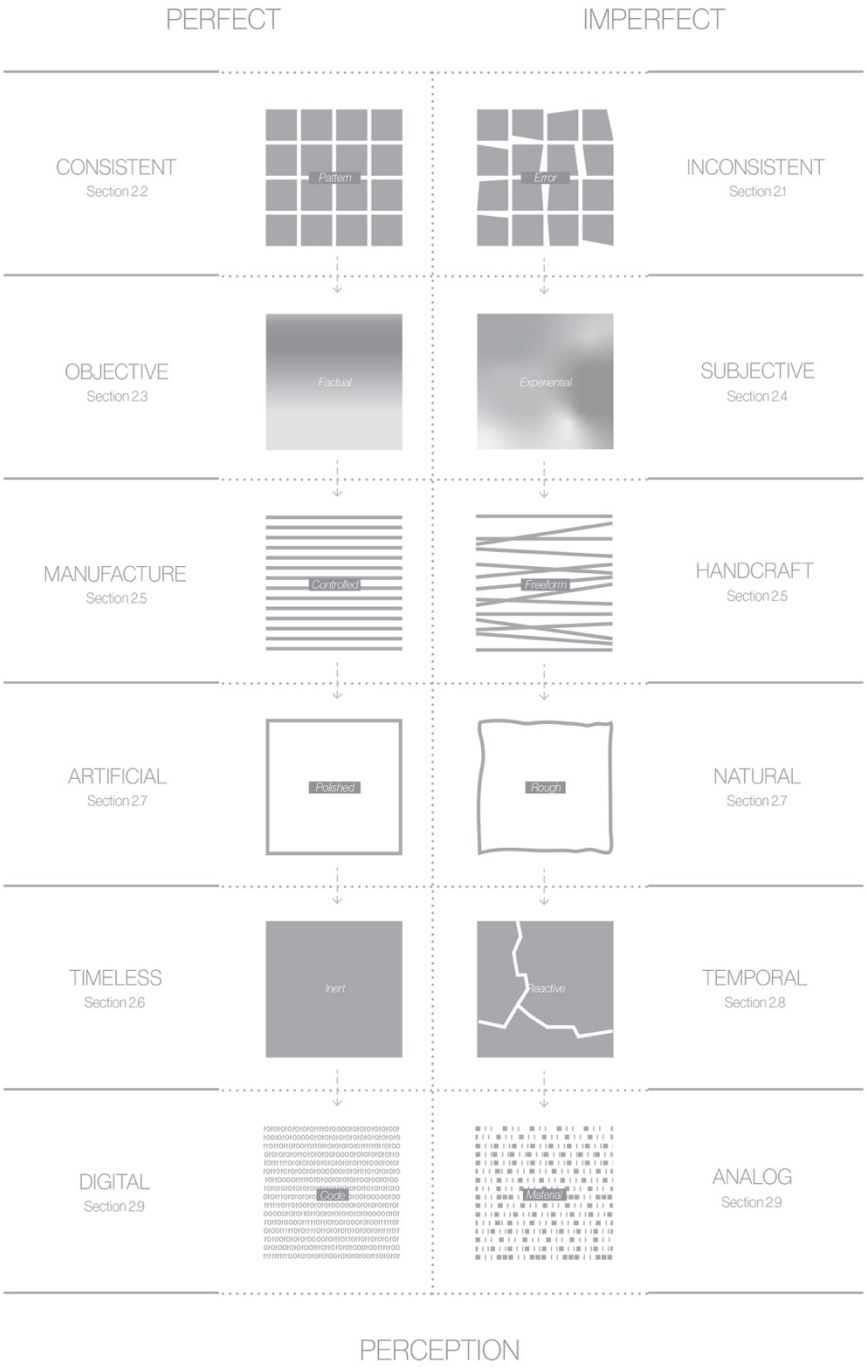

Figure 2: Content map comparing characteristics associated with the perception of perfect vs. imperfect materials and products discussed in background sections 2.1 – 2.9.

2 BACKGROUND

Incorporating uncertainty into the design process can be an added value. By examining contemporary and historic perceptions of imperfection in figure 2, we can better understand how to employ reactive biopolymer materials and digital fabrication tools to design products and structures that can accommodate environmental uncertainty.

2.1 The Perception of Inconsistency

The precision and efficiency of industrial technologies have made high standards of perfection more easily attainable. (Rognoli & Karana, 2014) The ability of mass manufacturing techniques to create perfect copies of industrial products has dramatically outcompeted craft-based production. Before the industrial revolution, the skill and knowledge necessary to achieve a level of material refinement and formal perfection comparable to current criteria would require considerable time and effort. However, the ubiquity of perfection enabled by standardized mass production has undermined its perceived value. Today, many artisans and craftspeople no longer aspire to traditional standards of perfection but instead attempt to glorify the inconsistency that is inherent in materials and handmade products. (Pitelka, 2005)

While inconsistency has traditionally been associated with low-quality, many designers have come to regard imperfection as desirable. (Pedgley, Şener, Lilley, & Bridgens, 2018) The uncontrolled and accidental results of imperfect production methods can lend authenticity and identity to an otherwise sterile set of mass-produced items. As a result, curated imperfection has in many cases become associated with quality. (Salvia, Ostuzzi, Rognoli, & Levi, 2011)

The increased cost of human labor and desire for sustainable design has reinforced this recent shift in the aesthetic appraisal of handcrafted items vs. manufactured products. (Walker, Evans, & Mullagh, 2019) Subsequently, many modern consumers are increasingly willing to pay a premium for objects made by hand possibly because of the higher cost and time associated with them. (Kruger, Wirtz, Boven, & Altermattc, 2004) In appreciating the inconsistency of handcrafted objects, consumer preferences imply higher value in human effort than in functional efficiency. (Fuchs, Schreier, Stijn, & Osselaer, 2015) Since the time allocated per manufactured item is typically negligible when compared to the time spent by an artist or craftsman making a similar item, it follows that consumers would place higher value in objects made by hand.

Due to the attention required to make objects by hand, many have come to desire imperfections and inconsistencies that are the traces of the human touch. (Lilley (2016) Textures and finishes that were once the result of working with materials through traditional tools, techniques and technologies have now become fetishized and replicated by industrialized methods for aesthetic rather than practical purposes. The trend for creating intentional references to traditional hand-crafted techniques exists in many products made from modern industrial manufacturing. It is present in digitally printed images in the appearance of hand-scored etchings or sawn logs that have a hand-hewn texture. In all cases, these objects contain the markers of former material and mechanical constraints that no longer affect their production.

For example, modern copper tableware is made with smooth surfaces with industrial machinery. However, many of the copper objects produced by these manufacturing processes are stamped out with molds that imitate the surface texture of copper objects that have been hammered by hand. The decision to include this reference to imperfection is in contrast with most modern objects that are relatively defect free.

These items nostalgically reference the aesthetic of the handmade even though the additional texture adds no direct functional value. This may be to evoke a feeling of familiarity with the object or to lend it the semblance of being handmade in order to increase its perceived value.

As another example, photography has shifted the pursuit of painting away from objective, realistic representation to that of subjective artistic expression. (Van Gelder & Westgeest, 2011) In much the same way, analog production methods have benefitted from establishing different qualitative metrics that distance their outputs from the high levels of consistency of mass-manufactured products. Unable to compete with assembly-line products to achieve the same standard of quality, crafted objects have found added value by exaggerating inconsistency in the working process. Rather than accepting imperfection as a negative attribution, we can intentionally exploit qualities of imperfection to elevate products to the status of the unique.

Inconsistency can lend character and personality to otherwise generic or unremarkable objects. By allowing objects to achieve their own identity, consumers can both recognize and empathize with unique objects that can allow them to reinforce their own identity through their material possessions. In this era of post-perfection aesthetics, inconsistency has become a marker of value.

2.2 The Perception of Consistency

Inherent visual biases and general rules of perception have guided both the appreciation of natural forms and influenced the aesthetic language of human crafts and industrial production methods. Human perception has developed to recognize patterns and create order from visual entropy to gain spatial awareness distinguish between objects in the environment. (Koffka, 1935) According to Gestalt psychology, the law of Prägnanz describes the idea that the experience of the world is simplified by human perception into simplistic forms that are regular and symmetric. In this way, humans organize and perceive three-dimensional space by grouping two-dimensional visual information into a hierarchy of forms within principles of similarity, proximity, continuity, and closure. (Palmer, 1999) Scenes exhibiting high degrees of order are easier for the mind to process and perhaps, as a result, appear more desirable or pleasant to view.

Visual preferences for human-made objects tend to favor order, but when it comes to natural materials, humans seem to value psychophysical qualities that exist between randomness and order. (E. Overvlieta & Soto-Faracobc, 2011) This includes objects in a series with shared visual characteristics and formal similarities that exhibit acceptable variation within a predefined set of rules. This would seem to correspond with the variable properties of natural forms that exhibit small deviations from established typologies. But what is considered attractive to humans can be both species and individually specific as colors, shapes, and patterns in the environment are perceived and interpreted differently between species. (Westphal-Fitch & al., 2012)

2.3 The (Objective) Definition of Perfection

Although perfection exists more as an aspiration than an entirely achievable pursuit, a definition of imperfection requires an understanding of commonly accepted characteristics of perfection. While perfection can take on a multiplicity of meanings according to context and interpretations with varying degrees of specificity we will broadly define perfection as a measurement of how closely the manifestation of an idea matches the conceptual purity of an idea. This realization can relate to the physical execution of an idea or how it is viewed or used. In the case of design and manufacturing, the term perfection can refer to the correlation of the physical form and material functionality of an item with its original design specifications.

Even though nearly every actualization will require some degree of compromise that is imposed by the constraints of production, it is not productive to claim that no object is perfect, and thus everything is imperfect. Instead of striving for perfection, most designers temper their expectations to create products that are "perfect enough," in which there is an acceptable amount of tolerance from which an object may stray from the standard. Beyond those acceptable limits of defects and inconsistencies is what we would consider imperfect.

Since the range of that tolerance is by nature subjective, what qualifies for perfection or imperfection is contestable. This uncertainty allows space to redefine what is a desirable amount of imperfection. Both personal and cultural factors influence the perception of beauty as it relates to inconsistency. The degree of refinement and consistency that determines whether an object can be considered aesthetically desirable is highly varied and is often at odds with characteristics associated with natural materials. (Karana, 2012)

Figure 3: A comparison of the original idealized condition of the Parthenon in an elevation drawing of the by J. Stuart & N. Revett in 1787 (top) with the current imperfect state in a photograph of the western façade of the Parthenon during renovation in 2008. (bottom) *(Piolle, 2008)*

Many of our contemporary notions of aesthetic perfection are heavily influenced by western classical traditions in architecture and sculpture. Greek architecture valued symmetry and perfection as a symbolic triumph of the intellectual order of humanity over the chaos of nature. However, the Parthenon on the Acropolis in ancient Athens, a seminal historical example of physical perfection, incorporates intentional physical imperfection to create the illusion of visual perfection. (Norwich, 2001) The perfect appearance of the building is possible through the optical refinements that physically distort the building.

As seen in figure 3, the appearance of perfection is achieved through the entasis of the columns compensates that for visual distortion by gradually thickening the central shaft of the columns to make them look straight as they would in a rendered façade elevation. Additionally, the distance between the columns is larger at the edges so that they appear regularly spaced, and the floor of the temple is curved upward so that it appears horizontally level. (Pollio, 1960) In this case, these physical imperfections were justified because they created an experience of perfection. These same desires for visual perfection have carried over to the present.

In considering these examples, we can acknowledge that the purposeful application of imperfection can yield results that conform to an alternate ideal of perfection. By allowing intentional inconsistencies to inform the design process, we can use them to support the more perfect realization of abstract ideas and human experiences.

Modernism	Values	Wabi-Sabi
Rational	Worldview	Intuitive
Universal Prototypical	Solution	Personal Idiosyncratic
Mass-produced / Modular	Manufacture	One-of-a-kind / Variable
Faith in Progress	Future	No Progress
Controllability	Nature	Uncontrollability
Technology	Romanization	Nature
People adapting to Machines	Adaptation	People adapting to Nature
Geometric (sharp, definite shapes and edges)	Organization	Organic (soft, vague shapes and edges)
The Box (rectilinear, precise, contained)	Geometry	The Bowl (free shape, open)
Manmade	Material	Natural
Slick	Finish	Crude
Well-maintained and Static	Maintenance	Accommodating Degradation and Attrition
Purity and Consistency	Expression	Corrosion and Contamination
Reduction of Sensory Information	Senses	Expansion of Sensory Information
Intolerant	Ambiguity	Comfortable
Cool	Temperature	Warm
Light and Bright	Brightness	Dark and Dim
Primary Values	Function	Not Important
Materiality	Perfection	Immateriality
Everlasting	Time	Temporal

Figure 4: (top) Chart comparing different values of Modernism vs. Wabi-Sabi ideology. *(Koren, 1994)*
(bottom) Craft comparison of Ikea 365+ mug from 2020 vs. raku tea cup from circa 1600's Japan. *(Kōetsu, 1600's)*

2.4 The (Subjective) Definition of Imperfection

Wabi-Sabi is an aesthetic philosophy that appreciates the imperfect, impermanent, and incomplete. The tradition places value in primitive forms made from natural materials in a rustic, humble, and sometimes unconventional manner. In the same way that Greek ideals of perfection have influenced western aesthetics, the concepts of Wabi-Sabi have contributed significantly to the conception of beauty in Japanese culture. However, Wabi-Sabi principles are mostly at odds with European sensibilities that are compared in figure 4. (Koren, 1994)

Wabi-Sabi embraces the inconstancy of the natural world to accept the illusion of permanence and the belief that all things are imperfect. The philosophy does not idealize a standard of perfection that works against nature in an attempt to control unpredictability. It values the use of materials that are vulnerable to the effects of weathering and human treatment to record climactic conditions.

How can we reconcile and combine Modernist ideals with Wabi-Sabi philosophy to synthesize a new approach to design that can fully explore the possibilities of new materials and production techniques?

Figure 5: Vermont white marble showing methods of constructing visual symmetry and order from book matched and repeated veining patterns. *(John, 2017)*

2.5 The Methods of Craft

A physical manifestation of the values of Wabi-Sabi can be found in traditional Raku pottery. The style's irregular forms are created through a hand-shaped process rather than the wheel-thrown process most pottery is made from. Inconsistencies in the temperature and exposure of the ceramic glazes that are fired in a kiln and cooled in water or air will determine the unique visual characteristics of each piece. (Rhodes, 1957) These imperfections are a celebrated byproduct of the production process.

The craft of ceramics has come a long way from the hand-crafted traditions of artisanal Raku pottery. Modern industrialized machinery has allowed manufacturers to produce large quantities of identical ceramic objects and building components cheaply and efficiently. On the other hand, these manufacturing methods prioritize consistent identical copies of a single design to impose restrictions on variability.

Despite the emphasis on uniformity, manufactured ceramic tiles often attempt to imitate the irregular patterns and textures of wood and stone. With porcelain inkjet printing, manufacturers can replicate the appearance of natural materials with high precision to create artificial products that appear virtually identical to the original. (Sanz, et al., 2012) If these perfect copies are aggregated together like the bottom vs. the top of figure 5, it is clear that they are all human-made. The consistency of these elements to one another is an indication of industrial methods of production.

While many existing manufacturing processes have stricter controls around product consistency, several craft traditions purposefully utilize complex, unpredictable material behaviors to generate aesthetically desirable results. Both paper and clay marbling techniques are employed to create detailed irregular patterns in figure 6 that are similar to the channels found in certain types of stone in figure 5.

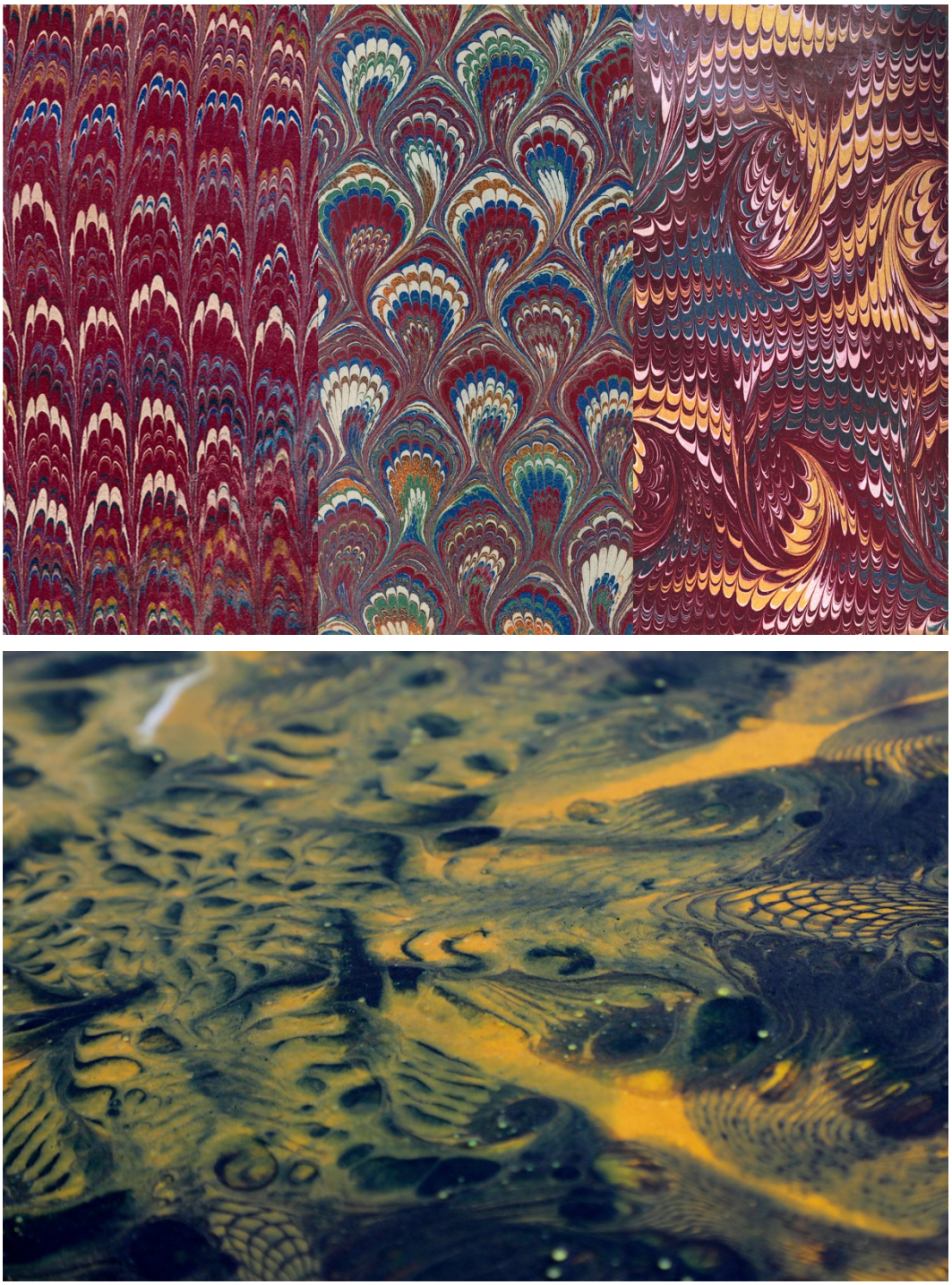

Figure 6: A comparison of traditional marbling techniques with machine-controlled mixing and pattern generation. (top) Marbled endpapers made using hand mixing techniques with pigments in water. *(Donin, 1875) (Ludwig, 1869)* (bottom) Marbled biopolymer patterns using CNC mixing paths with pigmented biopolymer hydrogels.

Paper marbling uses various color inks that are distributed, floated, and mixed on a liquid surface then transferred onto paper. The mixing technique and viscosity of the pigments are factors that determine the final pattern. (Woolnough, 1881) Clay marbling uses methods that are a 3-dimensional translation of 2-dimensional paper marbling techniques. Different colored clays are twisted and rolled into one another to create veined effects. These can be worked into irregular shapes, stamped forms, thrown pottery, or cut tiles.

Much like the examples mentioned above, working with biopolymers can result in products with unpredictable, dramatic behaviors depending on minute environmental differences. (Tai, et al., 2018) The higher viscosity of biopolymer hydrogels allows us to manipulate them in a manner that's between paper marbling and clay marbling. With our methods of multi-material hydrogel printing, we can control the various inherent inconsistencies of traditional marbling techniques to create visually and structurally complex yet consistently reproducible pieces. By documenting the behavior of these biopolymers in both air and water over time, we can understand the influence that specific fabrication techniques and material formulas have over the manufacturing process.

Figure 7: Historic and contemporary precedents that fetishize classical characteristics of aging and imperfection (top) Giovanni Battista Piranesi's etching of the ruins of the Mausoleum of Villa Gordiani in Rome in 1756. *(Piranesi, 1825-1839)* (bottom) Piero Fornasetti's "tema e variazioni" plate series. The variations on the theme of the woman's face shows fetishized signs of cracking and wear in classical fashions. The aesthetic mimics the qualities of traditional etching although the process of printing onto the plates uses modern techniques.

2.6 The Value of Age

Classical Greek aesthetic values have been passed from the Roman Empire through the Italian Renaissance, to the English Enlightenment and continue to influence our aesthetic preferences in the present day. The irony of this legacy is that such classical structures have survived as incomplete fragments experienced in a vastly imperfect state. Well-known images of temples with missing roofs and statues with broken arms in museums have inundated western culture as precedents for high art, beauty, and standards of perfection.

Although it was not the intention of Classical Greek and Roman architects and sculptors, the aging of their work inspired an aesthetic that glorified and replicated the elements of wear on their perfect forms. A famous series of engravings by the 18th-century Italian illustrator Giovanni Battista Piranesi surveyed views of the ruins of Rome to foster a renewed appreciation of Classical historical works in an imperfect state. Previously artists had attempted to replicate the original unbroken forms of Classical buildings and sculptures. However, Piranesi's work catalyzed a movement in art that fetishized ruins, elevating the aesthetic appeal of the imperfect state of these objects as incomplete forms. (Pinto, 2012)

Piranesi's etchings in figure 7 acknowledged that age had conferred an aura of value to Roman ruins that could allow an audience to visualize their history. Other designers, such as Fornasetti in figure 7, have appropriated the incomplete aesthetics of classical ruins to produce new pieces that appear aged. Gradually these trends that value pre-aged possessions have made their way into consumer culture.

During the 1970s, the punk subculture flaunted clothing that showed extreme signs of wear as an act of rebellion against mainstream values of newness and perfection. Visible signs of age previously signaled the end of a product's lifestyle, but the ripped aesthetic is now ubiquitous with distressed jeans and pre-torn jackets. Retailers commonly charge a premium for pre-worn clothing. The aesthetic of age is another commodity within a contemporary material culture that saturates the market with more new items each year.

Age in the optimal degree and context can demand a premium. For example, a cell phone from the 2000s would have little value today because the technology is largely obsolete. In contrast, a Bell telephone from the 1870s would commission a large amount of money despite being older and having less utility than a twenty-year-old cell phone. (Antique Telephones Ring a Bell with Collectors, 2018) Though this evaluation may be more related to sentimentality than functionality, objects that have successfully withstood aging are positively associated with durability and quality.

Since the imperfection caused by age is a record of the passing of time and proof of an object's ability to survive, proper design and material choices can allow gradual wear to cause objects to age gracefully through repeated use. However, there is an equally legitimate utility in degradation as there is in durability. Material temporality can be both functionally responsive and programmatically relevant.

2.7 The Natural in Artificial Materials

Synthetic materials were created due to scarcity and perceived shortcomings of natural materials. Initially, companies did not present synthetics as copies of natural materials but improved versions of natural materials at a heightened form that was unrestrained in its ability to resist the temporality of the material world. As conservationists placed synthetic materials under increased scrutiny for their environmental impacts, they became associated with being inferior or fake versions of natural materials. (Roosth, 2017)

Oftentimes, the same metric for resilience is used to assess value. A conventionally successful product or architectural structure is measured by its ability to withstand environmental wear or frequent use. However, there has been a recent shift in objectives to design products and structures for intentional decay instead of lasting durability in expectation of functional or aesthetic obsolescence. While some materials do not age gracefully, the aging of others is considered desirable from both an aesthetic and a performative perspective. (Lilley, Smalley, Bridgens, Wilson, & Balasundaram, 2016) The copper oxidation process is a good example of a material that naturally weathers in a manner that is aesthetically pleas.

The inherent material changes in copper have historically been accepted and appreciated as desirable aesthetic elements in architecture and sculpture. Many well-known sculptures that are today associated with the characteristic green patina of oxidized copper were initially orange and brown. The process can take up to 20 years depending on environmental conditions such as moisture and temperature. Different copper alloys and the use of oxidizing agents can be used to either speed up, slow down, fix or change the color of the patina. (Wang & Cho, 2009)

The patina serves both an aesthetic and functional purpose. It forms a protective surface layer over the copper that prevents further oxidations that would weaken the structure of the material. Corten steel weathers in much the same way by intentionally catalyzing material degradation. Over several months or years, the material will quickly turn from a dark grey to form a layer of orange rust that functions to protect the material in much the same way as copper in figure 8. (DeNardis, Rosales-Yeomansa, Boruckib, & Philipossianab, 2010)

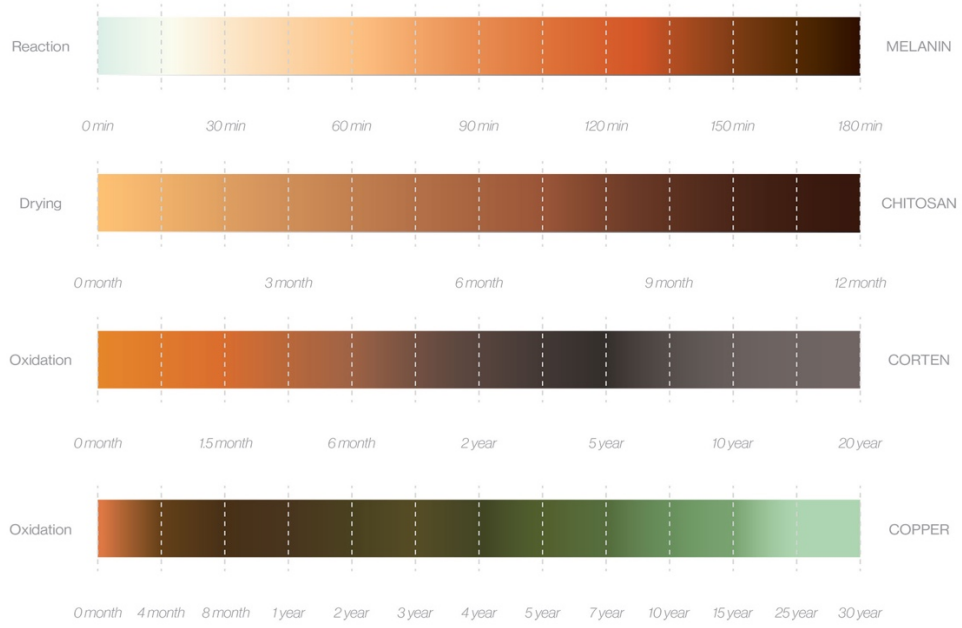

Figure 8: The range of color change and time period or change in melanin and biopolymers compared to that of metals caused by drying and oxidation.

Other organic materials also experience the positive effects of aging. Leather will darken and soften over time. Wood will dry out, discolor and rot. They will both inevitably dissociate and be reincorporated into the environment. (Ruel & Barnoud, 1985) While most natural materials biodegrade on their own, many artificial materials do not degrade and must be processed and recycled for reuse in new products.

2.8 The Lifecycle of Products

While environmental exposure will break down natural materials, manufactured materials often require human intervention to be absorbed and reused. With the increasing abundance of synthetic materials in the latter half of the 20th century, humans became responsible for finding new ecologically sustainable methods of reintroducing waste materials into either modified production cycles or existing ecological cycles.

The majority of contemporary reuse efforts focus on the collection and recycling of conventional plastics back into an industrialized manufacturing product cycle. However, material recovery facilities are highly resource intensive and unlike natural processes, there are material limitations to recycling PET and PP. (Hopewell, Dvorak, & Kosior, 2009)

- Virgin plastic material is needed to reform recycled plastics.
- Products with multiple materials or types of plastics must be separated.
- Plastics can only be recycled and reformed a limited amount of times.
- Recycled plastics become weaker through each reproduction cycle.

Instead of relying on inert synthetic materials that require large amounts of energy and equipment to be recycled, designers have renewed their interest in materials that can be naturally recycled by the environment. Timber and bamboo are examples of naturally occurring renewable resources that can be planted, harvested, and integrated into durable products and structures. Also, many other types of biomass that are less durable than traditional building materials may still have many potential applications. Despite popular interest, the use of biodegradable materials challenges commonly held expectations of permanence in objects and spaces.

With the abundance of technology and clothing that reaches obsolescence in short periods, programmatic decay can be considered a desirable attribute. Designers must find means to avoid unintentional or premature decay that impedes product utility or functionality by understanding the relationship of environmental stimuli and material characteristics that trigger different degrees of decay – from color, and shape-change to full disintegration.

Figure 9: The texture of grey felt acoustic panel made from recycled PET bottles resembles the veining patterns of white marble found in figure 2.

2.9 The Analog in Digital Fabrication

Traditional manufacturing methods can produce large quantities of identical items for relatively low costs but require sizeable investment to create new products with high degrees of variation. In contrast, objects made by hand can be more cheaply and quickly modified on an item by item basis to be personalized according to the needs of a given user. As a result, digital fabrication platforms have managed to compromise between the efficiency or reproducing and customizing designs. Tools such as laser cutters, 3D printers, and CNC mills are ubiquitous in fab labs across the world. The knowledge, software, and materials required to operate these machines are highly accessible to users who can then quickly prototype, iterate, test, and replicate designs. (Rosenberg & Oxman, 2010)

The ability to easily modify manufacturing methods allows fabricators to produce highly customized products for specific situations and users based on a design template. While these digital fabrication methods allow for higher levels of precision and consistency than analog prototyping, the software and hardware of these tools can be modified to produce unintended results. In some instances, designers have purposefully added entropy to controlled manufacturing systems to create a limited series of unique pieces such as the ceramics manufactured by Granby Workshop in figure 10. By bridging the analog and digital with new fabrication methods and design values, we can value the variation caused by material inconsistency and manufacturing imperfection. (Mogas-Soldevila, Duro-Royo, & Oxman, 2015)

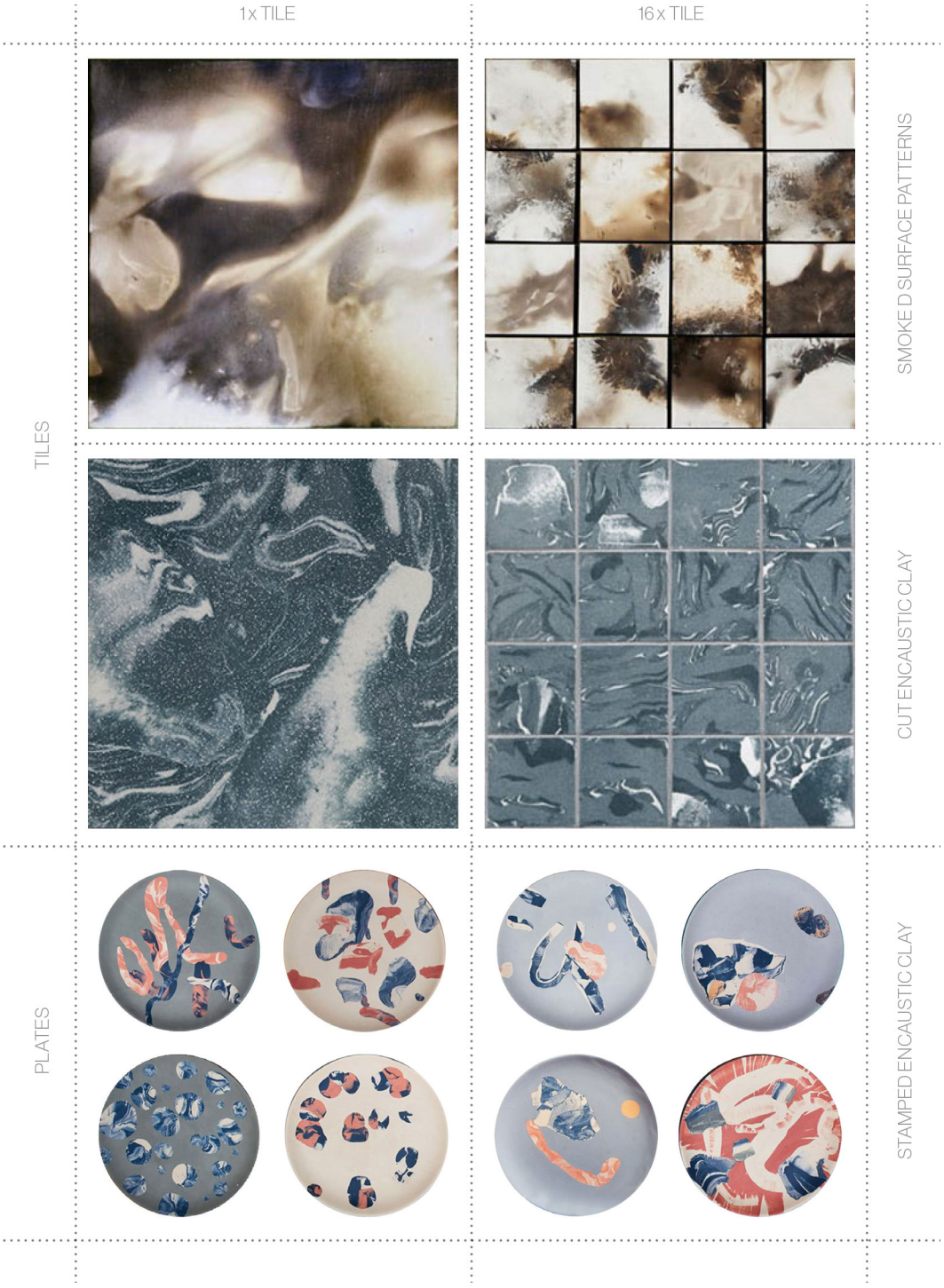

Figure 10: Ceramic tiles and plates from Assemble Studio's Granby Workshop that use intrinsic randomness of manufacturing to create unique aesthetic variations (top) smoked firing techniques (bottom) encaustic marbling.

2.10 The Excitement of Uncertainty

Designing for the unknown is an exploratory process that can result in surprising and unpredictable outcomes. By embracing the unknown, designers must accept the potential positives and negatives associated with the act of discovery. There is an ideal balance between rigid intention and flexibility in the face of uncertainty. While designers may direct their efforts towards accomplishing predefined goals, they should also be accepting towards creative possibilities that are outside of their preconceived intentions.

In some cases, the most unpredictable results are the most worthwhile. Inventions such as fiberglass or safety glass were discovered by accident by engineers who were attempting to find solutions for other problems but instead discovered processes for creating new materials with unique behaviors and applications. As an example, the discovery of fiberglass occurred when glass powder was injected into a metal layering gun that was supposed to fuse two glass blocks but instead produced a series of glass filaments. In another example, safety glass was supposedly discovered when a scientist dropped an unclean flask coated with plastic cellulose nitrate that did not shatter. (Innovations in Glass, 1999)

While the results of these experiments could be considered failures, the recognition that these were valuable in other applications beyond their initial intention turned potential failures into commercial successes. With a culture that promotes the value of unpredictability in problem-solving process, designers can more readily accept inconsistency and failure as an opportunity to learn and innovate.

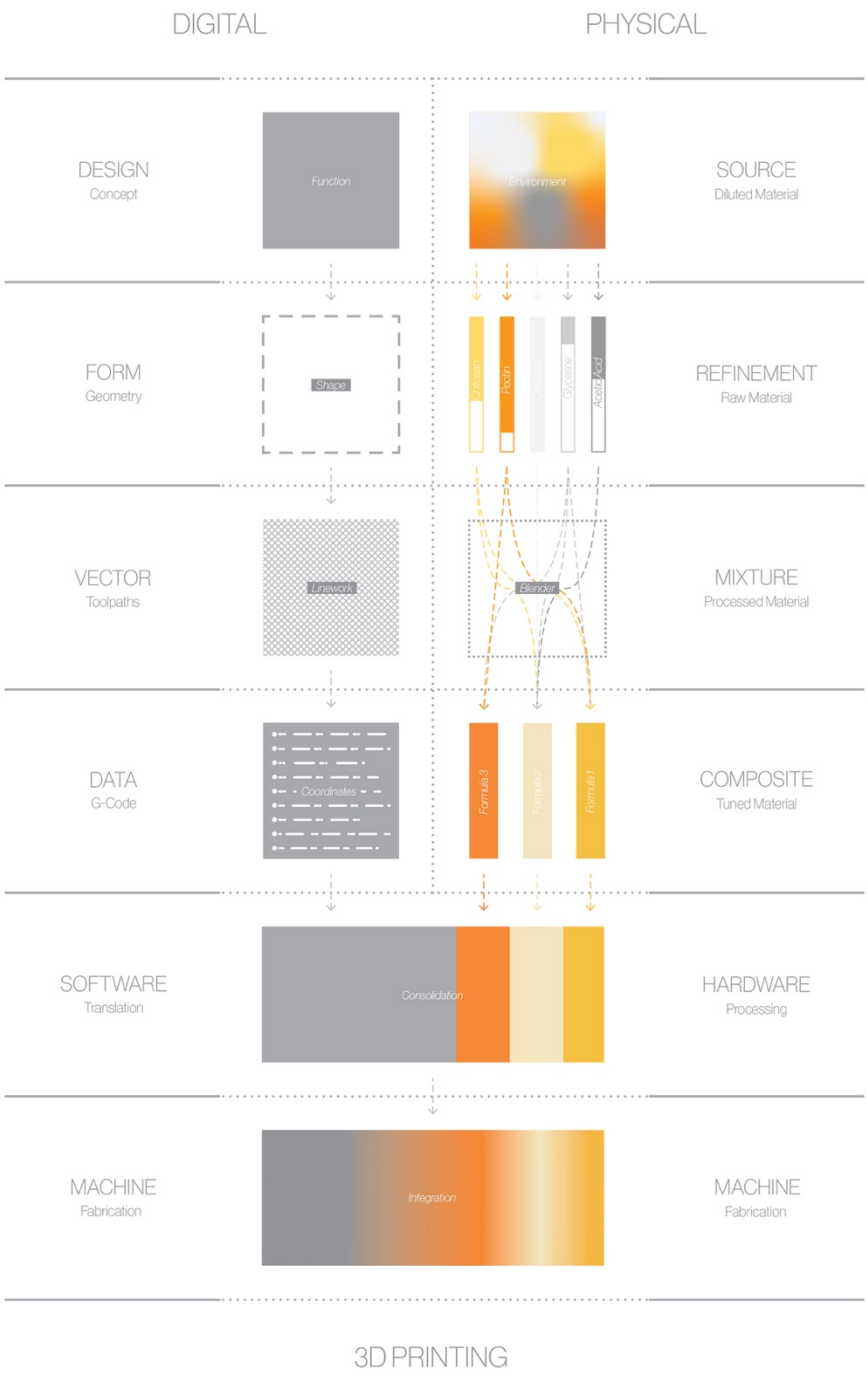

Figure 11: Diagram presenting the parallel process of transforming digital design parameters and physical material properties into extrudable biopolymer hydrogel 3D prints.

3 MATERIAL / MACHINE

The unpredictable behavior of products made from reactive materials can present a variety of performative challenges and negative aesthetic biases as explored in the previous section. In particular, the temperature and moisture sensitive properties of biopolymer hydrogels produce a high amount of uncertainty within multiple stages of the manufacturing process. In order to both compensate for and leverage the reactive qualities of these water-based organic materials, the Mediated Matter Group has designed and built a custom biopolymer 3D printer that integrates a digital fabrication workflow with physical material tunability to create objects that can functionalize natural behavioral indeterminacy.

To control unpredictable material behavior, we have established various design and fabrication protocols in order to manage undesirable material uncertainty while encouraging productive material indeterminacy as outlined in figure 11. Although the degradation of the biopolymers is inevitable, the measures seek to limit the circumstances in which the prints will prematurely ferment, lose shape, disintegrate, crack, or warp. This is achieved by controlling for printing parameters such as the extrusion speed, extrusion pressure, nozzle diameter and nozzle height as well as environmental factors such as the material of the print bed or the temperature and humidity of the print room.

At the same time, these procedures are flexible enough to allow for continued experimentation and are not intended to fully constrain the reactive qualities of the water-based materials. The fact that the printed biopolymer skins can change and react over time is a desirable feature of the material that has a practical potential and aesthetic appeal. The biggest challenge of working with biopolymers is finding the ideal balance between control and uncertainty.

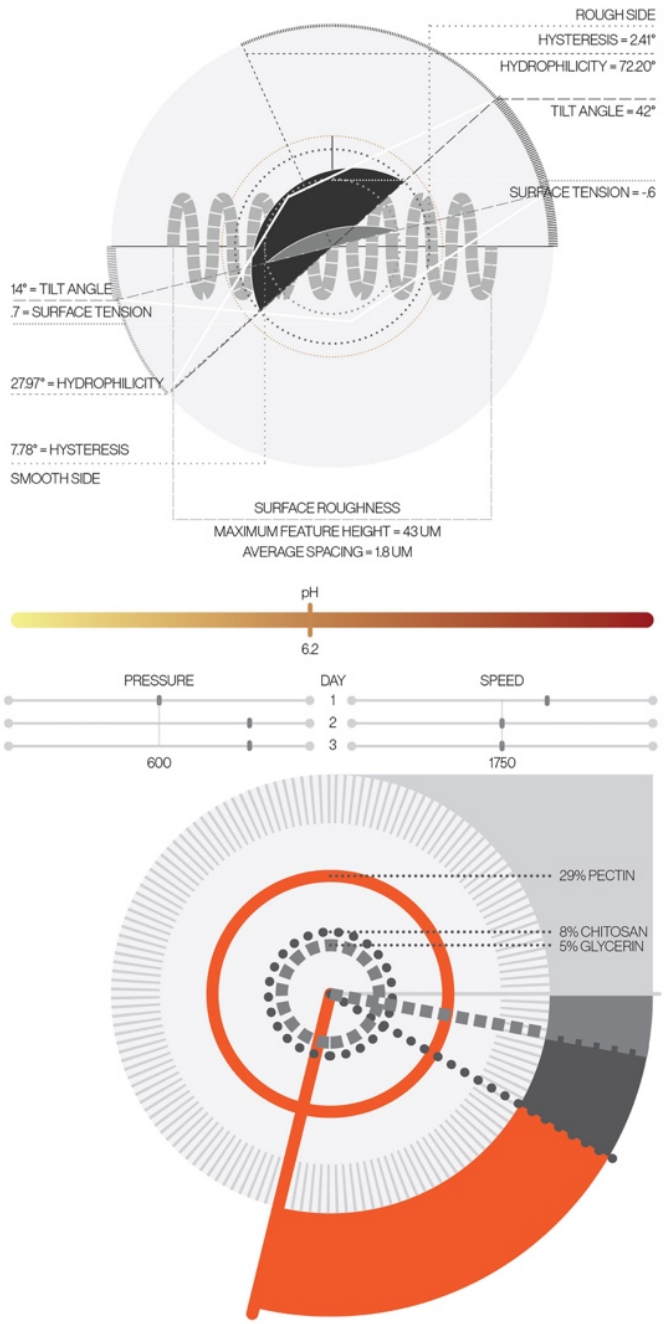

Figure 12: Pectin formula material property diagrams visualizing composition, pH, hydrophilicity, hysteresis, surface tension, surface roughness and printing parameters. (*https://designedecologies.com/Properties)*

3.1 Definitions of Material Indeterminacy

The complex relationship between precision additive manufacturing and environmentally responsive material characteristics is difficult to visualize in a consolidated format. It is difficult to represent the specific environmental conditions that effect different material qualities and understand how to constrain or modify the intensity of these effects by changing printing parameters or toolpaths. By consistently scaling and superimposing quantitative visual data, it is possible to compare information across different criteria in figure 12. This is useful in creating a visual vocabulary to act as a design reference to visually understand how to adjust fabrication settings and tune different material properties.

Based off of the historical and contemporary survey of imperfection, I will define three criteria for describing indeterminacy in biopolymer materials.

3.1.1 Visual

Inconsistencies in color, patterning, transparency, surface texture and geometry which result from manufacturing processes, material characteristics and effects of weathering.

3.1.2 Structural

Variations in stiffness, hydrophilicity and shape that occur over time from changes in the environment.

3.1.3 Functional

Multiple uses that change over a product's lifespan in response to the needs of users.

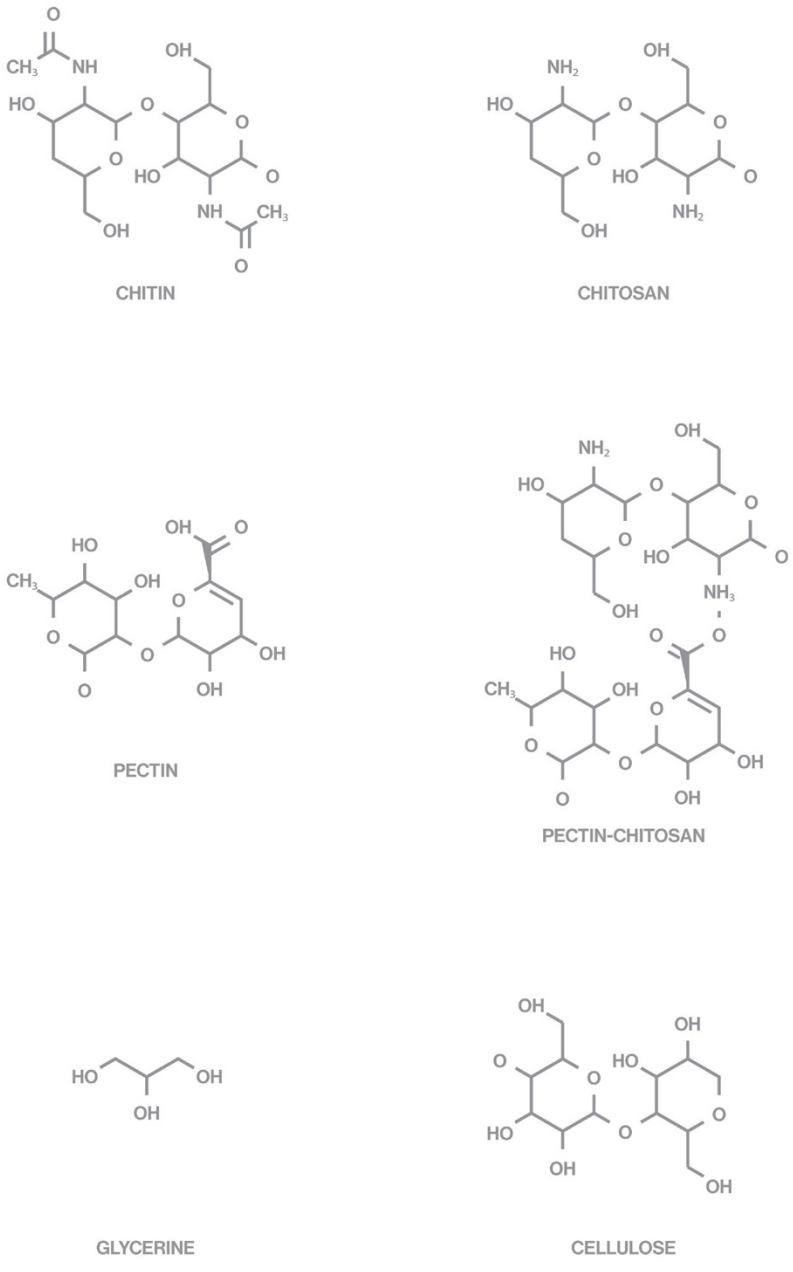

Figure 13: Structural formulas of biopolymer materials used in hydrogel mixtures.

3.2 Sources of Material Indeterminacy

3.2.1 Material

The material mixtures are based on a percentage value of volume to weight for water to powder. The primary ingredients are apple pectin, shrimp chitosan, vegetable glycerin, plant cellulose, and water in figure 13 with other organic additives that modify color and surface texture in figure 14.

Base Layer

The concentration of chitosan in our hydrogel base layer formulas is between 0% - 8%. Hydrogel mixtures containing more than 8% of chitosan will frequently cause jamming in thinner nozzles. In addition, the higher concentrations of chitosan come with a higher probability of warping and tearing as the hydrogel films dry on the print bed.

The formulas for the hydrogel base layer typically contain between 25% - 35% pectin. Anything more than 40% becomes difficult to blend into an extrudable solution. Hydrogels with a concentration of 25% pectin are relatively liquid and will diffuse outwards and mix more readily. On the other hand, hydrogels with a concentration of 32% pectin will have higher viscosity to remain more distinct when mixed. When pectin formulas of significantly different viscosities are blended, the resulting hydrodynamic interactions can generate complex surface patterns.

Surface Layer

The concentration of chitosan in our hydrogel surface layer formulas is between 5% - 7%, while the concentration of powdered cellulose in our hydrogel surface layer formulas are between 7% - 12%. The amount of acetic acid is consistently 5%.

The cellulose hydrogels dry much faster than the pectin hydrogels and can be printed in multiple consecutive layers because of their rigidity. The cellulose provides fibers form strong internal bonds that stick to the base layer and provide a more rigid structure to the dried hydrogel films. The surface layer is printed as lines rather than infills because of the high rate of shrinkage caused by the chitosan and acetic acid. Denser toolpaths printed using the cellulose hydrogels tend to tear themselves apart due to the internal forces caused by shrinkage.

Figure 14: Series of 360 ml cartridges containing colored pectin hydrogel. (left to right) Black – Charcoal, Dark Blue – Indigo, Dark Green – Spirulina, Green – Matcha, Yellow – Turmeric, Dark Red – Beet, Dark Brown – Cinnamon, Brown – Pomegranate, Light Orange – Chitosan, Orange – Standard, Light Tan – Calcium.

Fermentation

Each cartridge of hydrogels can contain approximately 360 ml of material. These are stored with a piston and a self-venting outlet cap to minimize the exposure of the hydrogels to oxygen that would catalyze fermentation. Even so, these materials have a limited shelf life. Pectin based materials tend to ferment and lose their consistent viscosity after a period of 3 – 7 days. Over time, the print parameters will change, and the speed and pressure need to be adjusted to accommodate the change in viscosity.

After the fermentation process reaches a certain point, the hydrogels will become too liquid to hold their forms and spread over the printing surface. The drying time for fermented materials typically increases and becomes more difficult to remove from the aluminum print bed. Depending on the temperature, different material formulas will ferment at different rates in figure 15.

In order to extend the shelf life of the pectin materials, the cartridges can be frozen to stop the fermentation process. During periods of high-volume production, the pectin hydrogels are mixed according to daily needs and stored in cartridges at colder temperatures in a refrigerator. While previous cellulose hydrogels hardened and become unextrudable between 1 – 3 days, newer material formulas have extended the printability of the material indefinitely.

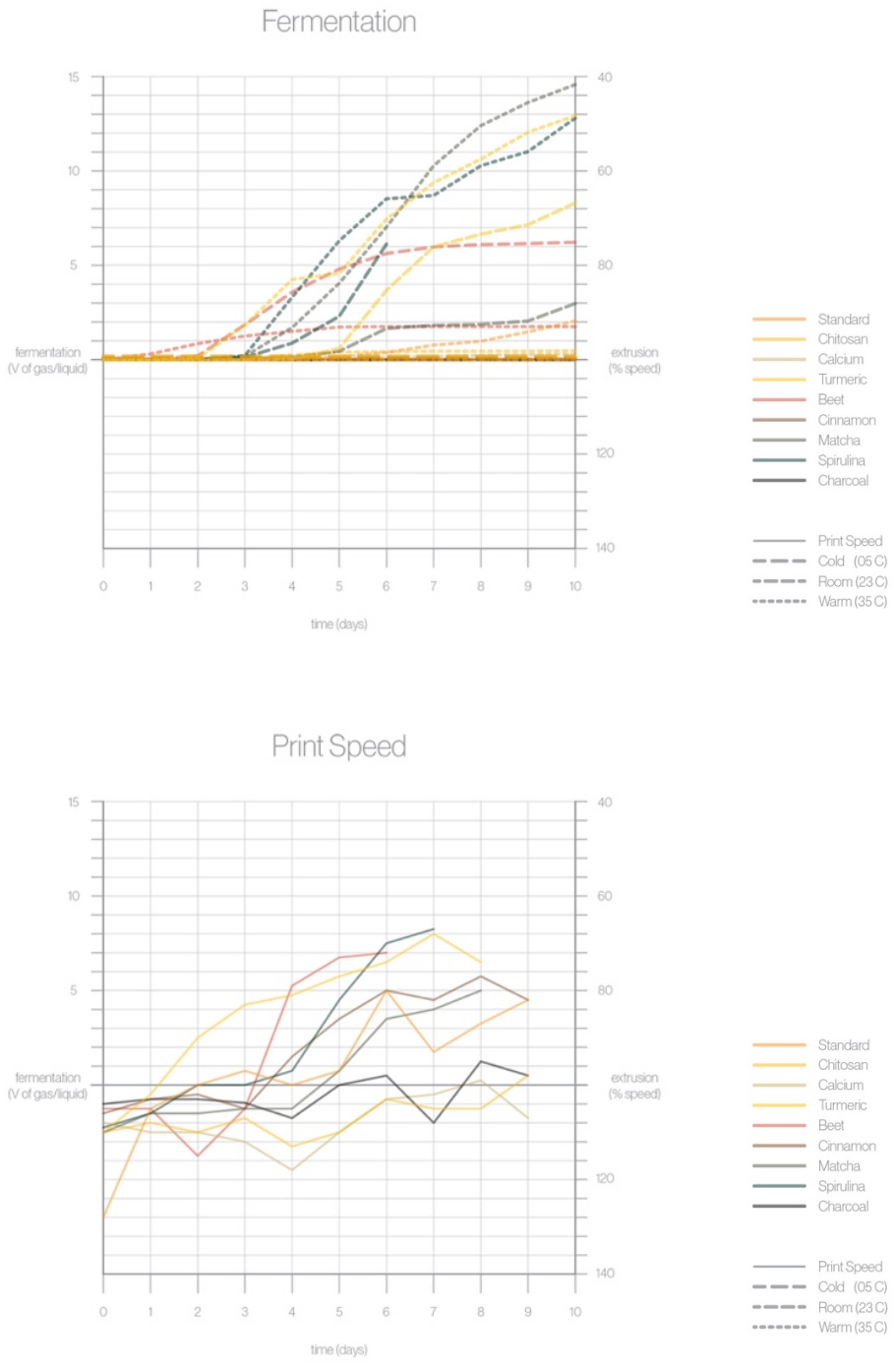

Figure 15: Correlation between fermentation rates and printing parameters in various pectin formulas. (top) Fermentation in warm, cold and room temperature (bottom) Changing extrusion parameters over 10 days.

3.2.2 Manufacture

A custom made 3 Axis CNC gantry controls the position of the print head over a 4' x 8' printing surface. The X and Y-axis of the machine are actuated by two pairs of NEMA 17 stepper motors that move along aluminum extrusion rails connected to timing belts. The Z-axis is controlled by a linear actuator that moves the print head with a worm screw. A fixed cartridge container with an airtight connector allows users to swap out cartridges easily. The entire printing assembly cost about $6,000.

End Effector

The end effector consists of a pneumatic system with a pressure regulator that pushes a piston into a cartridge to extrude material through a tip adaptor attached to a nozzle of varying diameters in figure 16. The size of the nozzle will control the width and precision of the extruded material on the toolpath. A thinner nozzle will extrude less material at a time to allow for higher degrees of precision. In comparison, a wider nozzle will extrude more material to allow for more efficient print times.

For purposes of consistency, we have chosen to use a 16-gauge diameter nozzle that allows a balance between precision and efficiency. The pressure and speed can be predefined or overridden mid-print to deposit more or less hydrogels on the print-bed. The printer is programmed to cut off the pressure and lift the nozzle as it moves between the start and endpoints of consecutive toolpaths. The nozzle height and diameter determine the precision of the biopolymer prints. Typically, the nozzle is 2-6 mm from the printing surface to ensure that the materials are being precisely extruded to the correct regions. If the nozzle is much farther away than 5mm, the hydrogels will extrude with slight inconsistencies that will cause coiling.

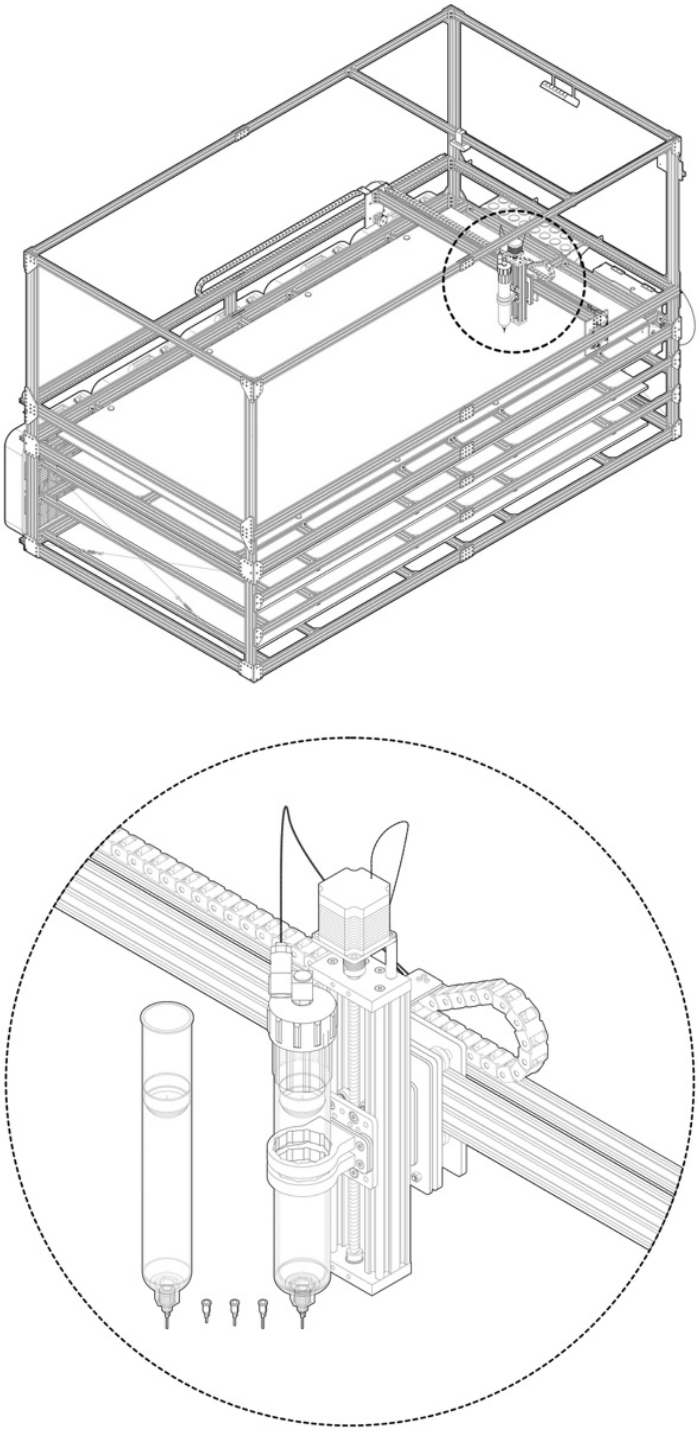

Figure 16: (top) Technical isometric drawing of the CNC biopolymer printing gantry showing print and drying beds. (bottom) Detail drawing of the end effector with removable cartridges and nozzles diameters.

Toolpaths

The toolpaths are typically generated as continuous vectors with minimal breaks using CAD software such as Rhino through scripting, parametric tools, or drawing manually. These programs are used to generate vector toolpaths that infill a closed shape with interior voids to make smooth hydrogel films or interconnected lattices from overlapping irregular toolpaths. The vector toolpath information is converted into G-Code by a grasshopper rhino plug-in that is opened by a Universal G-Code Sender before activating the microcontroller to operate the motor driver and pressure regulator in figure 17.

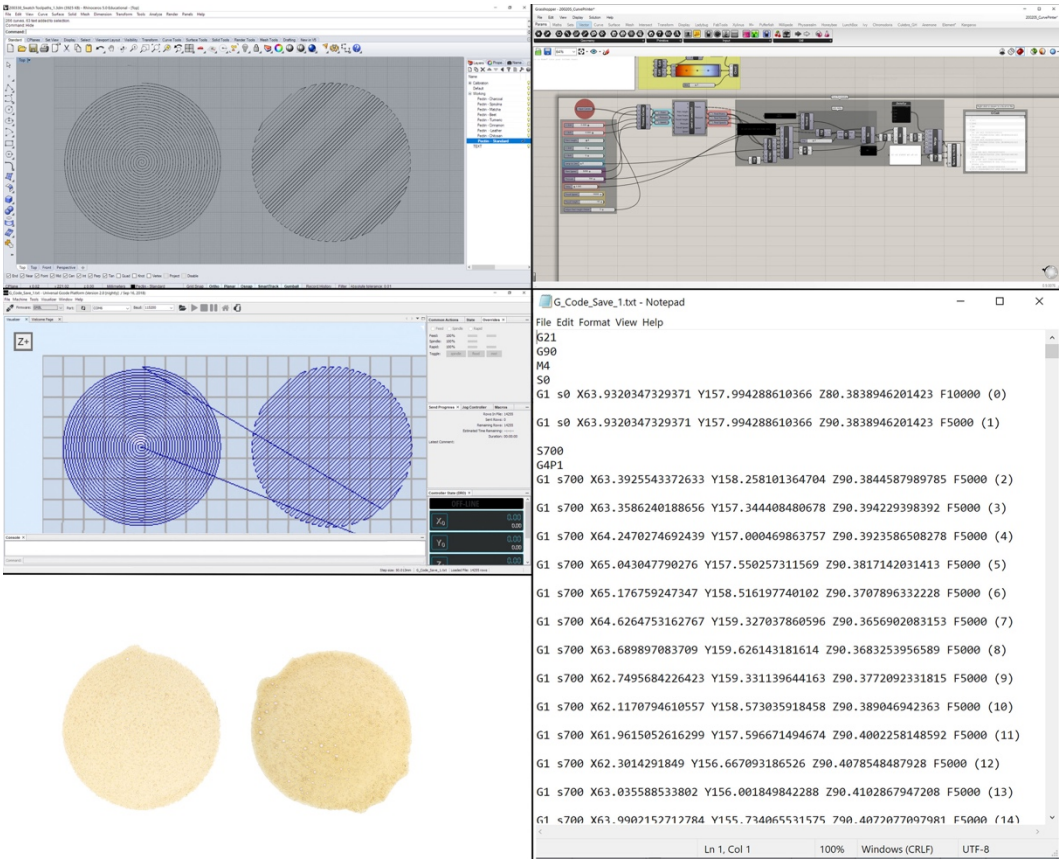

Figure 17: Digital printing process showing translation from vector paths in Rhino to G-Code coordinates in Grasshopper to UGS communication with printing gantry to physical print.

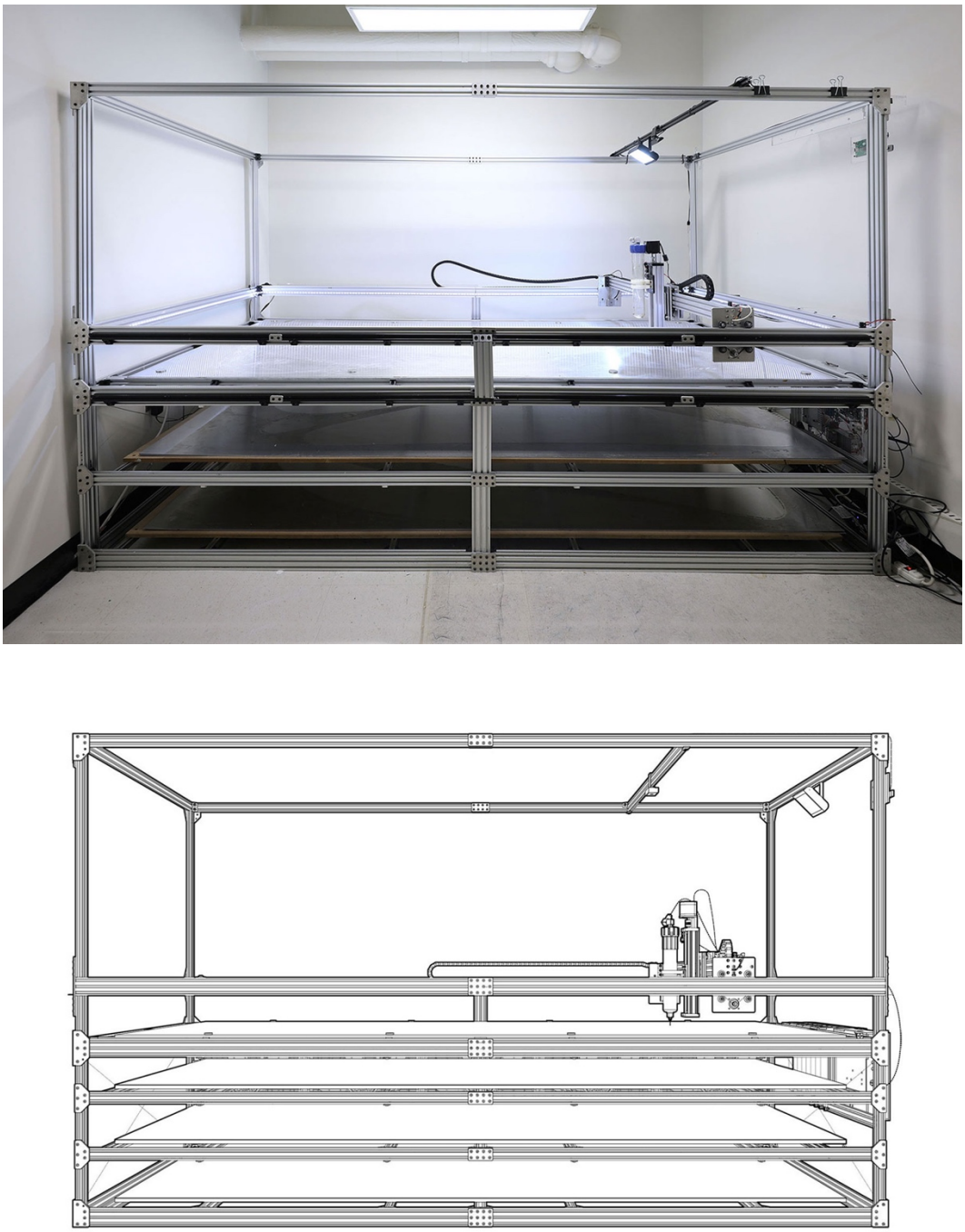

Figure 18: Biopolymer printing gantry photo with perspective elevation drawing showing set up in print room with end effector, print bed, drying beds and integrated lighting for imaging and recording experiments. (*https://designedecologies.com/Printer*)

Print Bed

The hydrogels are extruded onto a removable sheet of aluminum and allowed to dry in figure 19. Depending on the material formula, print thickness, room temperature, airflow, and humidity, the base layer of these prints will take somewhere between 18 to 36 hours to solidify and dry to a point at which they can be removed from the printing bed using chisels or scrapers. Once the hydrogels solidify on the aluminum bed, they must be removed within 4 – 8 days. If the hydrogels are allowed to dry on the print bed for extended periods, they risk rigidifying and sticking to the aluminum. After numerous tests, 1/16" x 4' x 8' aluminum sheet was chosen as an ideal printing surface for its smooth finish and lightweight rigid structure. The aluminum sheets are flattened, leveled, and fixed in place with a set of neodymium magnets that allow the print beds to be easily interchanged while ensuring they are precisely secured.

Swapping print beds avoids slowing down the production process with longer material drying times. In figure 18, the 3D printer is outfitted with two additional full-sized drying racks underneath the print bed with an array of five 20" box fans to circulate air and speed up the drying process without causing material cracking.

The design of the printer includes storage for additional cartridges of materials in addition to rails for mounting lighting and imaging equipment that can track and create time lapses of the printing and drying process.

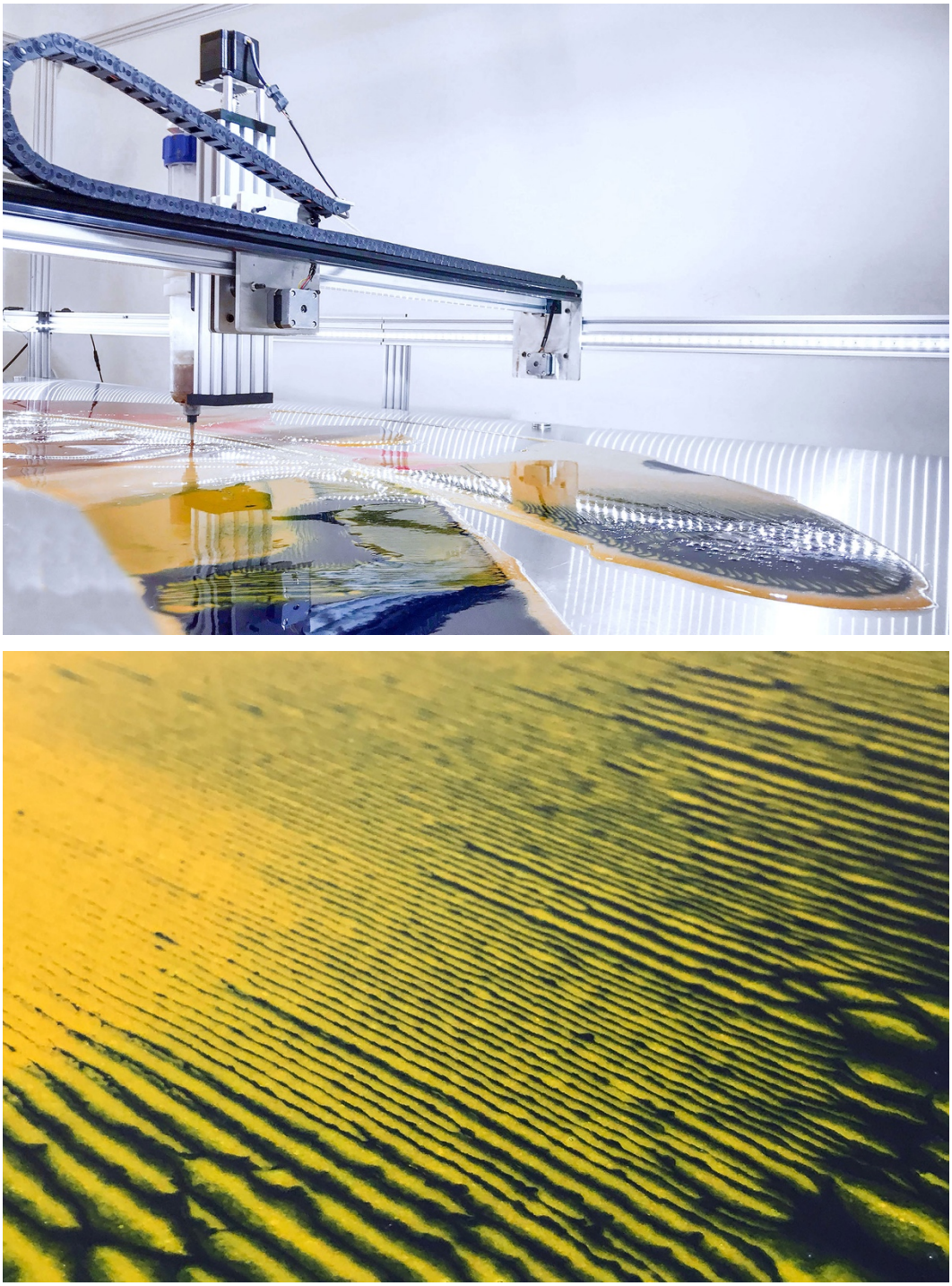

Figure 19: Biopolymer printer extruding pectin hydrogel onto aluminum print bed with close up of wet surface.

3.2.3 Environment

The biopolymer printer is located in a closed room that has temperature controls, a humidifier, and air circulation. Since the hydrogels are highly reactive to minute changes in the environment, varying the temperature and humidity of the printing space would require constant readjustment of other extrusion-based printing parameters. The temperature and humidity of the print room are regulated at about 70 degrees Fahrenheit with low humidity of about 40%. There are no windows to allow in sunlight that could otherwise affect the heating and drying of the hydrogel prints. The controlled environment allows the hydrogels to be printed under uniform conditions with greater predictability over the results of the fabrication process.

Drying

Experimentation with heating pads placed underneath the aluminum print beds yielded unreliable results. Although the higher temperatures caused the hydrogels to dry more quickly, the biopolymer surfaces experienced higher rates of tearing and warping while remaining attached to the print bed. Approximate room temperature environments allow adequate time for drying without causing excessive deformation.

Additionally, consistent airflow over the surfaces of the wet hydrogels can accelerate the evaporation of moisture within the material without causing considerable tearing or warping.

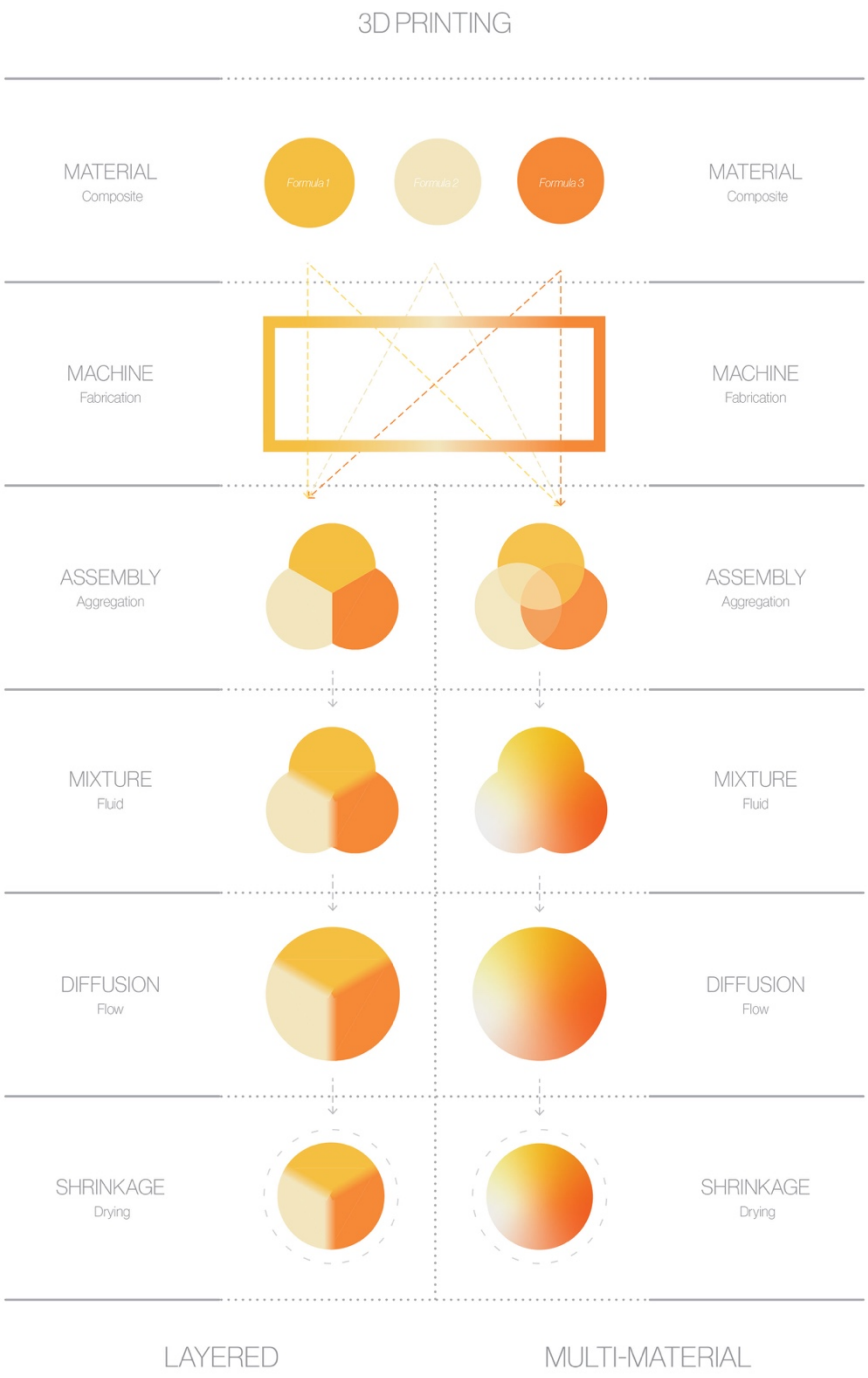

Figure 20: Diagram showing fabrication processes using layered vs. multi-material hydrogel 3D printing methods.

4 FABRICATION / METHOD

The biopolymer printer employs two primary methods for depositing materials on the print bed: layered printing and multi-material printing. While they both use the parallel computer controls and mechanical hardware, the toolpaths for each method of printing are generated using different techniques and extruded under different conditions in figure 20. The methods primarily diverge in the time period between successive printing sequences of different material compositions. With layered printing each sequence is extruded *on top* or *next to* the previous dry layer, whereas in multi-material printing each sequence is extruded *in to* the previous wet layer.

Each method can be adjusted to create distinct degrees of material diffusion and color gradation. Layered printing methods will produce biopolymer sheets with varied surface thickness with materials contained on distinct strata. In contrast, multi-material printing methods will create zones of material density in a continuous biopolymer sheet of uniform thickness. Biopolymer sheets printed with the two different methods using the same materials and toolpaths will appear and behave much different from one another.

4.1 Layered Printing

4.1.1 Print Order

Each biopolymer layer consists of different material formulas printed on top of one another after the previous one has dried. The base layer typically consists of a flexible pectin material formula to facilitate removal from the print bed. After this layer has dried for at least 18 hours, subsequent rigid layers of chitosan and cellulose material formulas are printed on top to provide additional thickness and structure.

4.1.2 Toolpath

The toolpaths fall into two categories of infills and lattices. The base layer is printed using infill toolpaths to create mostly continuous surfaces. Infill toolpaths are comprised of parallel or spiral vectors spaced equally between 1.5 mm to 2.5 mm apart. Adjacent regions can be printed with similar viscosity material mixtures to solidify as a single surface. In contrast, the surface layers are printed using lattice toolpaths in a variety of different patterns. Because of the high rates of shrinkage in the surface layer, the toolpaths are designed to avoid areas of significant density.

4.1.3 Nozzle Height

The distance of the nozzle from the print surface determines the precision of the printed toolpaths. With each successive layer, the nozzle height is adjusted to compensate. If the nozzle is too close to the print surface, the material will not extrude completely. If the nozzle is too far away, the material will be deposited on the print surface irregularly.

4.2 Multi-material Printing

4.2.1 Print Order

Each biopolymer layer consists of different material formulas printed into one another while they are still wet. The hydrogels can be blended on the print surface to create graded material transitions between regions. The base layer consists of an infill path with a lower toolpath density. The subsequent layers are printed directly into the first layer before it can begin to dry. Depending on the material formula and environment, hydrogels can be printed and mixed within 2 to 3-hours before they lose their fluidity and solidify. Hydrogel surfaces with the same materials and toolpaths will have noticeably different appearances because of the different order in which they're printed.

4.2.2 Toolpath

The base layer uses a low-density infill path and with high-density lattice paths for subsequent layers. The toolpaths deposit additional material and mix existing hydrogel layers already on the print bed. The pattern, direction, and speed of toolpaths affect how successive layers are mixed.

4.2.3 Nozzle Height

The depth of the nozzle in the hydrogels determine the layering of different materials and the layers mixed. Hydrogels can either be printed below, inside, and on top of materials on the print bed. Slight changes in the height of the nozzle can result in dramatically different appearances.

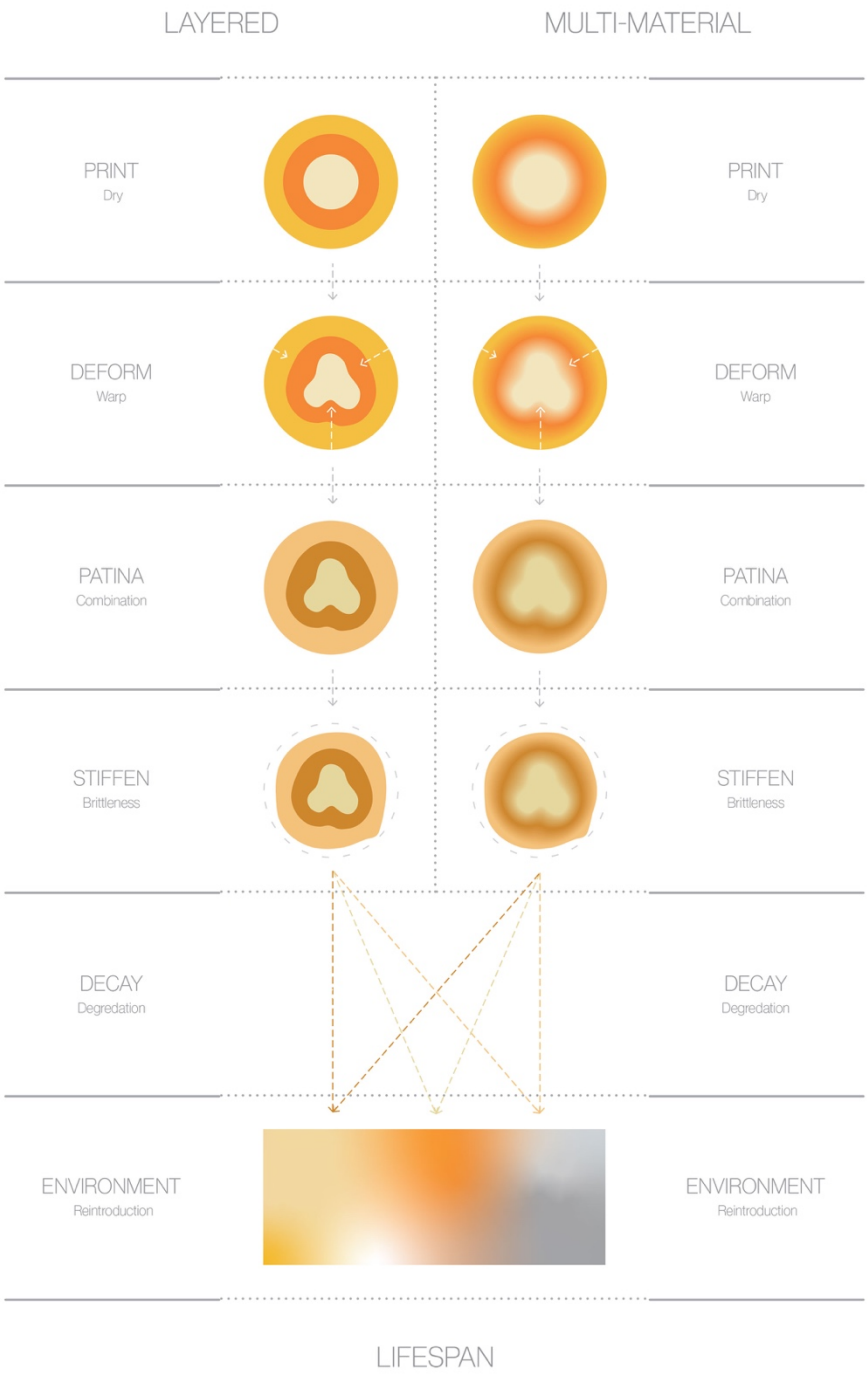

Figure 21: Diagram showing the general visual and structural changes of layered and multi-material biopolymer prints caused by drying, warping, tinting and stiffening over time.

5 TRACKING / QUANTIFICATION

Factors such as temperature and humidity continue to affect the behavior of the biopolymers in the weeks, months, and years post-production in figure 21. Over time the surfaces will curl and darken as the material continues to dry. The biopolymer prints will experience varying degrees of shape and color change that are accelerated and exaggerated by higher temperatures and dryer environments. Hydrogel mixtures containing more significant concentrations of chitosan will typically exhibit higher degrees of color, shape, and structural change more rapidly in figure 22.

5.1 Color

As the printed hydrogels dry, the materials darken in color. The standard pectin chitosan hydrogel formula dries into a light orange-yellow color. Over time, the prints will gradually change from a dark orange into a reddish-brown and eventually to a very dark brown. This behavior affects material mixtures that contain organic pigments to darken chitosan hydrogels containing turmeric, beet, spirulina, and matcha powder. Materials mixtures with pigments such as charcoal or indigo will not turn noticeably darker primarily because of their already dark appearance. In contrast, pectin material mixtures without chitosan will often lose their vibrant colors and turn lighter with a whitish surface coating when exposed to more humid environments.

5.2 Shape

As the printed hydrogels dry, the materials shrink. This process begins immediately after the biopolymers have been extruded onto the print bed with the most noticeable thinning and shrinkage occurring during the first 48 hours. Additional moisture loss

over time will cause the solidified surfaces to continue to shrink more slowly. The difference in rates of shrinkage of a top surface vs. a bottom surface will cause materials to deform from being flat to curved. The deformation is partially caused by adjacent regions that exhibit different levels of water loss. Exposure of a top surface to more air and heat will allow it to dry faster and deform more than the bottom surface. Pectin formulas containing chitosan and calcium will warp the most dramatically in environments with higher temperatures.

5.3 Structure

As the printed hydrogels dry, the materials become more rigid and brittle. With the gradual loss of moisture, the biopolymer surfaces lose their initial flexibility. Material formulas without chitosan will retain their flexibility for extended periods, while formulas containing calcium carbonate, cellulose, and chitosan will become rigid and brittle much more quickly. The pattern of the toolpaths and the air bubbles formed during extrusion and drying can create varied surface textures. Additionally, material formulas containing cinnamon and chitosan will exhibit a rougher surface texture.

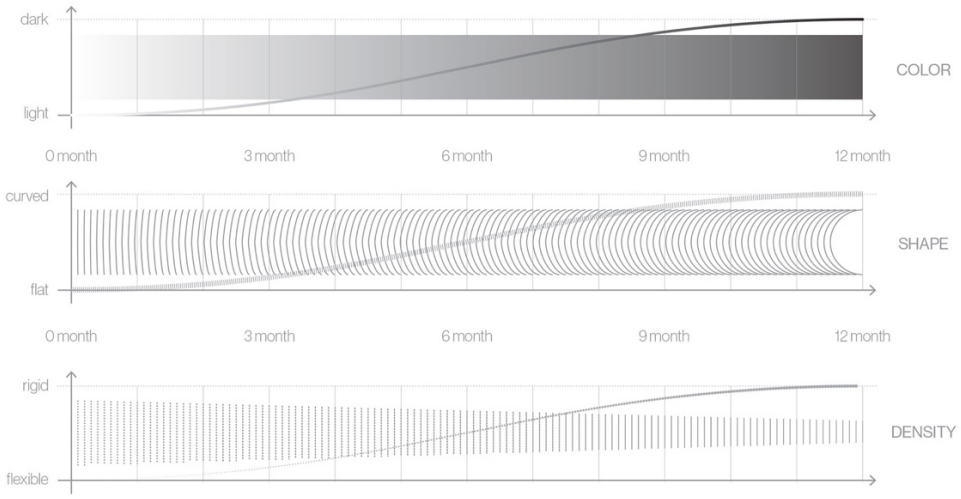

Figure 22: Diagrams showing general color, shape and structural changes in biopolymers over the course of a year.

6 CASE STUDIES

A large amount of external factors outside of the control of the fabrication environment affect the behavior of biopolymer prints over time. A set of experiments that each control for different designed variables were printed and recorded in order to test for and correlate the changes that result from various material mixtures, toolpaths, aggregated geometries, printing methods, climatic exposures and environments. The patterns of deformation and color change of the experiments 2-dimensional surfaces and 3-dimensional aggregate forms give insight into how materials composition and manufacturing methods can be adjusted to create programmable degradation that results in predictable shape, structure, and color change. By concentrating pectin hydrogels with higher concentrations of chitosan in distinct areas layered with oriented cellulose latticed, it is possible to drive more extreme material deformation in targeted regions within a single composite sheet of material. The strategic placement of pectin hydrogels with glycerine allows for areas of higher flexibility that can be folded and adhered to adjacent surfaces.

This series of 9 experiments have been grouped and labeled according to their relative global geometries, material composition and printing methods. The naming convention for each series contains a letter that corresponds to the general shape of each flat print (the letter O refers to the circular shape of the O swatch experiments while the letter X corresponds to the cross shape of the X swatch experiments). They were designed and printed between September 2018 and April 2019. Their visual and structural changes have been tracked from October 2018 to April 2020 for periods up to a year in length.

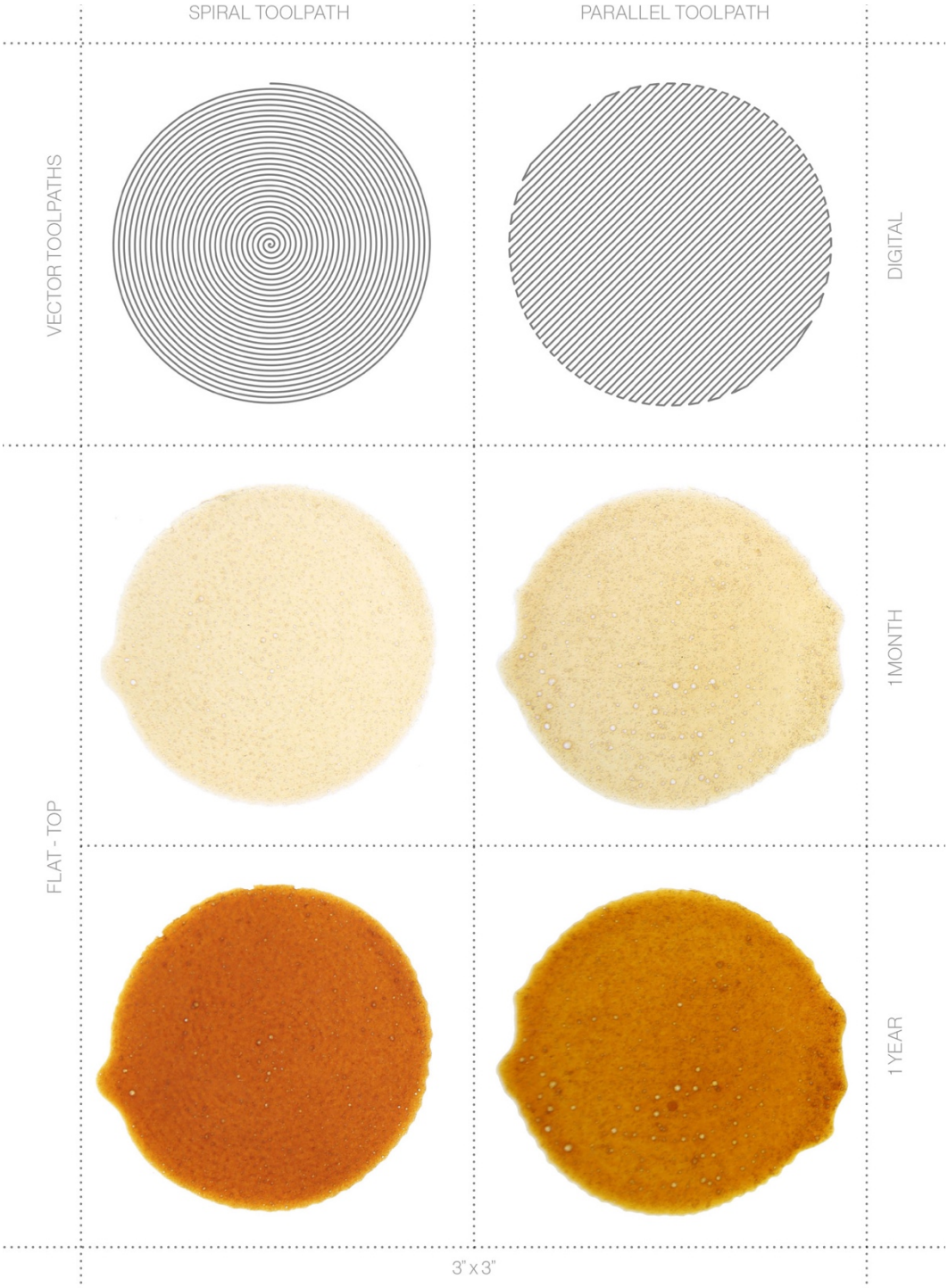

Figure 23: Pectin/chitosan mixture formula printed in circular diameter swatches with spiral and parallel toolpaths. (top) vector toolpaths, (middle) print after 1 month, (bottom) print after 9 months. 3" x 3"

6.1 O Swatch

These experiments examine how different material formulas and printing methods react to different environmental conditions. Each material formula is printed as a base layer of pectin in a 3" circular swatch with both a parallel and spiral infill toolpath. Additional swatches are then printed onto with separate layers of both white and black cellulose lattices. Three sets of swatches (base layer; base layer + white chitosan, base layer + black chitosan) are exposed to 4 elements over time: air, water, earth and fire in figure 24.

The visual changes of each material formula are tracked for various periods:

- Exposure to air is recorded every 3 months for a period of 9 months.
    - Changes in color and shape are visible in figure 23.
- Exposure to water is recorded every day for a period of 8 days.
    - Dramatic changes in solidity and composition are visible.
- Exposure to earth is recorded every 2 months for a period of 8 months.
    - Dramatic changes in color and shape are visible.
- Exposure to heat is recorded for the duration of 15s, 30s and 45s.
    - Dramatic changes in color and surface roughness are visible.

Figure 24: Matrix of O swatches showing tunable variation in material qualities using different pectin formulas, toolpaths, printing methods, heat and air exposures.

Ten different material formulas are tested:

- Standard: https://designedecologies.com/standard
- Chitosan: https://designedecologies.com/chitosan
- Calcium: https://designedecologies.com/calcium
- Turmeric: https://designedecologies.com/turmeric
- Beet: https://designedecologies.com/beet
- Cinnamon: https://designedecologies.com/cinnamon
- Matcha: https://designedecologies.com/matcha
- Spirulina: https://designedecologies.com/spirulina
- Indigo: https://designedecologies.com/indigo
- Charcoal: https://designedecologies.com/charcoal

The chitosan and calcium swatches exhibit the highest degrees of deformation and most dramatic color change over 4 months exposed to air. See appendix 9.2.1

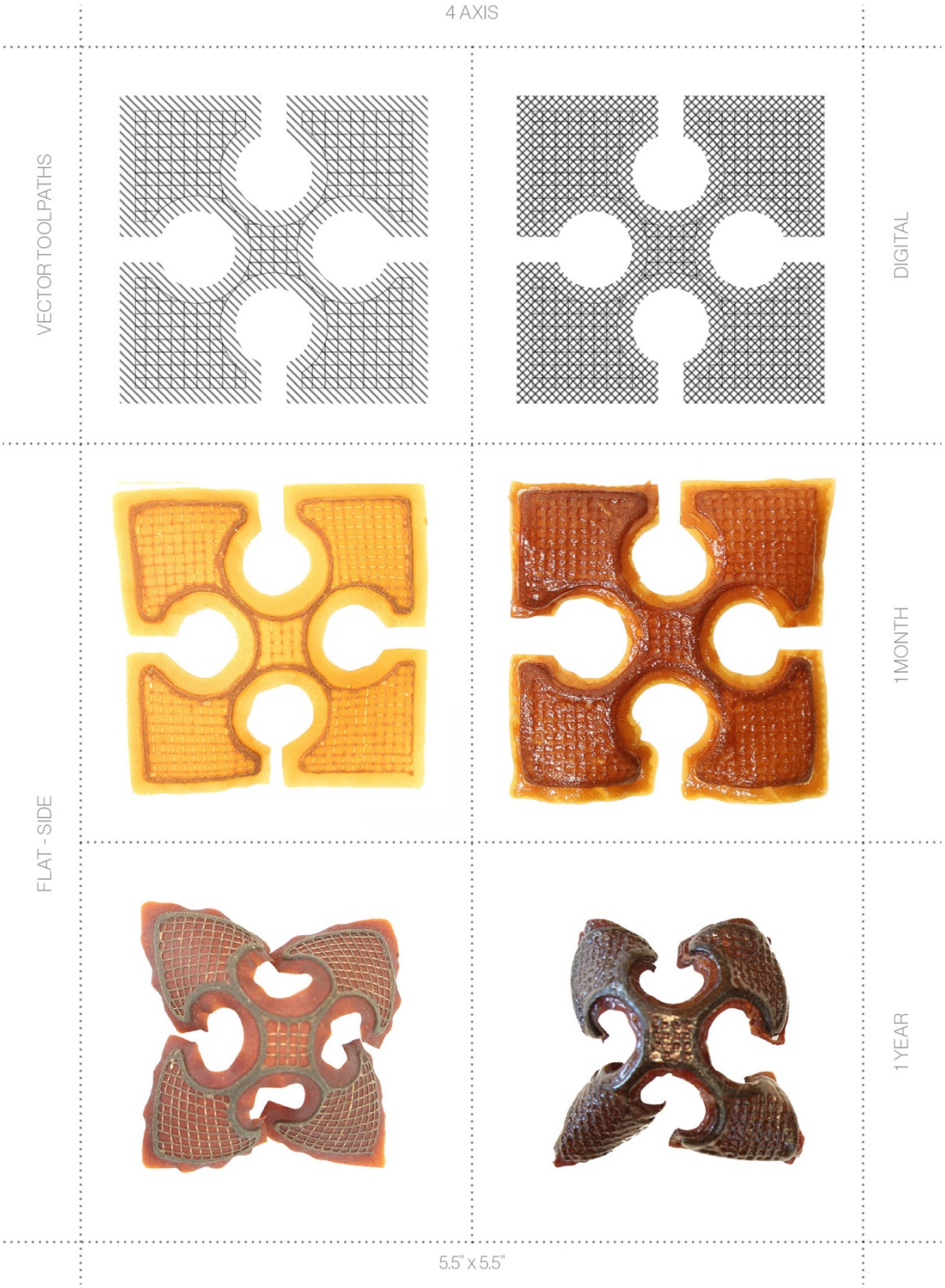

Figure 25: Comparison of the deformation of X swatch prints aged over 1 year with (left) pectin/chitosan and cellulose composition vs. (right) pectin/chitosan, cellulose, and pectin composition.

6.2 X Swatch

These experiments examine how different material formulas, print orders and toolpaths can affect deformation over time. Each material formula is printed with a base layer of pectin in a 5 ½" cross shaped swatch with a parallel infill toolpath. A layer of cellulose hydrogels is printed with variable density lattice patterns. In select swatches a 3rd layer of pectin hydrogel is printed either on top or below the cellulose layer. The breaks in the geometry of the X shape are intended to allow the surfaces to exhibit greater shape change over time. The collection of different swatches is then exposed to air in figure 26.

The visual changes of the swatches are tracked for a period of time.

- Exposure to air is recorded during the first month and at 12 months.
- Swatches are imaged with and without backlighting in plan and side view.
    - Changes in color and shape are visible in figure 25.

6 different sets of 4 swatches are tested that control for the same toolpaths but vary the material formula and print order: https://designedecologies.com/X-Swatch-1

- Pectin layer + Cellulose layer.
    - Minimal shape and color change.
- Pectin Chitosan layer + Cellulose layer.
    - Moderate shape and color change.
- Pectin Chitosan Acetic Acid layer + Cellulose layer.
    - Minimal shape and dramatic color change.
- Pectin layer + Cellulose layer + Pectin Chitosan layer.
    - Dramatic shape and color change.
- Pectin Chitosan layer + Cellulose layer + Pectin layer.
    - Dramatic shape and color change.

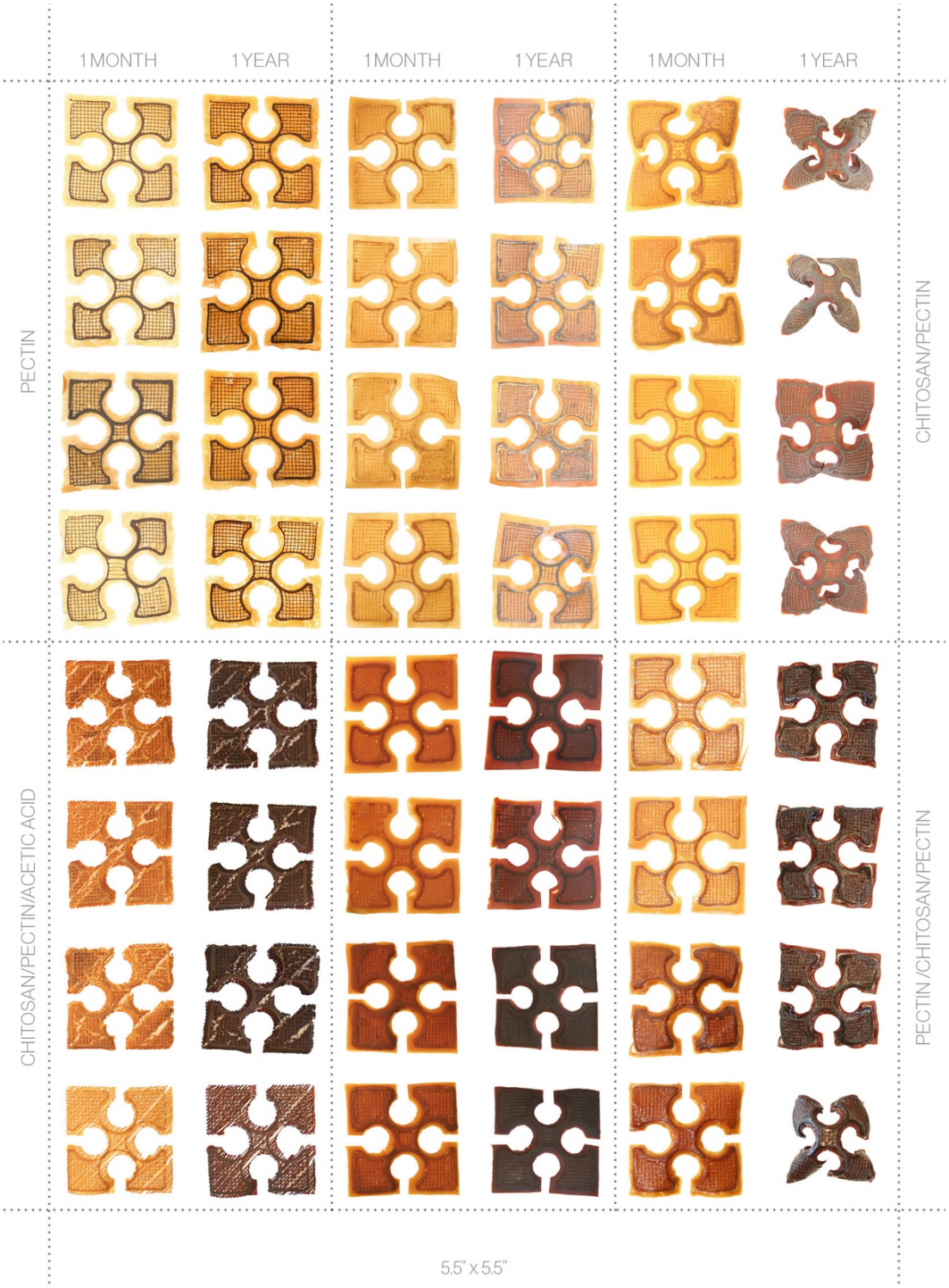

Figure 26: Matrix showing the deformation and color change of X swatches with different pectin formulas aged over 1 year with 1 – 2 layers of pectin and 1 layer of cellulose.

- Pectin Chitosan layer + Cellulose layer + Pectin Chitosan layer.
    - Dramatic shape and color change.

Multiple different sets of swatches are tested that control for material formula and print order but vary toolpaths: https://designedecologies.com/X-Swatch-2

- Pectin layer + Cellulose layer with 16 swatches.
    - Minimal shape and color change.
- Pectin layer + Cellulose layer + Holes with 12 swatches.
    - Minimal shape and color change.
- Pectin Chitosan layer + Cellulose layer with 8 swatches.
    - Moderate shape and dramatic color change.
- Pectin Chitosan layer + Cellulose layer Holes with 3 swatches.
    - Moderate shape and color change.
- Pectin layer + Cellulose layer + Pectin layer with 6 swatches
    - Dramatic shape and color change.
- Pectin layer + Pectin layer + Cellulose layer with 6 swatches
    - Dramatic shape and color change.
- Pectin layer + Cellulose layer + Pectin Chitosan layer with 2 swatches
    - Dramatic shape and color change.

The material composition and print order have a much more dramatic effect on shape change over time than does the variation of tool pathing in the cellulose layer. Although the lack of significant shape change in the sets that were testing for toolpathing may be due to different storage conditions that they were kept in. See appendix 9.2.2

Figure 27: Comparison of the deformation of X flower prints aged over 1 year with (left) pectin/chitosan and cellulose composition vs. (right) pectin/chitosan, cellulose, and pectin composition.

6.3 X Flower

These experiments examine how different material formulas can affect the deformation and color change of an aggregate, folded object over time. Each assembly is made of 8 folded X swatches printed with varying cellulose toolpath layers on top of a pectin base layer. Each swatch is folded and pinned at a different degree angle to nest within one another. The swatches are attached to one another from their central point. The collection of aggregated swatches is exposed to air.

The visual changes of the assemblies are tracked for a period of time.

- Exposure to air is recorded during the first month and at 12 months.
- Swatches are imaged with and without backlighting in plan and side view.
    - Changes in color and shape are visible in figure 27.

8 different sets of 8 swatch folded assemblies are tested that control for the same toolpaths but vary the material formula with 8 different types of pectin: Standard, Chitosan, Calcium, Turmeric, Beet, Matcha, Spirulina and Charcoal.
https://designedecologies.com/X-Flower

The assemblies do not exhibit extreme degrees of color or shape change largely due to their lack of chitosan content. Because the swatches are shrinking at the same rate and the connections between pieces are fairly flexible, the aggregate forms avoid tearing and deformation. See appendix 9.2.3

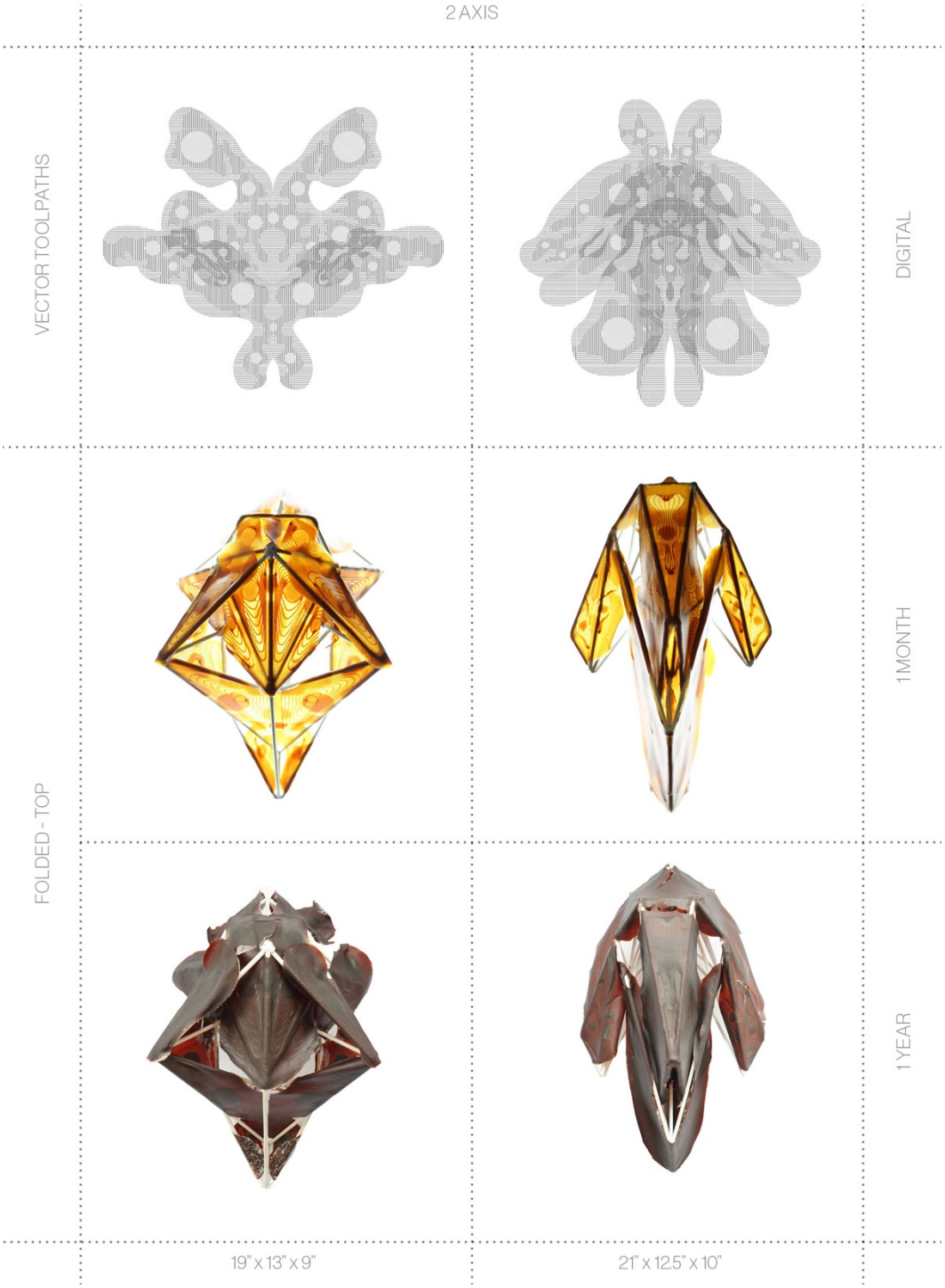

Figure 28: Comparison of the deformation of V skull prints aged over 1 year with different 2-dimensional geometries and 3-dimensional forms.

6.4 V Skull

These experiments examine how biopolymer surfaces wrapped over rigid structures may shrink and deform over time. Steel rod is welded into volumetric faceted frames. The hydrogel toolpaths are designed to match the shape and dimensions of specific areas on the frame. The base layer consists of a pectin chitosan sodium hydroxide formula that is printed as parallel infill paths. A second layer of pectin is printed as an infill onto areas that will bend around or attach to the steel frame. This layer has a higher concentration of pectin to allow for flexibility. When wet, the pectin can be stuck onto the metal frame. Once dry, the surface will adhere to the metal frame on its own. The last layer is a lattice toolpath of cellulose that adds structural rigidity to the areas between the folds in the biopolymer skin.

The visual changes of the wrapped frames are tracked for a period of time.

- Exposure to air is recorded during the first month and at 12 months.
- Frames are imaged with and without backlighting in plan, back and side view.
    - Changes in color and shape are visible in figure 28.

3 wrapped frames of different sizes with 2, 3 and 4 biopolymer surfaces with duplicates are tested that control for the same materials and print orders but vary the 3-dimensional geometries: https://designedecologies.com/V-Skull

The biopolymer skins tend to shrink over the rigid metal frames to tear in some areas and decohere from the frame in others. There is significant color change. See appendix 9.2.4

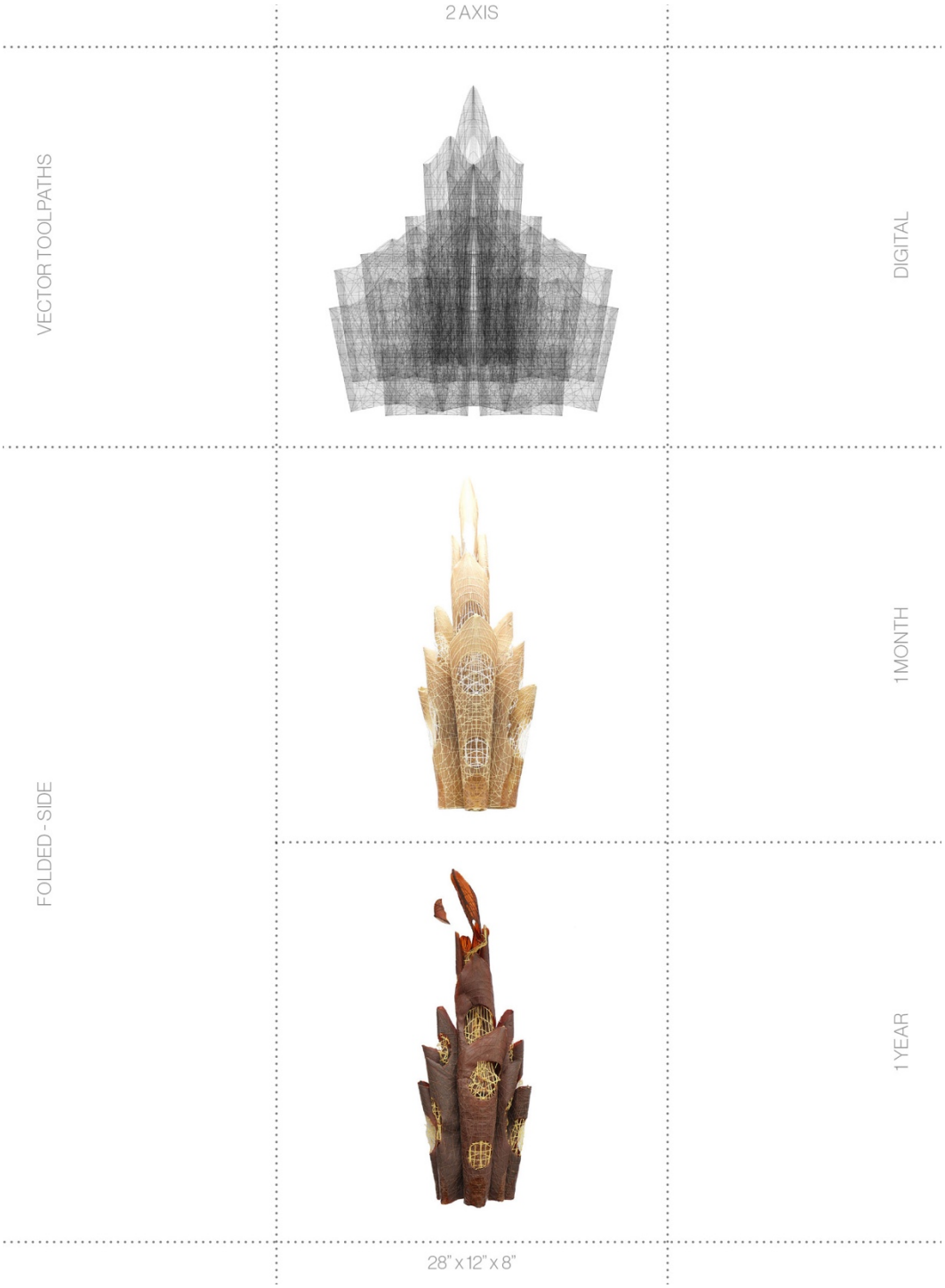

Figure 29: Comparison of the deformation of U fold aggregate prints aged over 1 year.

6.5 U Fold

These experiments examine how centrally aggregated and nested biopolymer surfaces may deform over time. A series of bilaterally symmetric prints are composed of a pectin chitosan infill base layer with a cellulose lattice surface layer. The center lines of each print have a region of pectin infill printed above the cellulose lattice. A set of 10 different prints are clamped along the wetted central pectin spine to adhere all surfaces together. The edges of each of these surfaces are exposed to a humidifier and folded into adjacent surfaces.

The visual changes of the aggregate surfaces are tracked for a period of time.

- Exposure to air is recorded during the first month and at 18 months.
- Folded shapes are imaged with and without backlighting in plan view.
    - Changes in color are visible in figure 29.

1 nested aggregate of 16 biopolymer surfaces are tested that control for the same materials and print orders but vary the 3-dimensional geometries: https://designedecologies.com/U-Fold

Although the symmetrical aggregate does not experience major deformation, portions have cracked due to internal pressures. There is significant color change. See appendix 9.2.5

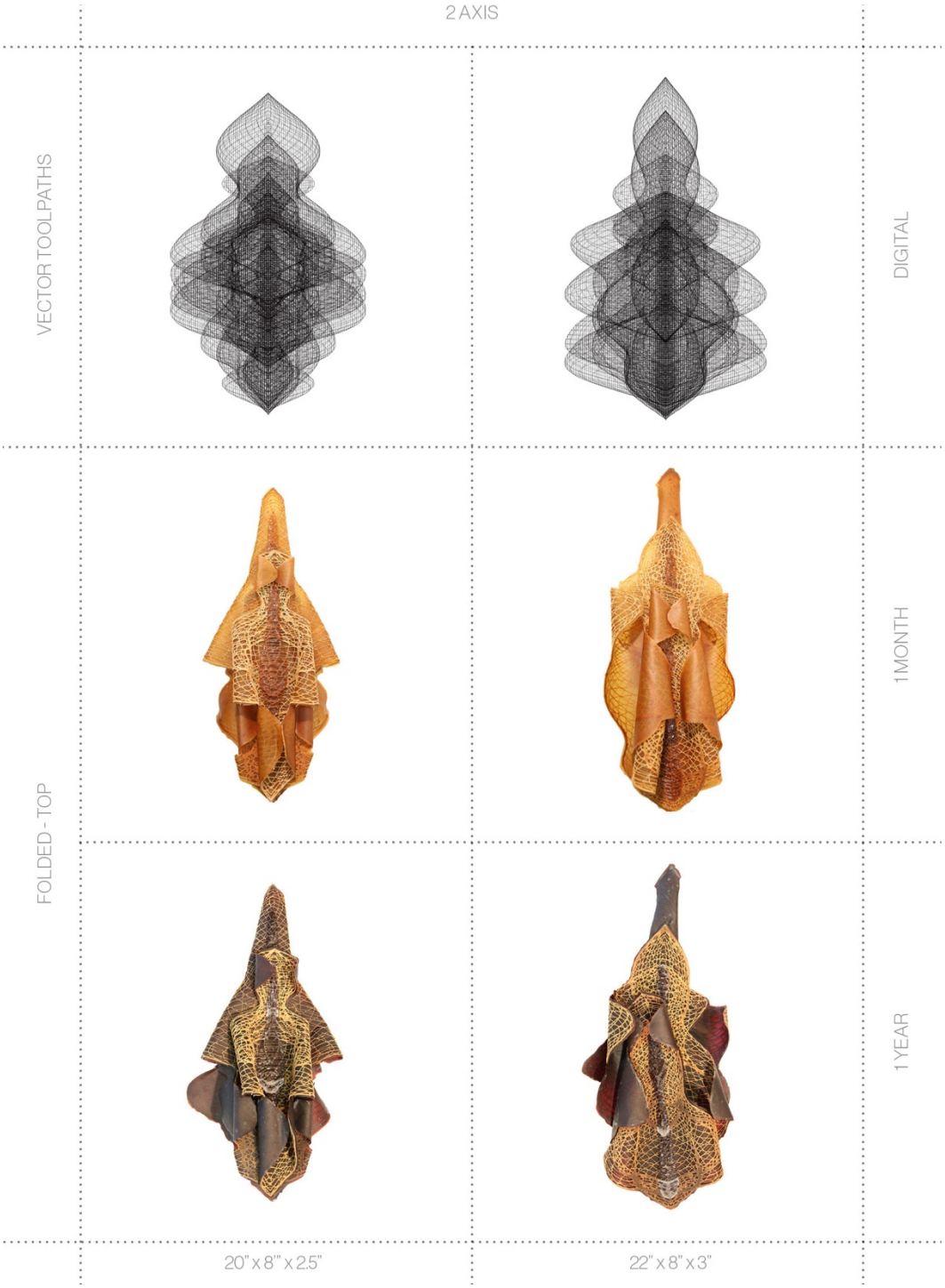

Figure 30: Comparison of the deformation and color change of T fold prints aged over 1 year with different 2-dimensional geometries and 3-dimensional forms.

6.6 T Fold

These experiments examine how centrally aggregated and folded biopolymer surfaces may deform over time. A series of bilaterally symmetric prints are composed of a pectin chitosan infill base layer with a cellulose lattice surface layer. The center lines of each print have a region of pectin infill printed above the cellulose lattice. A set of 4 different prints are clamped along the wetted central pectin spine to adhere all surfaces together. The edges of each of these surfaces are exposed to a humidifier and folded into adjacent surfaces.

The visual changes of the aggregate surfaces are tracked for a period of time.

- Exposure to air is recorded during the first month and at 12 months.
- Folded shapes are imaged with and without backlighting in plan view.
    - Changes in color and shape are visible in figure 30.

2 folded aggregates of 4 biopolymer surfaces are tested that control for the same materials and print orders but vary the 3-dimensional geometries: https://designedecologies.com/T-Fold

Although the aggregates are shaped symmetrically, they do not deform consistently on either side of a single piece. There is significant color change. See appendix 9.2.6

Figure 31: Comparison of the deformation and color change of Y fold prints aged over 1 year with different 2-dimensional geometries and 3-dimensional forms.

6.7 Y Fold

These experiments examine how radially aggregated and folded biopolymer surfaces may deform over time. A series of bilaterally symmetric prints are composed of a pectin chitosan infill base layer with a cellulose lattice surface layer. The cellulose surface layer is generated to align to specific vectors that encourage creasing the surfaces along predefined ridges. The center lines of each print have a region of pectin infill printed above the cellulose lattice. Regularly spaced holes on the print allow the surfaces to be clamped and joined together. Two sets of 3 identical prints are clamped along the wetted central pectin spine to adhere all surfaces together. The edges of each of these surfaces are exposed to a humidifier and creased along the toolpaths.

The visual changes of the aggregate surfaces are tracked for a period of time.

- Exposure to air is recorded during the first month and at 12 months.
- Folded shapes are imaged in plan and angled view.
    - Changes in color and shape are visible in figure 31.

2 folded aggregates of 4 biopolymer surfaces are tested that control for the same materials and print orders but vary the 3-dimensional geometries: https://designedecologies.com/Y-Fold

Although the aggregates are shaped symmetrically, they do not deform consistently on either side of a single piece. There is significant color change. See appendix 9.2.7

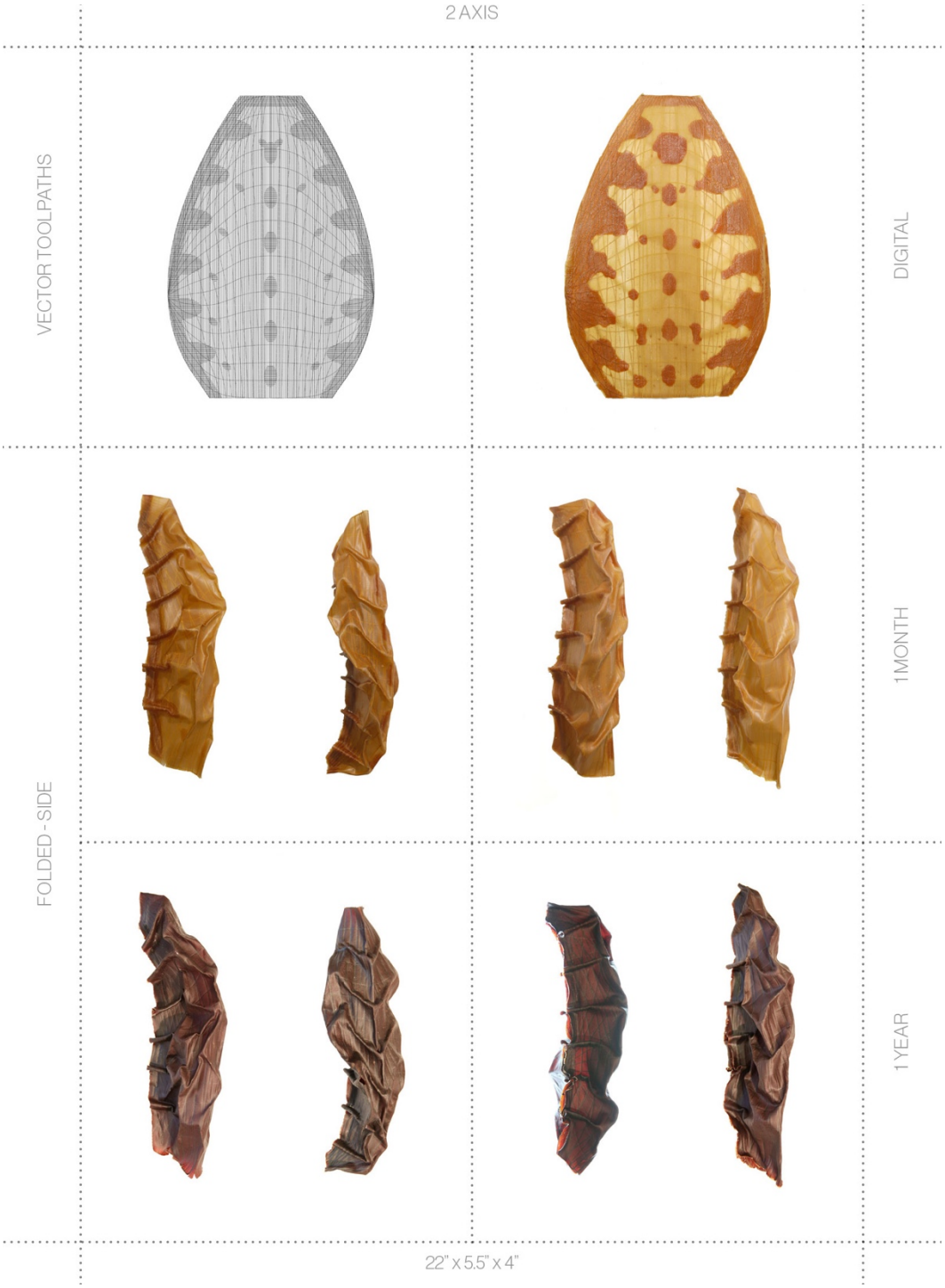

Figure 32: Comparison of the deformation and color change of I crease prints aged over 1 year with different 3-dimensional forms.

6.8 I Crease

These experiments examine how creased biopolymer surfaces may deform over time. A series of bilaterally symmetric prints are composed of a pectin chitosan infill base layer with a cellulose lattice surface layer. The edges of each print have a region of pectin infill printed above the cellulose lattice. The edges of each of these surfaces are wet and folded over to connect to themselves. The volume is pinched and creased along its ridges.

The visual changes of the creased surfaces are tracked for a period of time.

- Exposure to air is recorded during the first month and at 12 months.
- Folded shapes are imaged in plan and side view.
    - Changes in color and shape are visible in figure 32.

4 creased surfaces are tested that control for the same materials, toolpaths and print orders but vary 3-dimensional geometries: https://designedecologies.com/I-Crease

The pieces experience moderate shape change and significant color change. See appendix 9.2.8

Figure 33: Comparison of the deformation and color change of + crease prints aged over 1 year with different 2-dimensional geometries and 3-dimensional forms.

6.9 + Crease

These experiments examine how creased biopolymer surfaces may deform over time. A series of radially symmetric prints are composed of a pectin chitosan infill base layer with a cellulose lattice surface layer. The cellulose surface layer is generated to align to specific vectors that encourage creasing the surfaces along predefined ridges. The sides and ridges of each print have a region of pectin infill printed above the cellulose lattice. The edges of each of these surfaces are exposed to a humidifier and creased along the toolpaths.

The visual changes of the creased surfaces are tracked for a period of time.

- Exposure to air is recorded during the first month and at 12 months.
- Folded shapes are imaged in plan and side view.
    - Changes in color and shape are visible in figure 33.

4 sets of 2 biopolymer surfaces with 2, 3, 4 and 6 axis of symmetry are tested that control for the same materials, toolpaths and print orders but vary the 3-dimensional geometries: https://designedecologies.com/Crease

The pieces experience significant non-symmetric shape and color change. See appendix 9.2.9

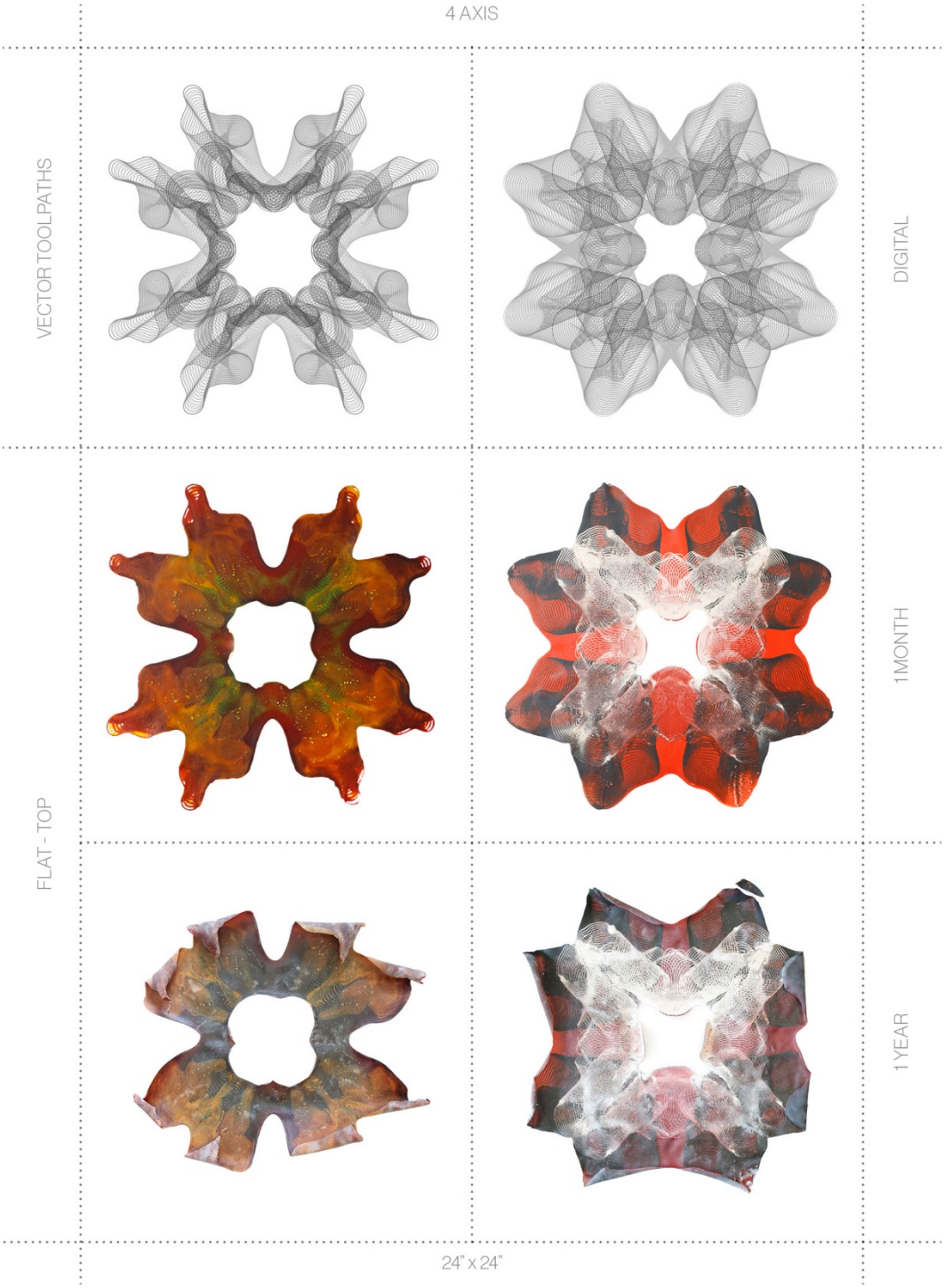

Figure 34: Comparison of the deformation and color change of * flat prints aged over 1 year with different 2-dimensional geometries and 3-dimensional forms.

6.10 * Flat

These experiments examine how multi-material biopolymer surfaces will change over time. A series of radially symmetric prints are composed of a pectin infill base layer containing pigmented additives that are printed into one another while still wet.

The visual changes of the creased surfaces are tracked for a period of time.

- Exposure to air is recorded during the first month and at 12 months.
- Folded shapes are imaged in plan and side view.
    - Changes in color and shape are visible in figure 34.

64 multi-material biopolymer surfaces with 3, 4, 5 and 6 axes of symmetry are tested that vary materials, toolpaths and print orders: https://designedecologies.com/

The pieces experience minimal shape and color change. See appendix 9.2.10

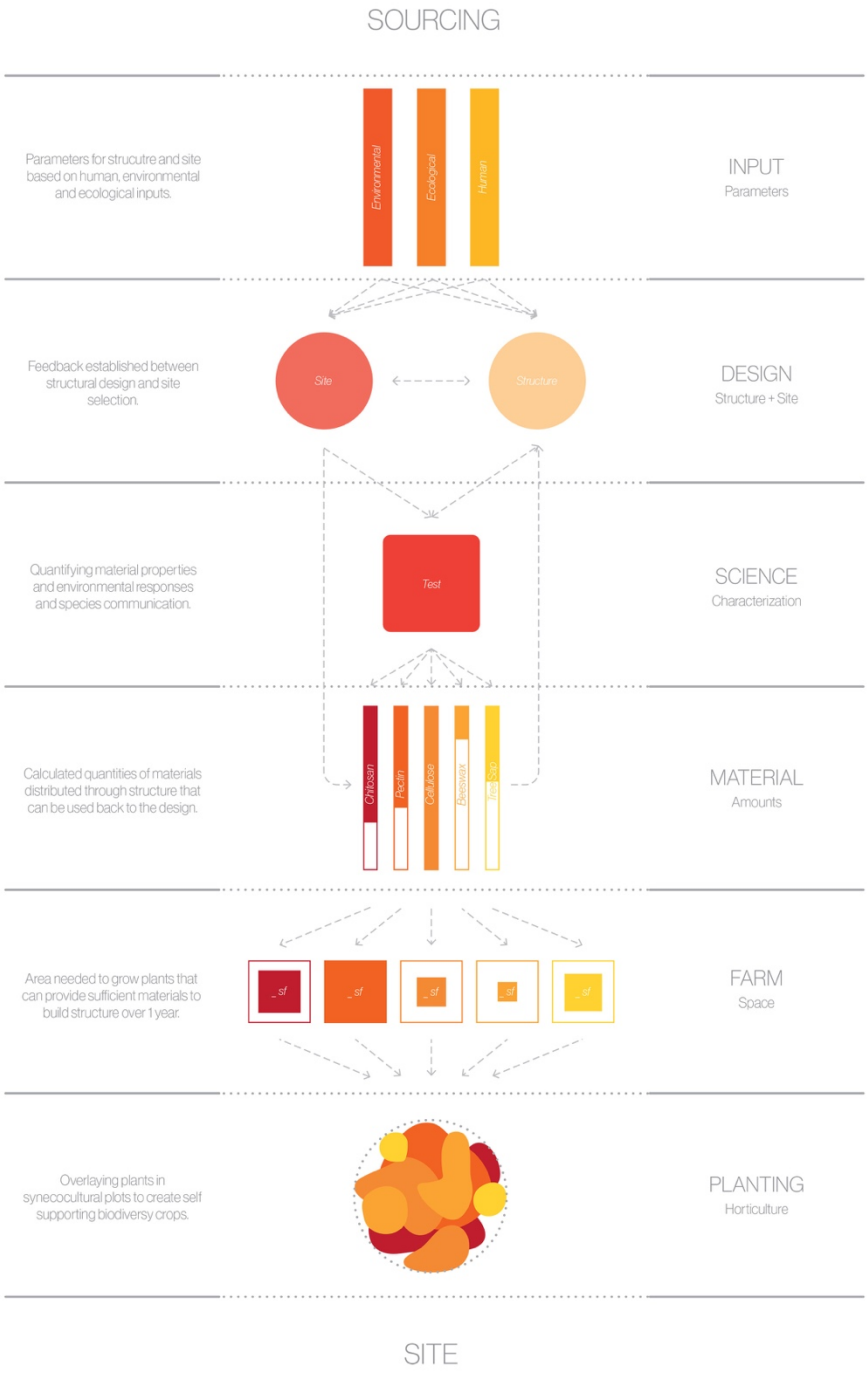

Figure 35: Diagram illustrating the design and implementation process for creating site specific structures from locally grown materials capable of reacting to the climate and organisms in an ecology.

7 CONCLUSION

Although the case studies were made as explorations in 2-dimensional pattern generation and 3-dimensional form finding within the constraints of the biopolymer materials and CNC gantry rather than to serve a specific function, they provide meaningful insight into the use of biopolymers in structures and products made from site sourced materials in figure 35.

7.1 Application

Chitosan, pectin and other biopolymers are broadly appealing because they require few resources and create low environmental impacts. These materials are largely non-toxic to both people and the environment. Chitosan is already widespread in the food and beverage industry as both a nutritional additive, antimicrobial coating and disposable packaging. In biomedicine, there is promising potential for chitosan to be used in drug delivery and tissue engineering because of its biocompatibility, antibacterial properties and ease of processing into different forms. (Crini & Lichtfouse, 2019) In building components, biopolymers can be incorporated into mortars or concrete to augment their functionality. (Plank, 2004)

Biopolymers offer a potential alternative to conventional single-use plastics in a variety of industries. Although the material properties of pectin and chitosan are not ideal for durability, their ability to quickly decay in natural environments is ideal for short-term use products. (Rydz, Musioł, Zawidlak-Węgrzyńska, & Sikorska, 2018) The increasingly widespread adoption of these materials comes with a social shift towards environmentally responsible materials and technologies that value imperfection and temporality over permanence.

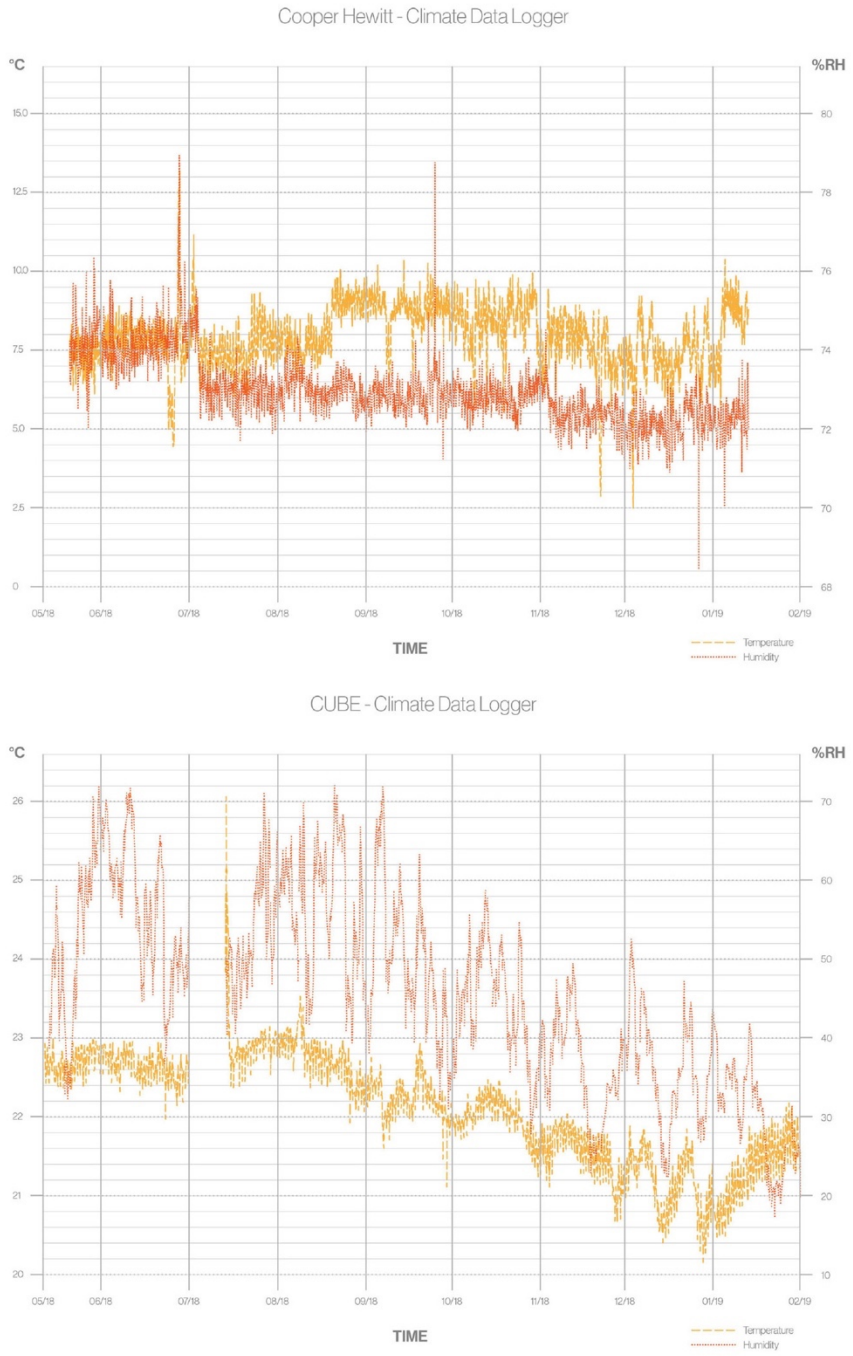

Figure 36: Diagrams illustrating changes in temperature and relative humidity from May 2019 – February 2020 responsible for color and shape change in the biopolymer prints located in (top) the CUBE Design museum and (bottom) Cooper Hewitt Design Museum.

7.2 Physical Exhibition

The biopolymer experiments have been displayed in museums such as the Cooper Hewitt and CUBE in 2019, the MoMA in 2020, and the upcoming SF MoMA show in 2021. The pieces have shown noticeable effects of aging and color change during the exhibitions due to the different environmental conditions in each venue. The pieces were publicly displayed from periods of three to nine months.

The + Crease prints shown in the CUBE museum in the Netherlands experienced dramatic visual changes that were noticeable to visitors during the nine months between the beginning of to the end of the exhibition in figure 36. The 3-dimensional forms gradually sagged and hardened because of the way they were hung and secured at points with pins against the vertical display board. The biopolymer prints in this series contained higher concentrations of chitosan that caused increased shape and color change.

The * Flat prints shown in the Cooper Hewitt in New York experienced far less dramatic visual changes than the + Crease prints during the same nine-month period. Not only were these pieces flat, but they were secured to the vertical display board with netting that evenly distributed forces that may otherwise have caused irregular deformation. The biopolymer prints in this series contained little or no chitosan that would have contributed to shape and color change.

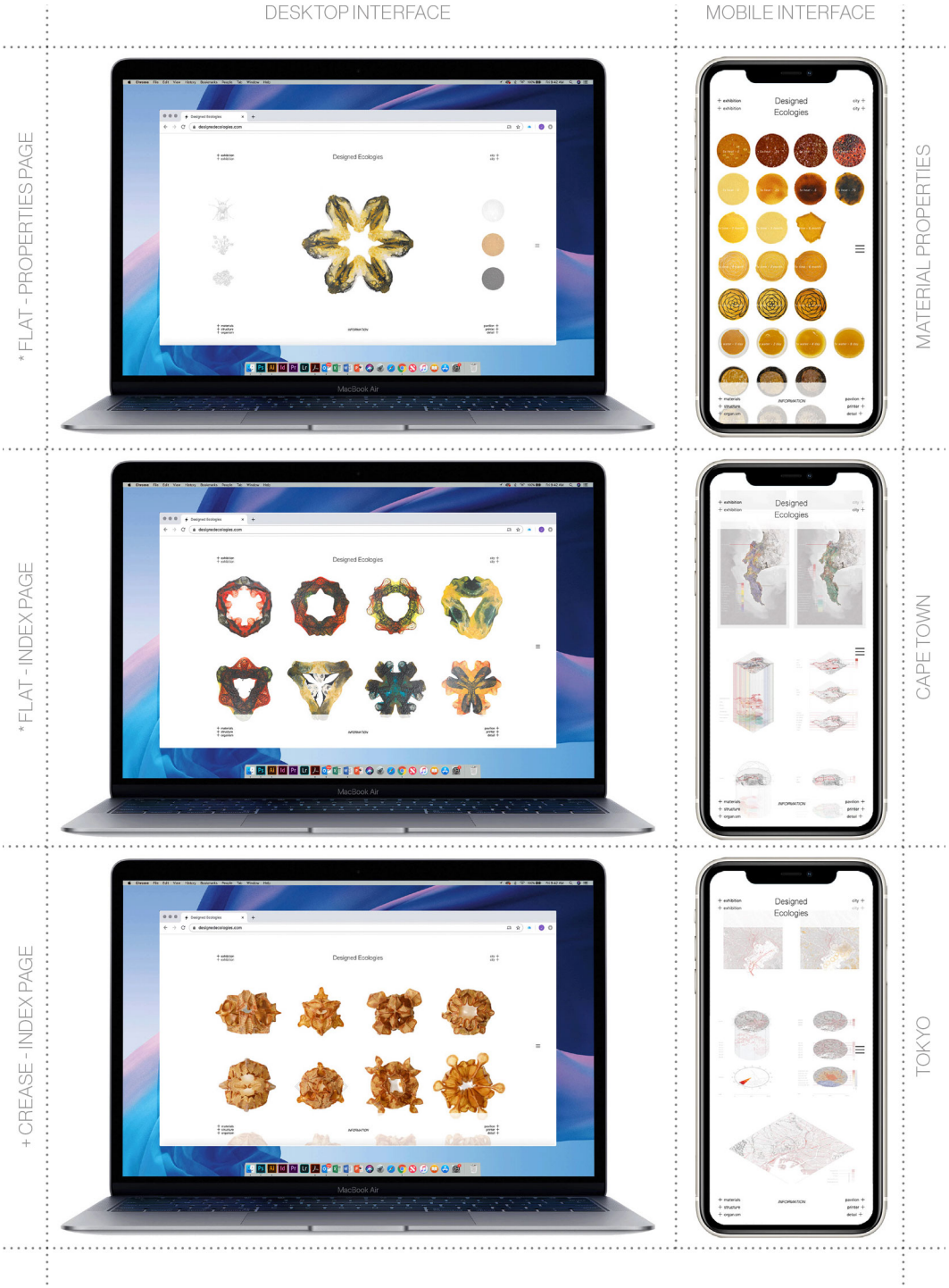

Figure 37: Website pages displayed on computer and mobile formats with homepage and case study pages with dynamic slideshow and scrolling interfaces to compare toolpaths and material deformation over time.

7.3 Digital Platform

Unlike this thesis document, which will be set static and unchanged in both pdf and print formats, the website is an ever changing medium of expression. The website at https://designedecologies.com/ in figure 37 is an ongoing project that will be continually added to, modified, and improved over time.

When attempting to describe inherently visual characteristics, text has its limitations. In addition, figures containing static images and diagrams are not well suited to showing the behavioral trends of these biopolymer materials. To accommodate these shortcomings, the website presents the material experiments in an easily accessible format. Animations and superimposed slideshow images allow for a more intuitive comparison that tracks the shape deformation and color change of all of the biopolymer experiments over time. Additionally, the design of the website allows visitors to navigate between images and data in a non-linear format for a more detailed understanding of the relationship between the design, materials, and fabrication of the biopolymer prints.

With new research and technology, biopolymers will find increasing relevance in different fields and with various applications. As the nature of communication online evolves, so will the way this project is understood. The presentation of the website will adapt over time with access to new information in much the same way these biopolymer materials react to changes in the environment.

Figure 38: Matrix of * Flat prints arrayed in a 7 x 10 grid with human for scale demonstrating diversity in form and color for tunability.

7.4 Preservation

The preservation of biodegradable materials that are intentionally designed to decay may seem counterproductive. In contrast, conservation is a priority for artwork in the context of a museum, and there are expectations of returning artwork in the same condition as it is received. Typically, perceived damages that result from natural weathering diminish an artwork's financial value. Thus, museum galleries maintain a steady temperature and humidity levels as well as limit exposure of artwork to direct sunlight. If the goal is to slow material changes and preserve the pieces as they appear after printing, the biopolymer experiments can be stored in between sheets of packing foam and wax paper in a dry, cold and dark with limited fluctuations in temperature and humidity.

However, the unique subjective beauty of these biopolymer experiments resides in their ability to degrade. The controlled museum environment deprives visitors from experiencing temporal changes in the artwork. The biopolymer pieces are perhaps better suited to be displayed in the natural environment in which they can freely react to unforeseen conditions. With this temporality in mind, we can shift the role of museums to expose audiences to meaningful experiences instead of the permanent artifacts traditionally in their collection. Museums can preserve the artistic experience while allowing the physical piece to behave outside of the interests of conservation by recording and documenting artwork that intentionally degrades over time. Continuing off of the legacy of movements in earth art, video art, and installation art, the acceptance of natural decay in artwork shifts the tangible value of art away from a tradable commodity that has verifiable ownership. An elevated aesthetic appreciation of the degradation of artwork in a museum can lead to a greater social acceptance for the imperfect and uncertain nature of objects in our daily lives.

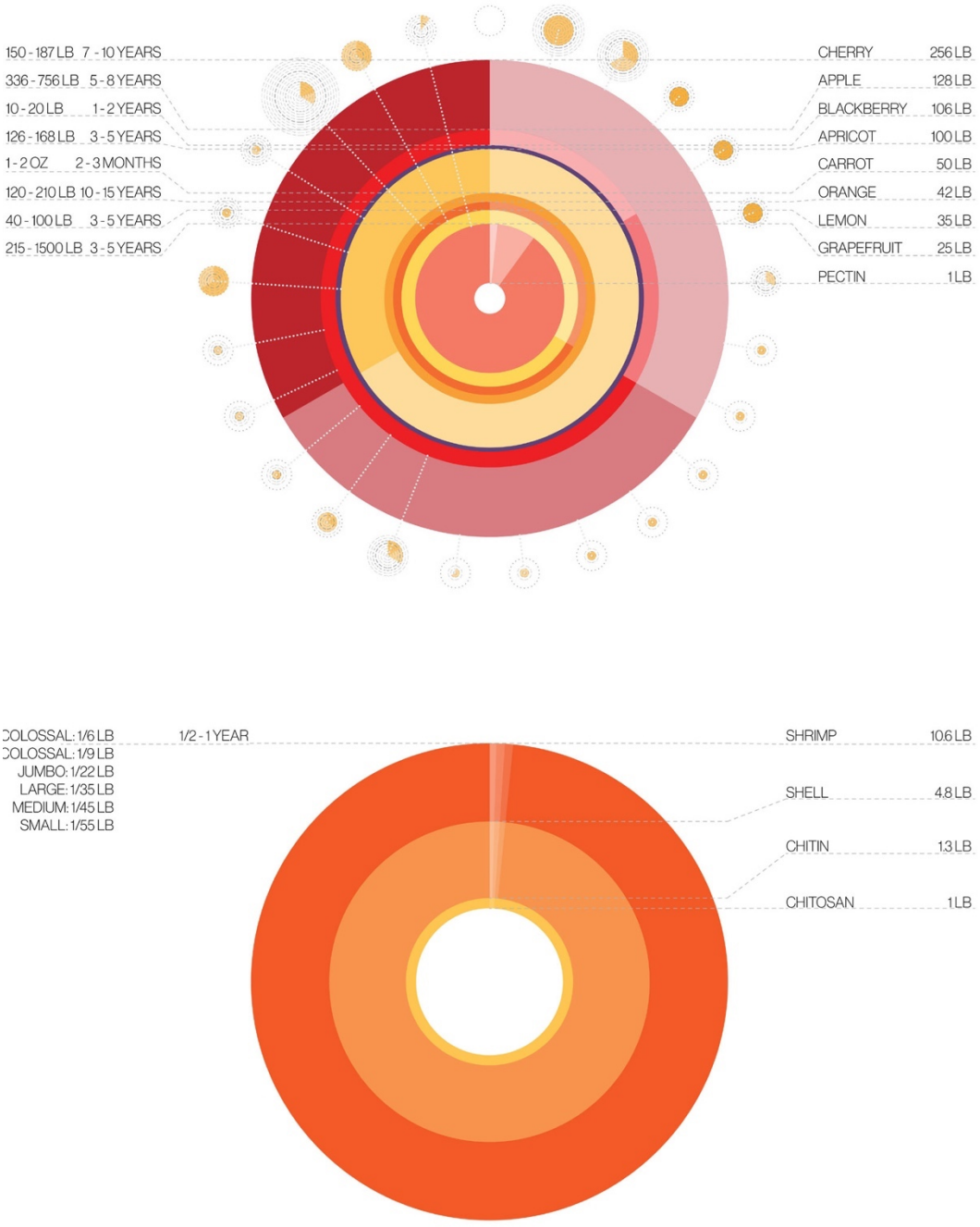

Figure 39: Diagrams illustrating the yield of pectin from various fruit trees *(Baker, 1997)* and chitosan from shrimp *(Islam, Khan, & Alam, 2017)* with the number of organisms and amount of time needed to naturally grow and refine 1 lb. of materials in an ecosystem.

7.5 Future Directions

Biopolymer additive manufacturing offers the possibility of site-specific bio-fabrication through the natural aggregation and sourcing of raw biological materials by creating microclimates to support the growth of specific plants and insects.

7.5.1 Material Sourcing

The need to control our environment is familiar to most people, yet by nature, the other living organisms that we share our spaces with are problematic to predict. Cultural standards of cleanliness and the desire to isolate our living quarters from the perceived uninhibited chaos of the external environment have contributed to this approach of sanitizing our living environments. While most contemporary buildings attempt to create habitats exclusively for humans that are hostile to the existence of these other organisms, foreign matter will inevitably infiltrate our personal spaces. With this in mind, architects and designers must consider how to make products, spaces, and structures that can better coexist with and host other organisms in order to produce mutually beneficial outcomes.

By encouraging architectural and ecological symbiosis at various scales, a design process and fabrication system can be customized to fit a variety of sites and deployed on an agricultural scale to farm the raw materials used in the construction of buildings while remaining sensitive to local flora and fauna. Theoretical precedents such as Laugier's primitive hut provide the conceptual basis for establishing a symbiotic relationship to ecologies throughout the entire lifespan of a building to create a self-sufficient hybrid structure capable of sustaining a diverse ecosystem while producing resources for construction and maintenance.

In determining the types of inputs which can cause minute changes to functionalize the behavior of multiple species of organisms, plants and animals can be exposed to designed structures that can encourage organisms to aggregate materials into specialized forms within their natural habitat.

7.5.2 Organism Communication

Current experiments in bio-fabrication occur inside the highly controlled enclosure of a research lab and museum gallery that isolate species in simulated scenarios. There has been less exploration to deploy bio-fabrication with species in an unmediated natural environment. Such an approach would expand the traditional awareness of an architectural site as a complex ecosystem rather than a reductive series of spatial parameters.

By combining the customization and precision of robotic fabrication with environmentally responsive materials, these tools and design processes have the potential to establish initial design parameters and experimental protocols for constructing non-anthropocentric objects. Using the materials, machines, and workflows developed for biopolymer printing, architects, engineers, and scientists have the tools to create structures that can communicate with and modify the behavior of organisms across ecological niches. With these tools, we can encourage organisms to independently aggregate materials and utilize these materials in building site-specific structures that encourage environmental wellbeing.

7.5.3 Ecological Integration

The dynamic set of interactions and relationships between various organisms and environments over time is challenging to comprehend and express. A prerequisite

for designing for such a complex network of interdependent variables requires the definition of a vocabulary and series of parameters that can be used to quantify and express the relationships between different aspects of a single ecology. Further investigation of species-specific pest and pollinator syndromes can generate structures made from biopolymers that can sensitively affect various ecologies. These habitats could be used to promote the environmental health and ecological integration of architectural structures by attracting pollinators, repelling predators, and providing nutrients for plant growth. By diagraming the causal chains and dependencies of multiple actors that share a given site, it is possible to bring about dramatic changes through minute yet targeted interventions. While making ecological modifications that produce unintended consequences may be easy, having control and predictability over the process can be extremely difficult.

Rather than establishing productive landscapes that take the form of large-scale conventional monocultures, architects can design structures that will create differentiated microclimates that encourage plant and animal biodiversity that can result in improved environmental health. By taking an active role in assisting the vegetative dynamics of sites, this project will create an augmented ecosystem based on principles shared with regenerative agriculture and synecoculture. These ideas can be taken a step further to create a method of open-field agriculture that uses organisms to aggregate natural resources and materials into self-assembled built forms without requiring artificial interventions in the form of plowing, fertilizers, or chemicals. These environmental structures could consolidate a large variety of plant and insect species that can coexist in their natural state and support each other's needs while contributing to the overall functionality of the soil. The process of decay can create beneficial outcomes in the environment by releasing a cocktail of beneficial nutrients, bacteria, and seeds to encourage plant growth that can support environmental wellbeing.

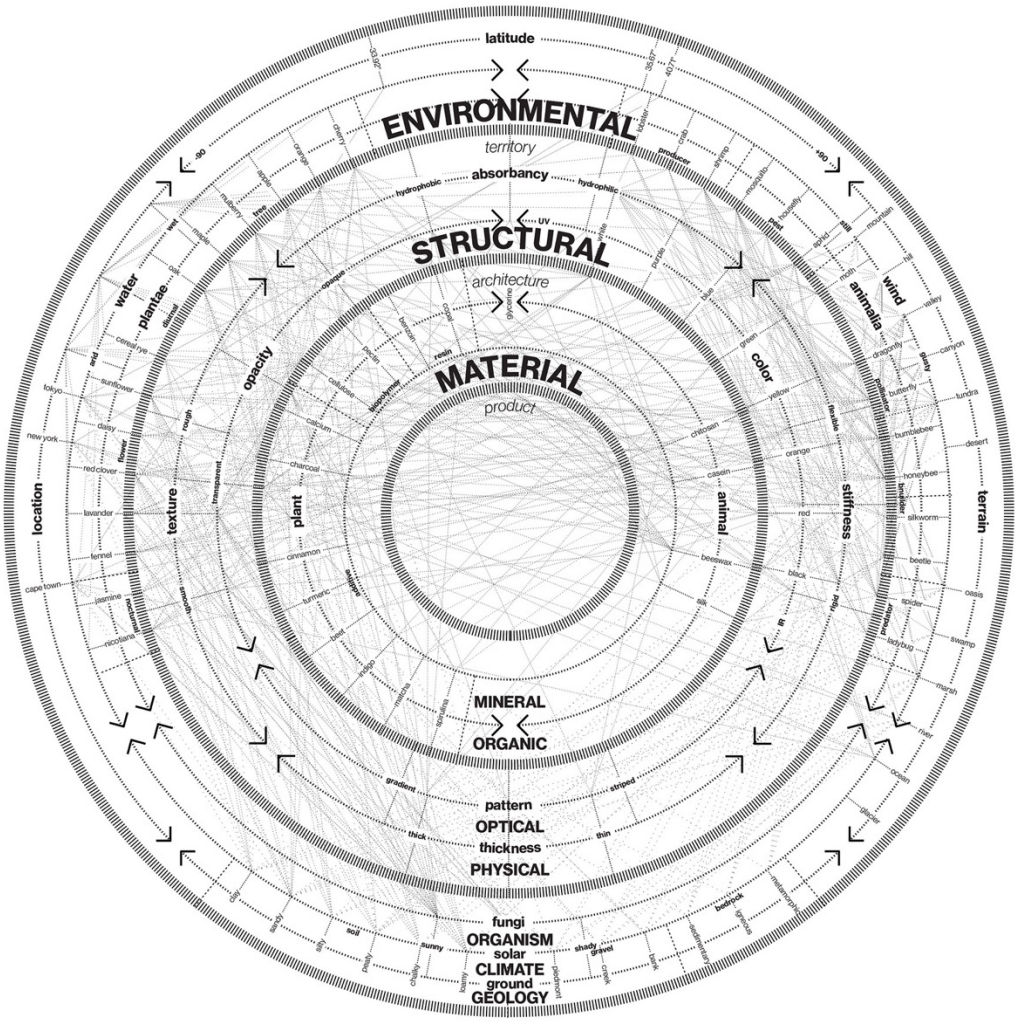

Figure 40: A scalar network diagram showing the complex web of relationships between materials, structures and environments within a select grouping of pollinating insects and geographical sites.

7.5.4 Scalar Networks

Territorial: *Environmental*
- Geology:
  - Location: *New York City, Tokyo, Cape Town*
  - Terrain: *Mountain, Hill, Valley, Canyon, Tundra, Desert, Oasis, Swamp, Marsh, River, Ocean, Glacier*
  - Ground:
    + Bedrock: *Metamorphic, Igneous, Sedimentary*
    + Gravel: *Bank, Creek, Piedmont*
    + Soil: *Loamy, Chalky, Peaty, Silty, Sandy, Clay*
- Climate:
  - Solar: *Sun - Shade*
  - Water: *Arid - Moist*
  - Wind: *Still - Gusty*
- Organism:
  - Plantae: (case studies)
    + Flower: *Nicotiana, Jasmine, Fennel, Lavender, Clover, Daisy, Rye*
    + Tree: *Oak, Maple, Mulberry, Apple, Orange, Cherry*
  - Animalia: (case studies)
    + Producer: *Lobster, Crab, Shrimp*
    + Pest: *Mosquito, Housefly, Aphid*
    + Pollinator: *Moth, Dragonfly, Butterfly, Bumblebee, Honeybee*
    + Builder: *Silkworm. Beetle*
    + Predator: *Spider, Ladybug, Finch, Blue Jay*

Structural: *Architectural*
- Physical:
  - Thickness: *Thick - Thin*
  - Stiffness: *Flexible - Rigid*
  - Texture: *Smooth - Rough*
  - Absorbency: *Hydrophobic - Hydrophilic*
- Optical:
  - Color: *White, Black, Purple, Blue, Green, Yellow, Orange, Red*
  - Opacity: *Transparent - Opaque*
  - Pattern: *Gradient - Striped*

Product: *Material*
- Organic:
  - Biopolymer: *Pectin, Cellulose, Calcium, Charcoal*
  - Additive: *Cinnamon, Turmeric, Beet, Indigo, Matcha, Spirulina*
  - Resin: *Copal, Benzoin*
- Mineral: *Laterite, Basalt*

With a culture that promotes the value of unpredictability in problem-solving process, designers can more readily accept inconsistency and failure as an opportunity to learn and innovate. New research and technology have allowed biopolymers to find increasing relevance in different fields and with various applications. As the nature of communication online evolves, so will the way this project is understood. By promoting a culture that accepts and values intentional inconsistencies, we can design with, by, and for uncertainty to create value out of the unknown in broad applications across multiple scales.

8 WORKS CITED

Amato, I. (1998). *Stuff: Materials World.* Harper Collins.

Antique Telephones Ring a Bell with Collectors. (2018, August 30). Retrieved from Live Auctioneers: https://www.liveauctioneers.com/news/be-smart/antique-and-vintage-telephones-ring-a-bell-with-collectors/

Ashby, M. F., Gibson, L. J., Wegst, U., & Olive, a. R. (1995). The Mechanical Properties of Natural Materials. I. Material Property charts. *Proceedings of the Royal Society A: Mathematical, Physical and Engineering Sciences, 450*(1938), 123-140.

Baker, R. A. (1997). Reassessment of Some Fruit and Vegetable Pectin Levels. *Journal of Food Science, 62*(2), 225-229.

Bechthold, M., & Weaver, J. (2017). Material Science and Architecture. *Nature Reviews Materials, 2.*

Belgacem, M. N., & Gandini, A. (2008). *Monomers, Polymers and Composites from Renewable Resources.* (M. N. Belgacem, & A. Gandini, Eds.) Elsevier.

Bensaude-Vincent, B. (2001). Construction of a Discipline: Material Science in the United States. *Historical Studies in the Physical and Biological Sciences, 31*(2), 223-248.

Bray, W., & Upcott, W. (1872). Diary and Correspondence of John Evelyn. London: Bell & Daldy.

Chapman, J. (2014). Meaningful Stuff: Toward Longer Lasting Products. *Materials Experience: Fundamentals of Materials and Design*, 135-143.

Cogner, A. (2007). *A Comparative Analysis of Sugar Concentrations in Various Maple Species on the St. John Campus.*

Crawford, D. L. (1980). *Meat Yield and Shell Removal Functions of Shrimp Processing.* Oregon State Univeristy: Marine Advisory Program.

Crini, G., & Lichtfouse, E. (2019). *Sustainable Agriculture Reviews 35: Chitin and Chitosan: History, Fundamentals and Innovations.* (G. Crini, & E. Lichtfouse, Eds.) Springer.

DeNardis, D., Rosales-Yeomansa, D., Boruckib, L., & Philipossianab, A. (2010, May). Studying the effect of temperature on the copper oxidation process using hydrogen peroxide for use in multi-step chemical mechanical planarization models. *Thin Solid Films, 518*(14), 3903-3909.

DeSilvey, C. (2006). Observed Decay: Telling Stories with Mutable Things. *Journal of Material Culture, 11*(3), 318-338.

Donin, L. (1875). Die Nachfolge Christi. Vienna.

Doordan, D. P. (2003). On Materials. *Design Issues, 19*, 3-8.

Duro-Royo, J. (2015). *Towards Fabrication Information Modeling (FIM): Workflow and Methods for Multi-scale Trans-disciplinary Informed Design.* Cambridge: Massachusetts Institute of Technology.

Duro-Royo, J., & Oxman, N. (2015). Towards Fabrication Information Modeling (FIM): Four Case Study Models to Derive Designs informed by Multi-Scale Trans-Disciplinary Data. *Materials Research Society*.

Duro-Royo, J., Van Zak, J., Ling, A., Tai, Y.-J., Hogan, N., Darweesh, B., & Oxman, N. (2018). Designing a Tree: Fabrication Informed Digital Design and Fabrication of Hierarchical Structures. *Proceedings of the IASS Annual Symposium.*

E. Overvlieta, K., & Soto-Faracobc, S. (2011, January). I can't believe this isn't wood! An investigation in the perception of naturalness. *Acta Psychologica, 136*(1), 95-111.

Evans, E., Mader, E., & Marla, S. (2010). *Managing Alternative Pollinators: A Handbook for Beekeepers, Growers and Conservationalists.* College Park: Sustainable Agriculture Research and Education.

Fuchs, C., Schreier, M., Stijn, M., & Osselaer, V. (2015, March 1). The Handmade Effect: What's Love Got to Do with It? *Journal of Marketing, 79*(2), 98-110.

Hopewell, J., Dvorak, R., & Kosior, E. (2009, July 27). Plastics Recycling: Challenges and Opportunities. *Philosophical Transactions of the Royal Society B, 364*(1526), 2115-2126.

Hounshell, D. A., & Smith, J. K. (2006). *Science and Corporate Strategy: Du Pont R and D. 1902-1980.* Cambridge, UK: Cambridge University Press.

(1999). *Innovations in Glass.* Corning, NY: The Corning Museum of Glass.

Islam, S., Khan, M., & Alam, N. (2017, May 29). Production of chitin and chitosan from shrimp shell wastes. *Journal of the Bangladesh Agricultural University, 14*, 253.

John, J. S. (2017). Vermont White Marble. Wikimedia - Creative Commons.

Jones, C. A. (2006). *Sensorium: Embodied Experience, Technology and Contemporary Art.* Cambridge: MIT Press.

Köhler, K. (1929). *Gestalt Psycology.* New York: Liveright.

Kōetsu, H. (1600's). Cclay, pitted, covered with glaze having patches; vertical incisions near lip, under glaze (Raku ware). Wikimedia - Creative Commons.

Kanigel, R. (2007). *Faux Real: Genuine Leather and 200 Years of INspired Fakes.* Philadelphia: University of Pennsylvania Press.

Karana, E. (2012). Characterization of 'natural' and 'high quality' materials to improve perception of bio-plastics. *Journal of CLeaner Production, 37*(1), 316-325.

Keating, S. J. (2016). *From Bacteria to Buildings: Additive Manufacturing Outside the Box.* Cambridge: Massachusetts Institute of Technology.

Kerrod, R. (1986). *Structures and Materials.* New York, NY: Silver Burdett.

Koffka, K. (1935). *Principles of Hestalt Psychology.* New York: Harcourt, Brace.

Kolarevic, B., & Klinger, K. (2008). *Manufacturing Material Effects: Rethinking Design and Making in Architecture.* Oxford, UK: Routledge.

Koren, L. (1994). *Wabi-Sabi for Artists, Designers, Poets and Philosophers*. Berkeley, CA: Stone Bridge Press.

Kruger, J., Wirtz, D., Boven, L. V., & Altermattc, T. W. (2004, January). The Effort Heuristic. *Journal of Experimental Social Psychology, 40*(1), 91-98.

Laugier, M.-A. (1755). *An Essay on Architecture*. London: Osborne and Shipton.

Lee, N. A., Weber, R. E., Kennedy, J. H., Zak, J. V., Duro-Royo, J., & Oxman, N. (2019). Multi-Material Printing of Multi Lengthscale Bio-composite Membranes. *Proceedings of the IASS Annual Symposium*.

Lilley, D., Smalley, G., Bridgens, B., Wilson, G. T., & Balasundaram, K. (2016, July 5). Cosmetic obsolescence? User perceptions of new and artificially aged materials. *Materials & Design, 101*, 355-365.

Ling, A. (2018). *Design by Decay, Decay by Design*. Cambridge, MA: Massachusetts Institute of Technology.

Ludwig, K. J. (1869). The snakes of Australia an illustrated catalogue.

May, C. D. (1990). Industrial Pectins: Sources, Production and Applications. *Carbohydrate Polymers, 12*, 79-99.

Mogas-Soldevila, L. (2015). *Water-based Digital Design and Fabrication: Material, Product. and Architectural Explorations in Printing Chitosan and its Composites*. Cambridge: Massachusetts Institute of Technology.

Mogas-Soldevila, L., Duro-Royo, J., & Oxman, N. (2015). Form Follows Flow: A Material-driven Computational Workflow for Digital Fabrication of Large-Scale Hierarchically Structured Objects. *Acadia - Computational Ecologies: Design in the Anthropocene*.

Morse, E., Dantan, J.-Y., Anwer, N., Söderberg, R., Moroni, G., Qureshif, A., . . . Mathieu, L. (2018). Tolerancing: Managing uncertainty from conceptual design to final product. *CIRP Annals, 67*(2), 695-717.

Norwich, J. (2001). *Great Architecture of the World*. Boston, MA: Da Capo Press.

Ofori, G. (2000). Greening the Construction Supply Chain in Singapore. *European Journal of Purchasing & Supply Management, 6*(3-4), 195-206.

Palmer, S. E. (1999). *Vision Science: Photons to Phenomenology.* Cambridge MA: MIT Press.

Parisi, S., Rognoli, V., & Garcia, C. A. (2016, September). Designing materials experiences through passing of time: Material driven design method applied to mycelium-based composites. *Celebration & Contemplation, 10th International COnference on Design & Emotion.*

Pedgley, O., Şener, B., Lilley, D., & Bridgens, B. (2018). Embracing Material Surface Imperfections in Product Design. *International Journal of Design, 12*(3).

Peniche, C., Argüell, W. M., & Goycoolea, F. M. (2008). Chitin and Chitosan: Major Sources, Properties and Applications. In *Monomers, Polymers and Composites from Renewable Resources* (pp. 517-542). Elsevier.

Pinto, J. A. (2012). *Speaking Ruins: Piranesi, Architects and Antiquity in Eighteenth-Century Rome.* Ann Arbor: University of Michigan Press.

Piolle, G. (2008, July 20). Western facade of the Parthenon during its restoration, Acropolis of Athens, Greece. Wikimedia - Creative Commons.

Piranesi, G. B. (1825-1839). Le Antichità Romane. In *Opere di Giovanni Battista Piranesi, Francesco Piranesi e d'altri.* (Vol. 2). Paris: FIrmin Didot Freres.

Pitelka, M. (2005). *Handmade Culture: Raku Potters, Patrons, And Tea Practitioners In Japan.* Honolulu, USA: University of Hawai'i Press.

Plank, J. (2004, October 1). Applications of Biopolymers and other Biotechnological Products in Building Materials. *Applied Microbiology & Biotechnology, 66*(1), 1-9.

Pollio, M. V. (1960). *The Ten Books on Architecture.* (M. H. Morgan, Ed.) New York, NY: Dover.

Pye, D. (1968). *The Nature of Art and Workmanship.* London, UK: A&C Black.

Rhodes, D. (1957). *Clay and Glazes for the Potter.* New York, NY, USA: Greenberg.

Rognoli, V., & Karana, E. (2014). Toward a New Materials Aesthetic Based on Imperfection and Graceful Aging. In E. Karana, O. Pedgley, & V. Rognoli, *Materials Experience* (pp. 145-154). Oxford, UK: Butterworth-Heinemann.

Roosth, C. (2017). *Synthetic: How Life Got Made.* Chicago, IL: University of Chicago Press.

Rosenberg, J., & Oxman, N. (2010, October). Material-based Design Computation: An Inquiry into Digital Simulation of Physical Material Properties as Design Generators. *International Journal of Architectural Computing, 5*(1), 25-44.

Ruel, K., & Barnoud, F. (1985). Degredation of Wood by Microorganisms. In T. Higuchi, *Biosynthesis and Biodegradation of Wood Components.* London, UK: Academic Press.

Rydz, J., Musioł, M., Zawidlak-Węgrzyńska, B., & Sikorska, W. (2018). Present and Future of Biodegradable Polymers for Food Packaging Applications. In A. M. Grumezescu, & A. M. Holban, *Biopolymers for Food Design* (Vol. 20). Elsevier.

Salvia, G., Ostuzzi, F., Rognoli, V., & Levi, M. (2011, October). The value of imperfection insustainable design: the emotional tie with perfectible artefacts for longer lifespan. *(2011) Sustainability in Design : Now! Challenges and Opportunities fo Design Research, Education and Practice in the XXI Century.*

Sanz, V., Reig, Y., Feliu, C., Bautista, Y., Ribes, C., & Edwards-Schachter, M. (2012, September). Technical Evolution of Ceramic Tile Printing. *Journal of Imaging Science and Technology, 56*(5), 401-407.

Seeley, T. D. (2010). *Honeybee Democracy.* Princeton: Princeton University Press.

Tai, Y.-J. (2018). *Towards Material-informed Techtonics.* Cambridge, MA: Massachusetts Institute of Technology.

Tai, Y.-J., Bader, C., Ling, A., Disset, J., Darweesh, B., Duro-Royo, J., . . . Oxman, N. (2018). Design (for) Decay: Parametric Material Distribution for Hierarchical

Dissociation of Water-based Biopolymer COmposites. *Proceedings of the IASS ANnual Symposium*.

Van Gelder, H., & Westgeest, H. (2011). *Photography Theory in Historical Perspective*. Oxford, UK: Wiley-Blackwell.

Van Zak, J., Duro-Royo, J., Tai, Y.-J., Ling, A., Bader, C., & Oxman, N. (2018). Parametric Chemistry: Reverse Engineering Biomaterial Composites for Robotic Manufacturing of Bio-Cement Structures across Scales. *Challenges for Technology Innovation, 217*(223), 217-223.

Walker, S., Evans, M., & Mullagh, L. (2019). Meaningful practices: The contemporary relevance of traditional making for sustainable material futures. *Craft Research, 10*(2), 183-210.

Wang, J.-P., & Cho, W. D. (2009). Oxidation Behavior of Pure Copper in Oxygen and/or Water Vapor at Intermediate Temperature. *ISIJ International, 49*(12), 1926-1931.

Webster, C., Onokpise, O., Abazinge, M., Muchovej, J., Johnson, E., & Louime, C. (2014). Turning waste into usable products: a case Study of extracting chitosan from blue crab. *American Journal of Environmental Sciences, 10*(4), 357-362.

Westphal-Fitch, G., & al., e. (2012). Production and perception rules underlying visual patterns: effects of symmetry and hierarchy. *Philosophical Transactions of the Royal Society B: Biological Sciences*, 2007-2022.

Woolnough, C. W. (1881). *The Whole Art of Marbling as Applied to Paper, Book Edges, etc.* London, UK: George Bell and Sons.

9 APPENDIX

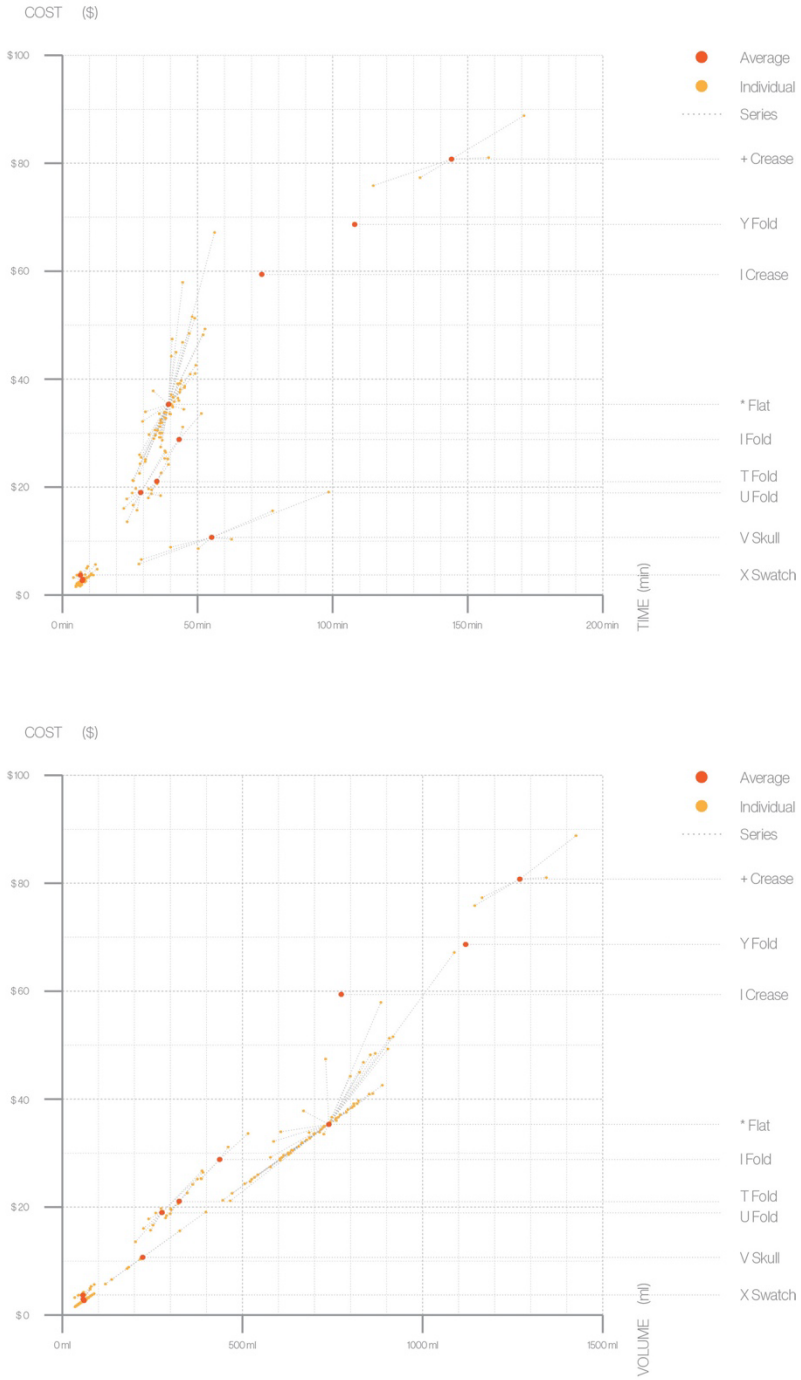

Figure 41: Charts showing relative distribution of material amount, cost and printing time for 9 case studies

9.1 Material Properties

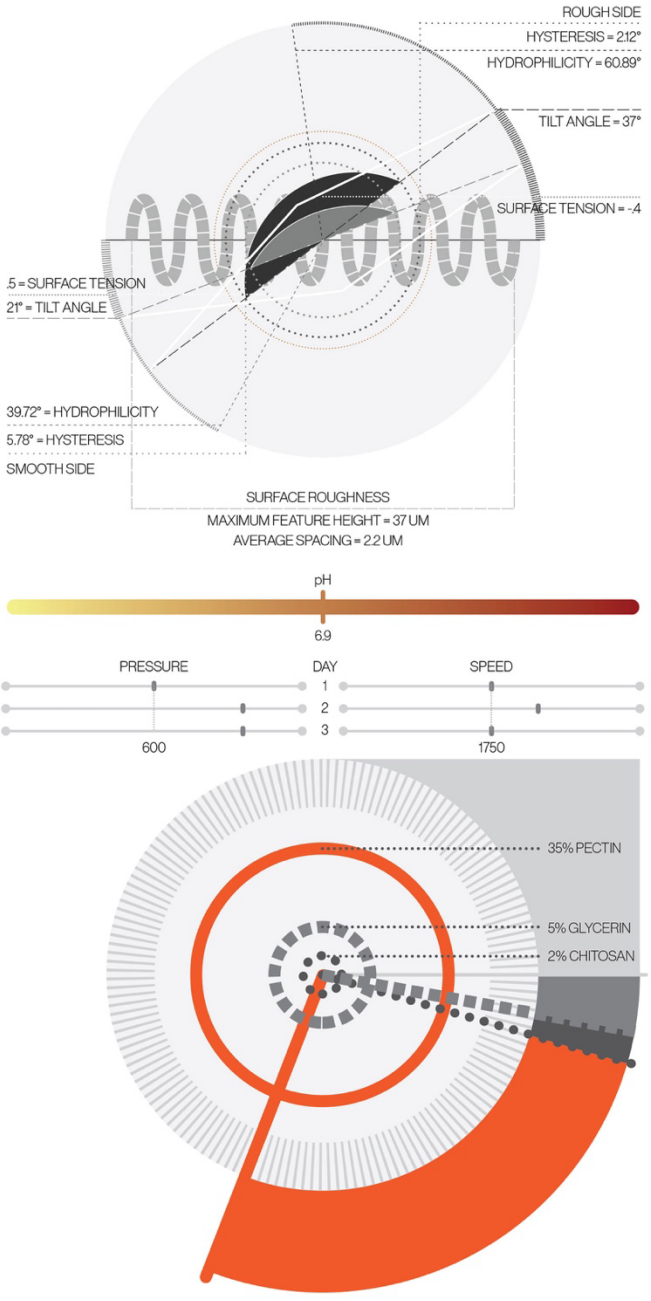

Figure 42: Pectin formula #1 - material property diagram showing composition, pH, hydrophilicity, hysteresis, surface tension, surface roughness and printing parameters in a single integrated graphic.

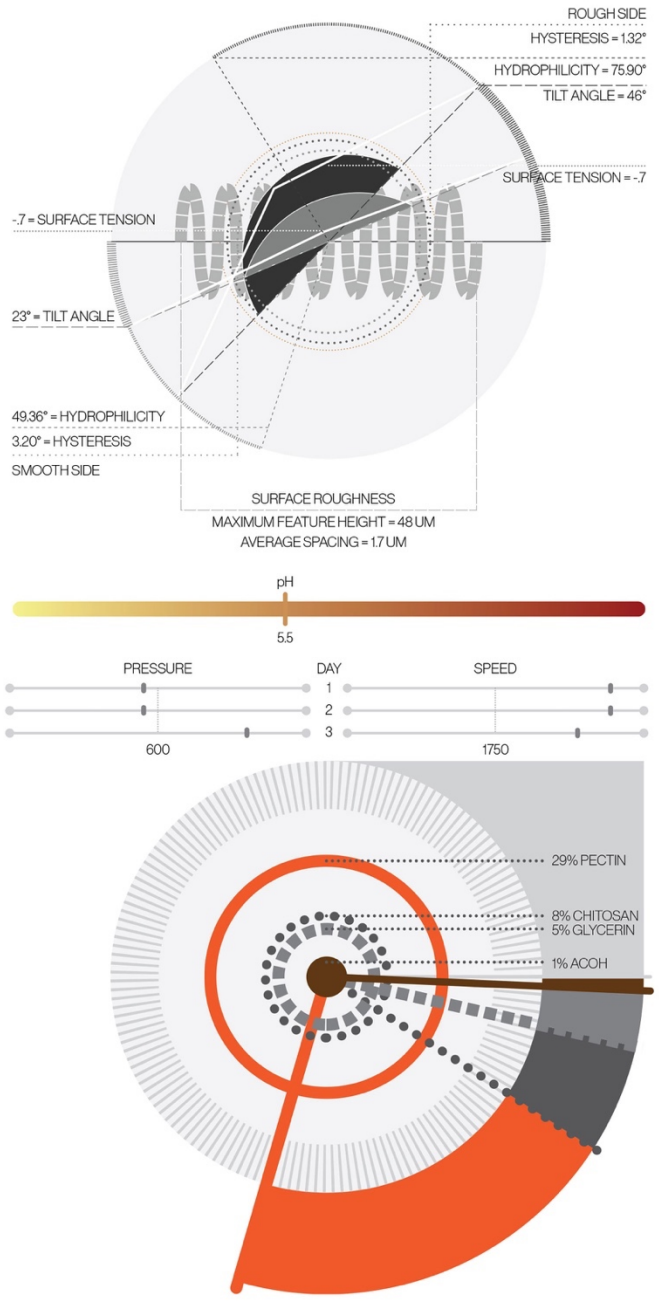

Figure 43: Pectin formula #3 - material property diagram showing composition, pH, hydrophilicity, hysteresis, surface tension, surface roughness and printing parameters in a single integrated graphic.

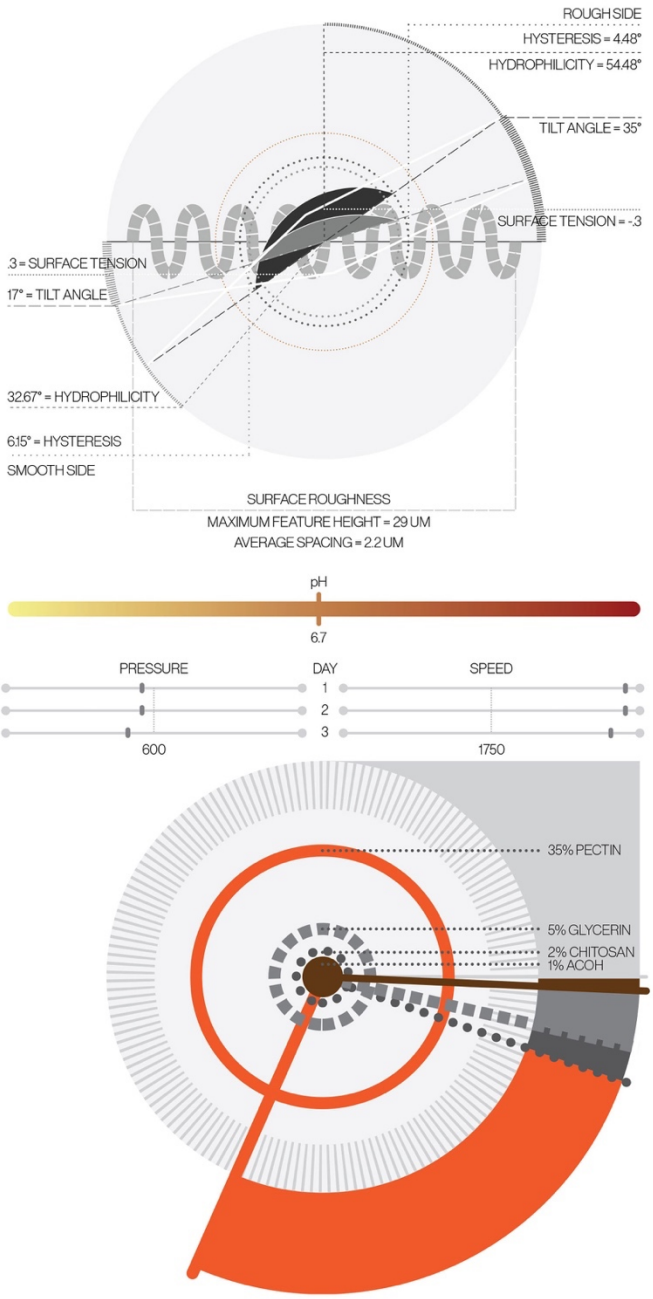

Figure 44: Pectin formula #4 - material property diagram showing composition, pH, hydrophilicity, hysteresis, surface tension, surface roughness and printing parameters in a single integrated graphic.

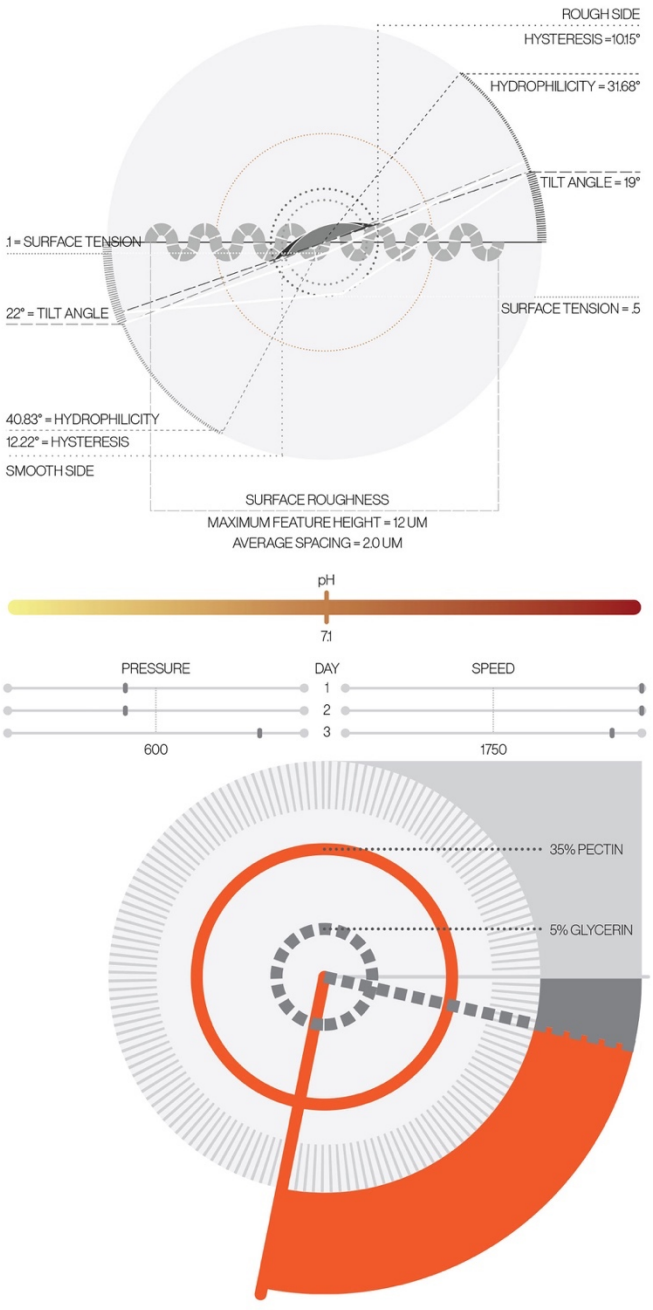

Figure 45: Pectin formula #5 - material property diagram showing composition, pH, hydrophilicity, hysteresis, surface tension, surface roughness and printing parameters in a single integrated graphic.

9.2 Material Sourcing

Figure 46: Diagrams illustrating the yield of chitosan from lobster and crab *(Webster, et al., 2014)* with the number of organisms and amount of time needed to naturally grow and refine 1 lb. of material in an ecosystem.

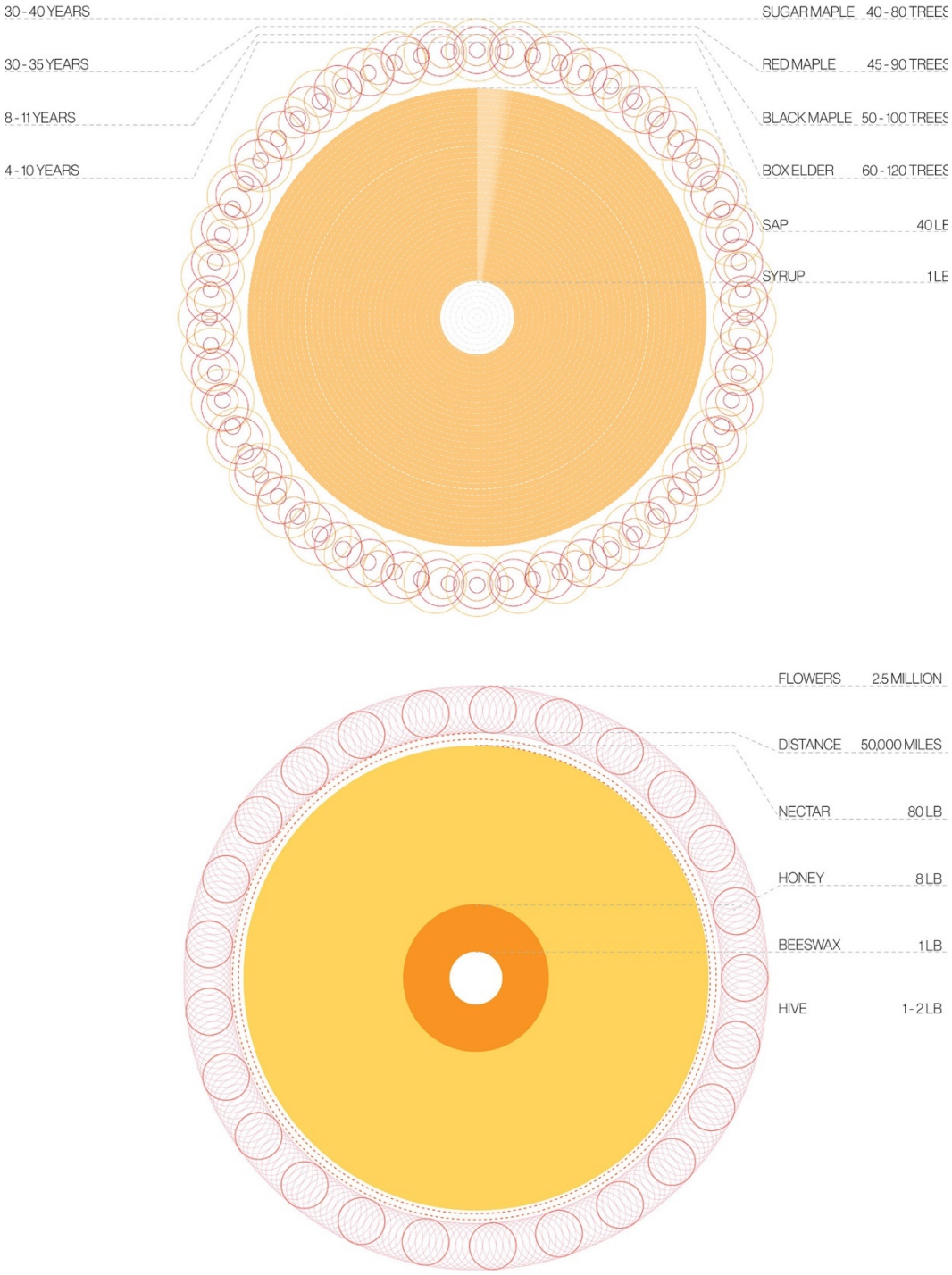

Figure 47: Diagrams illustrating the yield of honey from bee hives and tree sap from trees *(Cogner, 2007)* with the number of organisms and amount of time needed to naturally grow and refine 1 lb. of materials in an ecosystem.

9.3 Case Studies

9.3.1 O Swatch

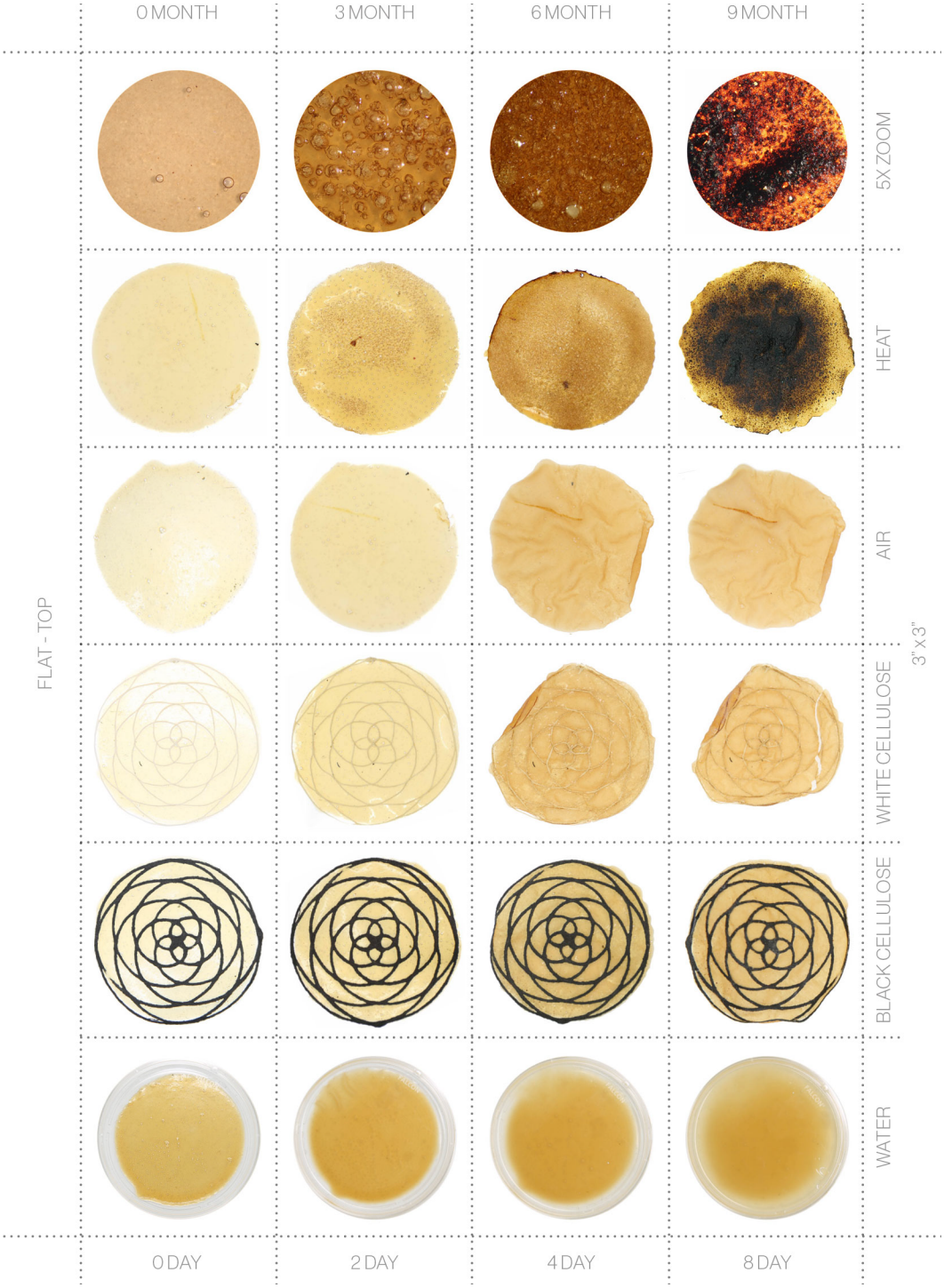

Figure 48: Matrix of O Swatch - Standard pectin formula comparing color change and deformation in response to exposure to heat, air and moisture over time.

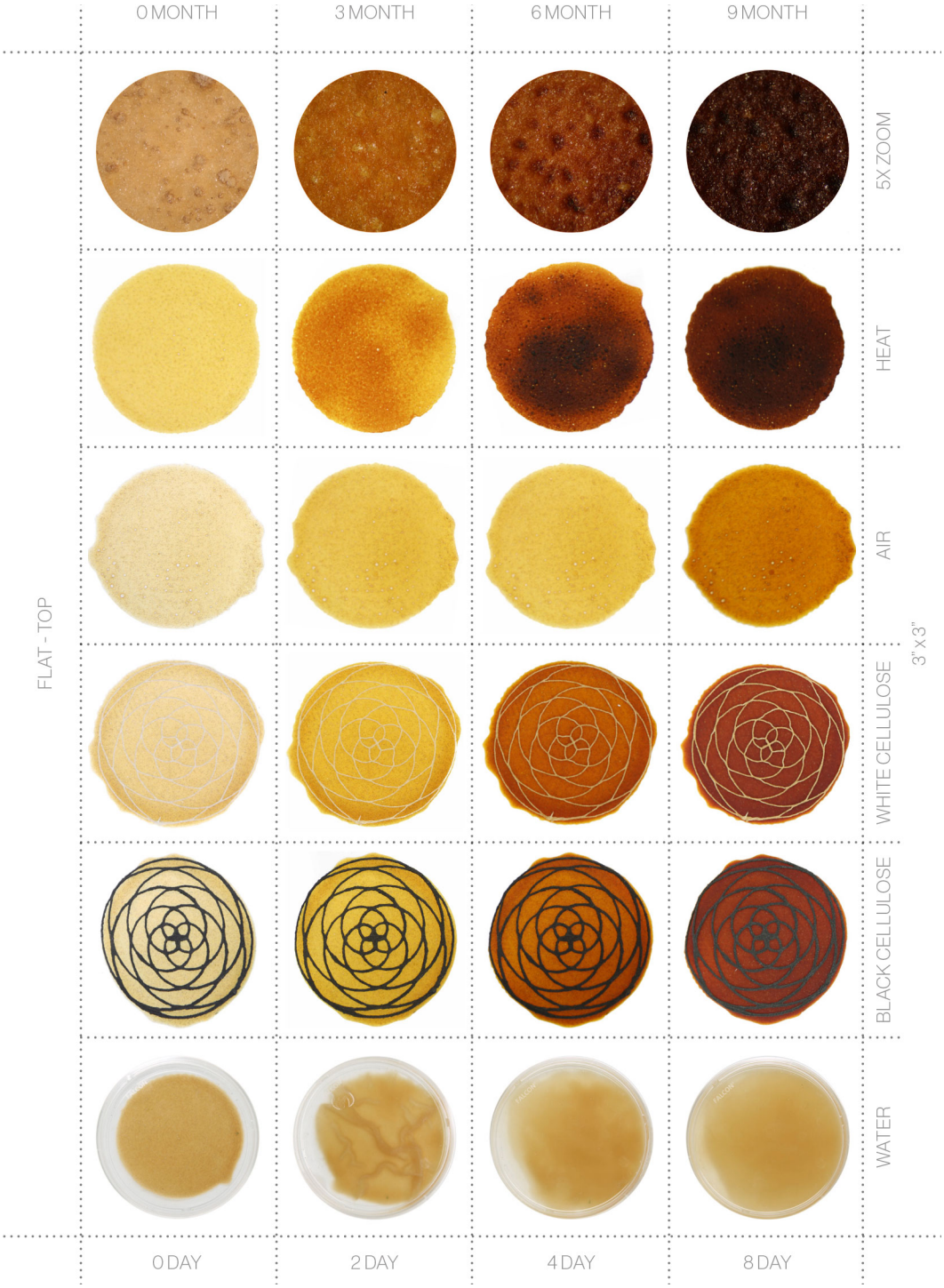

Figure 49: Matrix of O Swatch - Chitosan pectin formula comparing color change and deformation in response to exposure to heat, air and moisture over time.

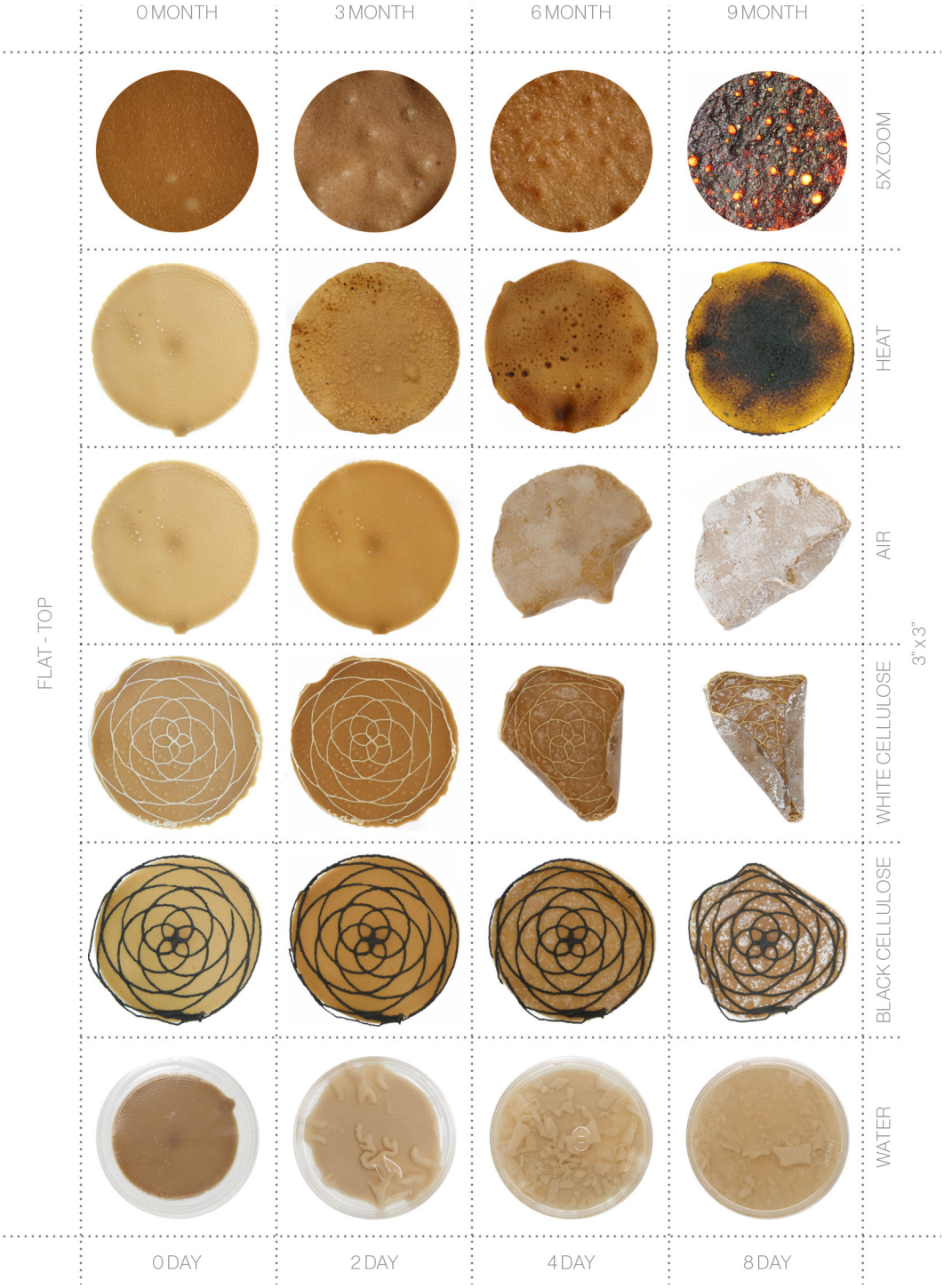

Figure 50: Matrix of O Swatch - Calcium pectin formula comparing color change and deformation in response to exposure to heat, air and moisture over time.

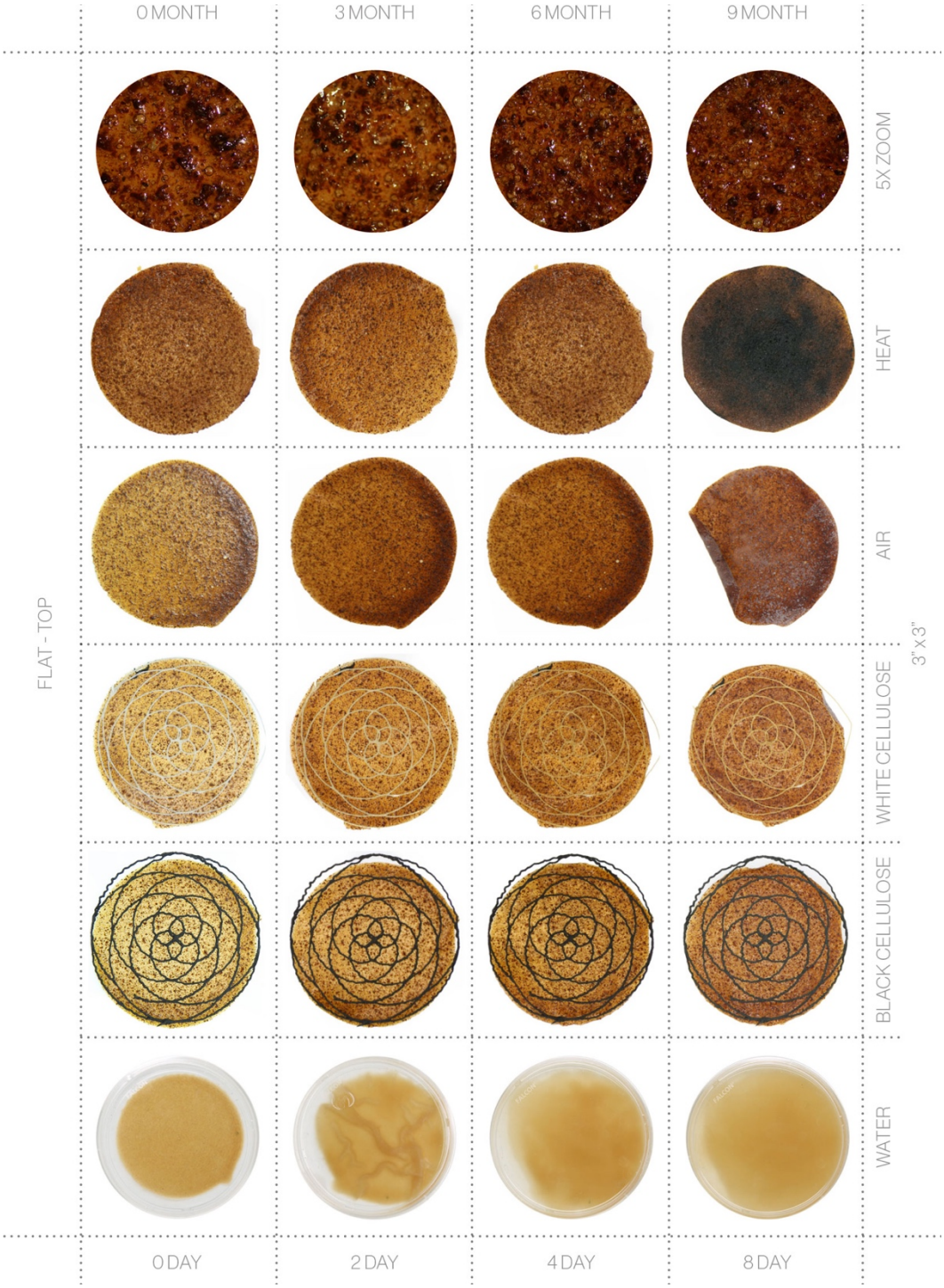

Figure 51: Matrix of O Swatch - Cinnamon pectin formula comparing color change and deformation in response to exposure to heat, air and moisture over time.

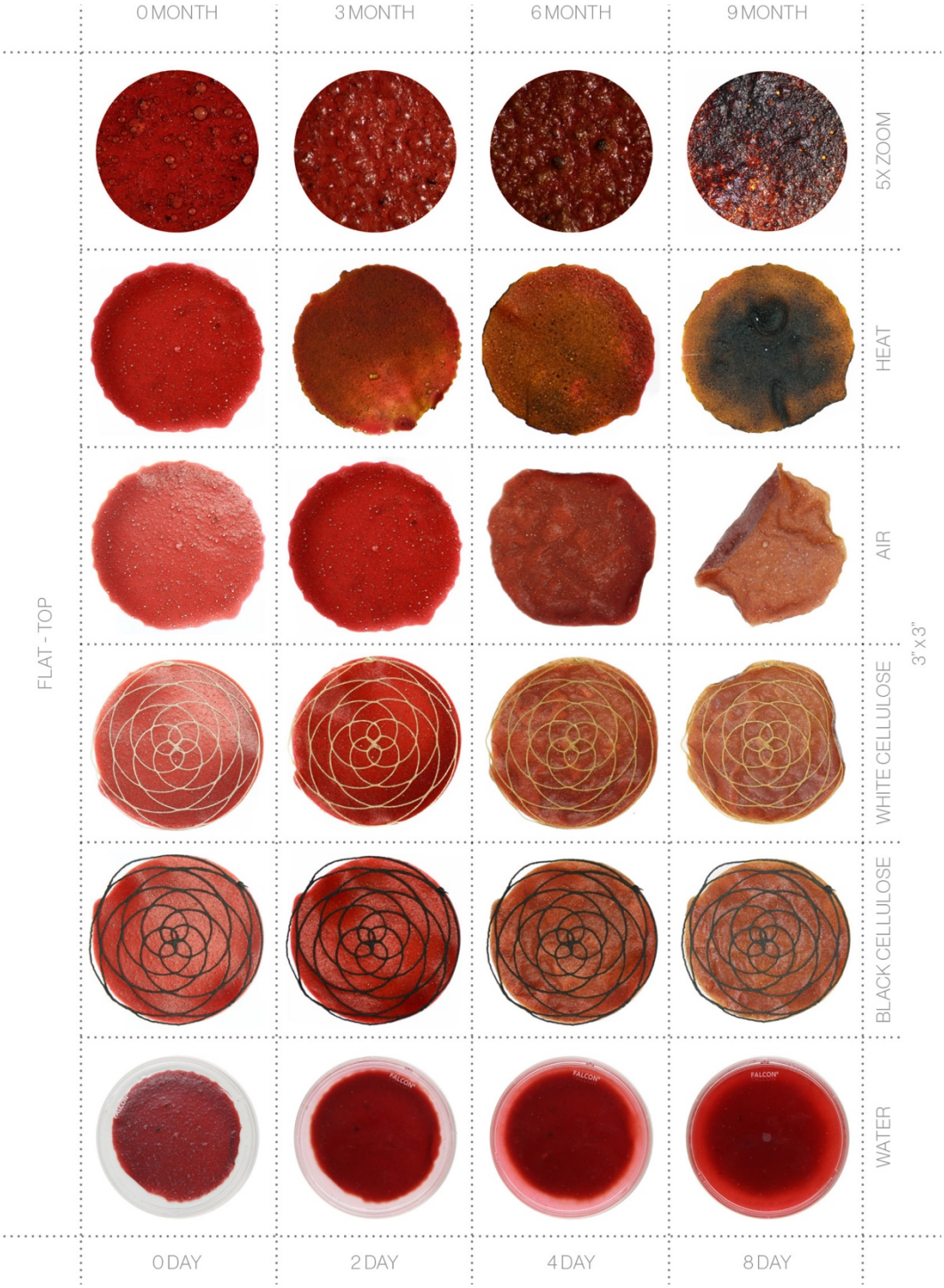

Figure 52: Matrix of O Swatch - Beet pectin formula comparing color change and deformation in response to exposure to heat, air and moisture over time.

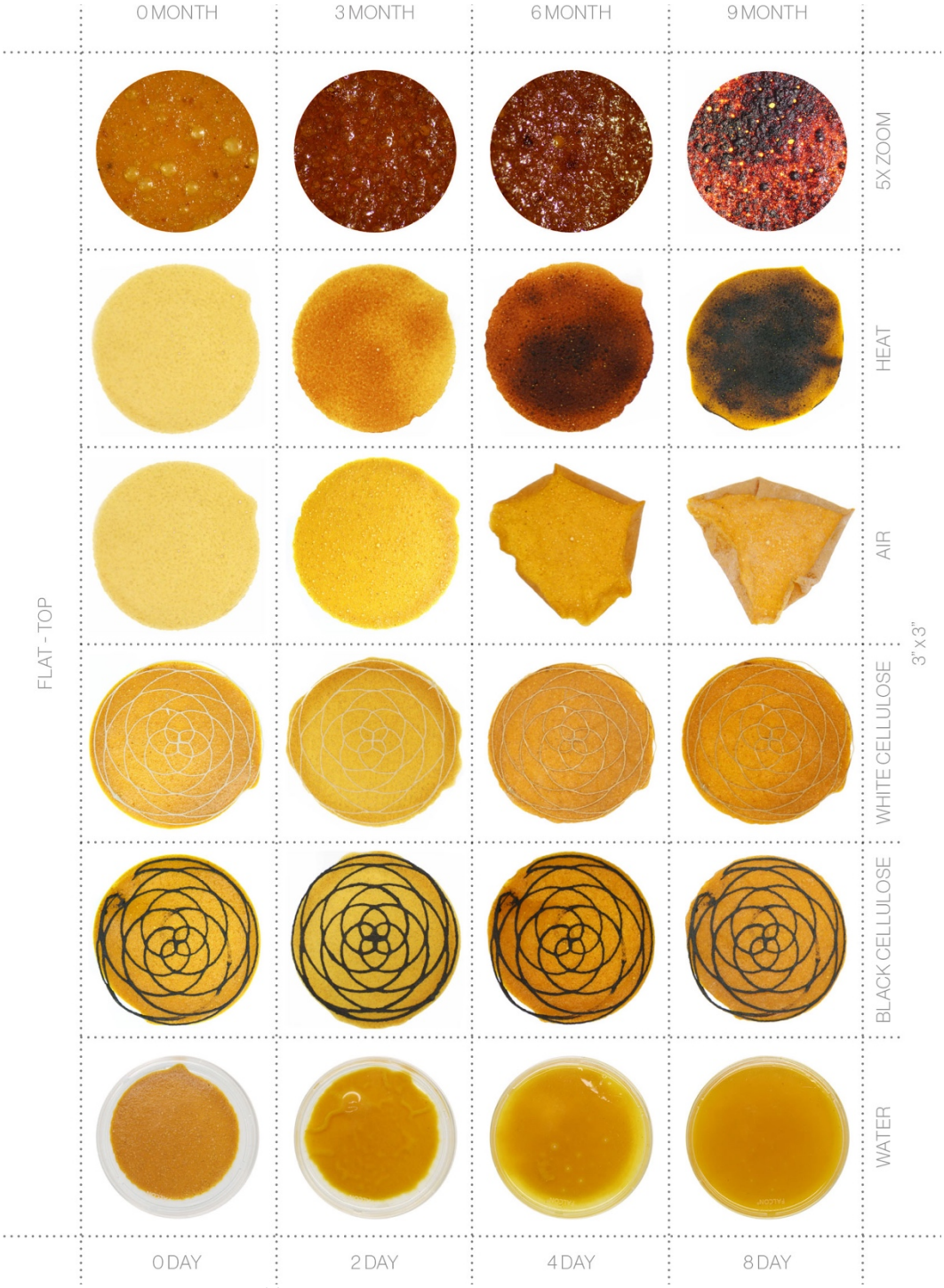

Figure 53: Matrix of O Swatch - Turmeric pectin formula comparing color change and deformation in response to exposure to heat, air and moisture over time.

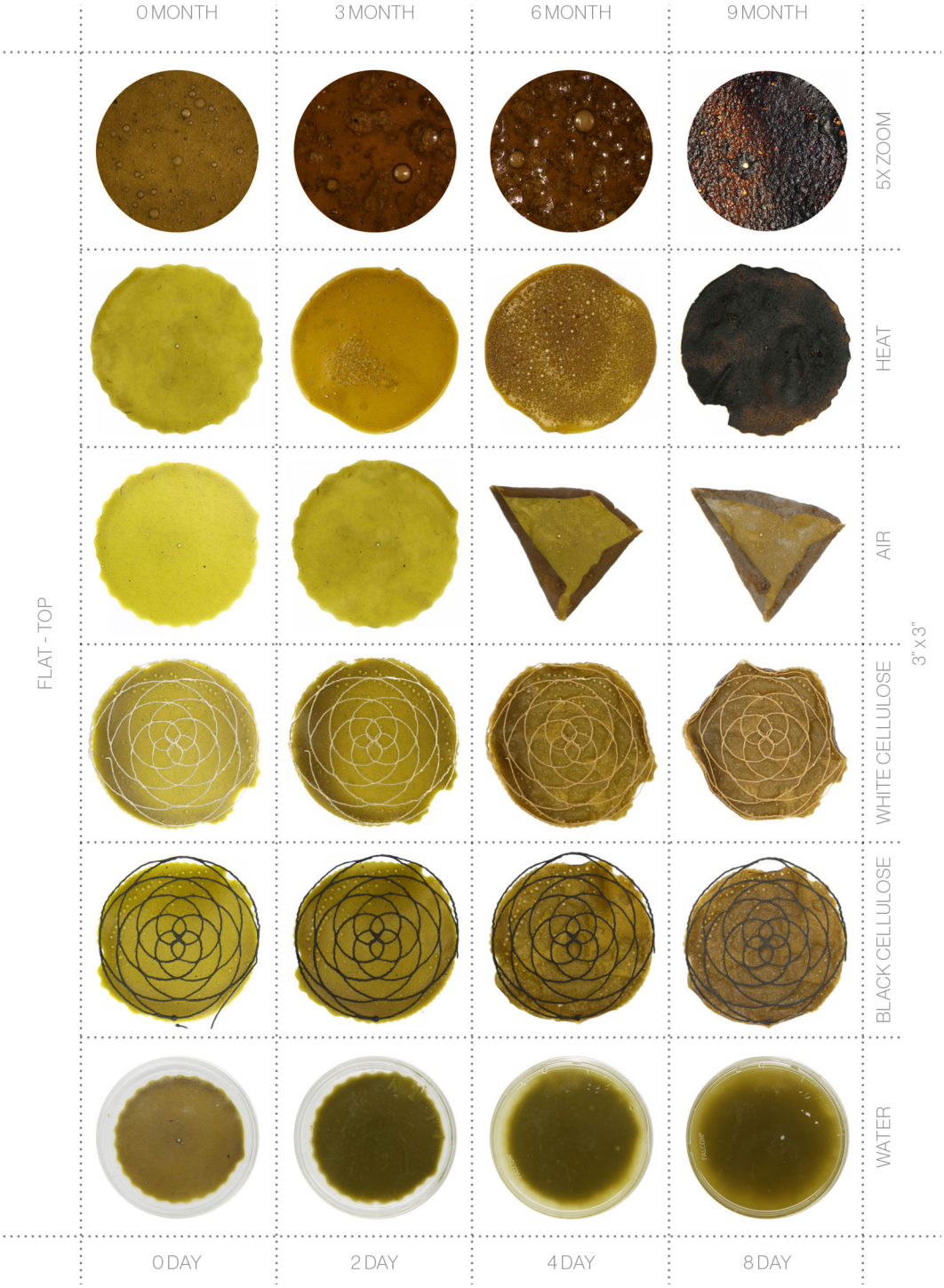

Figure 54: Matrix of O Swatch - Matcha pectin formula comparing color change and deformation in response to exposure to heat, air and moisture over time.

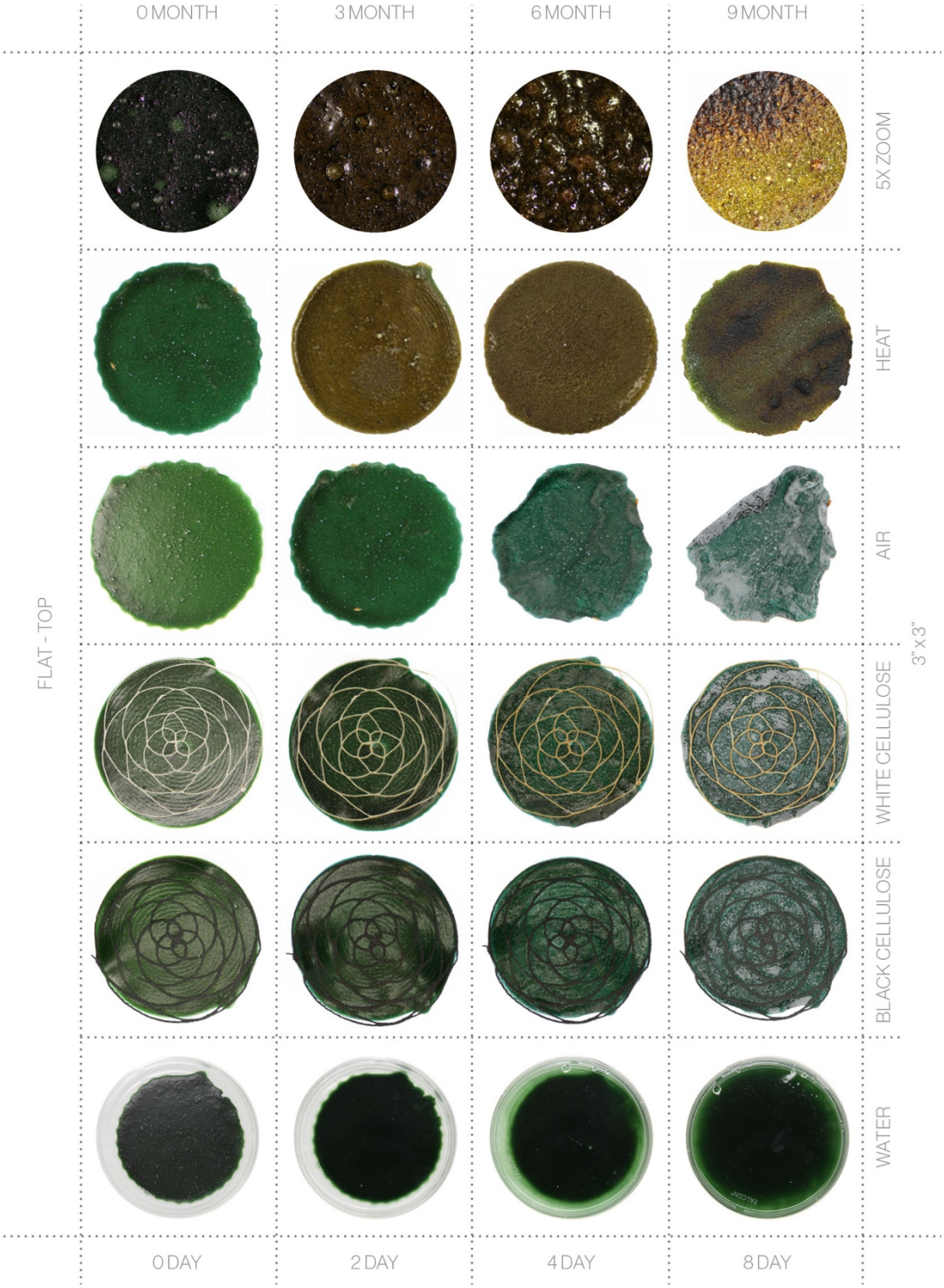

Figure 55: Matrix of O Swatch - Spirulina pectin formula comparing color change and deformation in response to exposure to heat, air and moisture over time.

Figure 56: Matrix of O Swatch - Indigo pectin formula comparing color change and deformation in response to exposure to heat, air and moisture over time.

Figure 57: Matrix of O Swatch - Charcoal pectin formula comparing color change and deformation in response to exposure to heat, air and moisture over time.

9.3.2 X Swatch

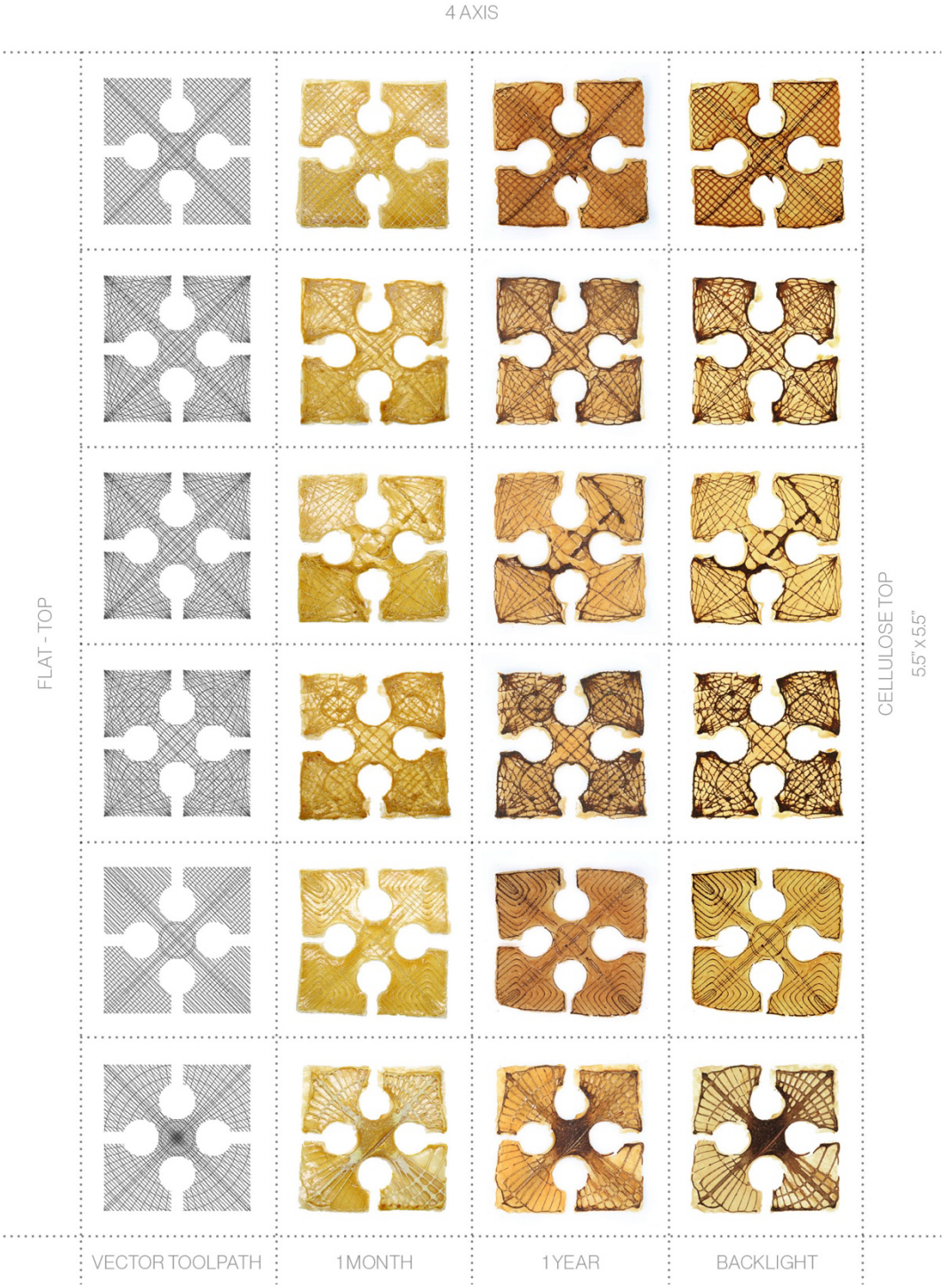

Figure 58: Matrix of X Swatch – Standard pectin and cellulose toolpaths comparing the color change and deformation of prints exposed to air over 1 year.

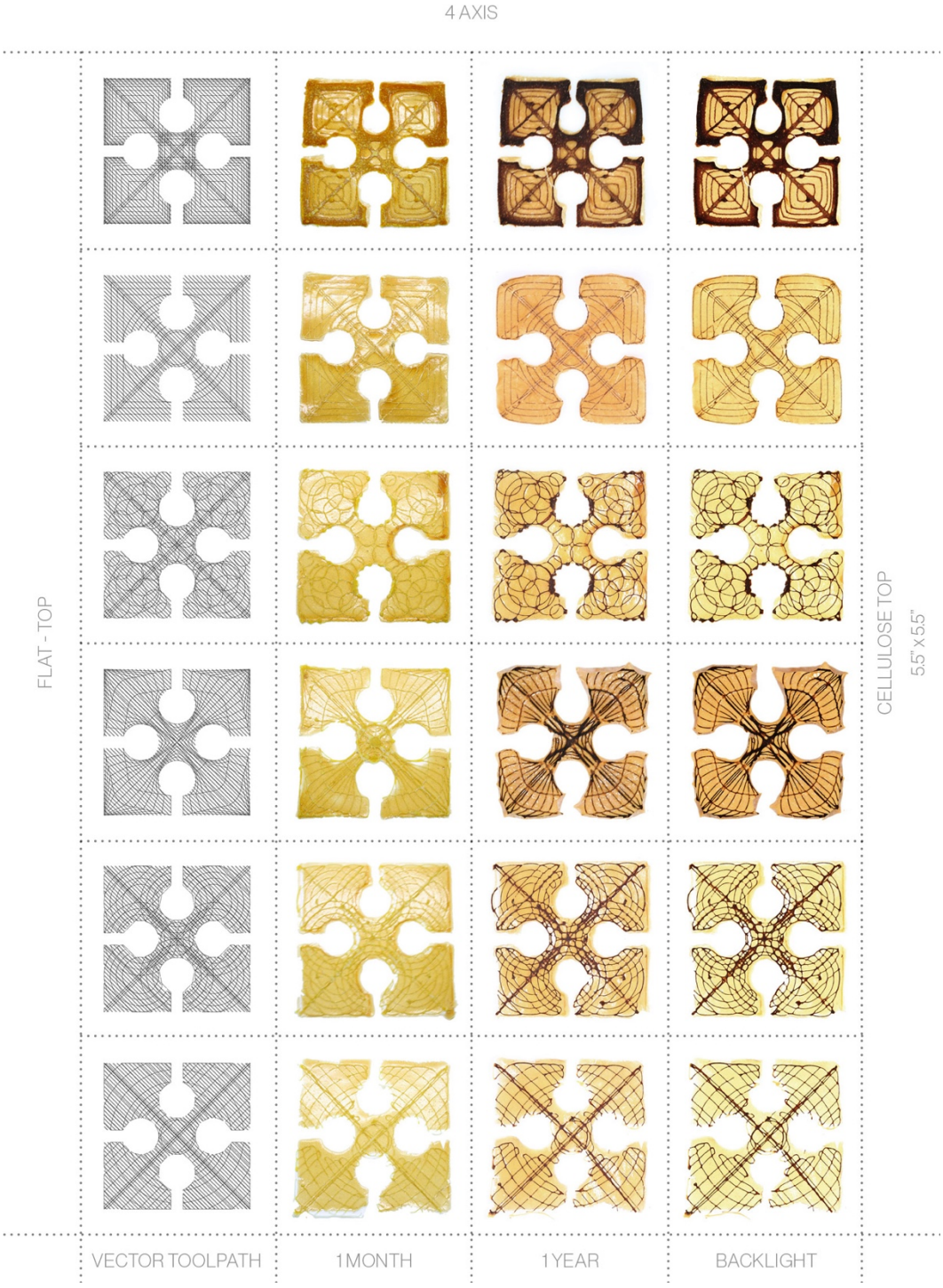

Figure 59: Matrix of X Swatch – Standard pectin and cellulose toolpaths comparing the color change and deformation of prints exposed to air over 1 year.

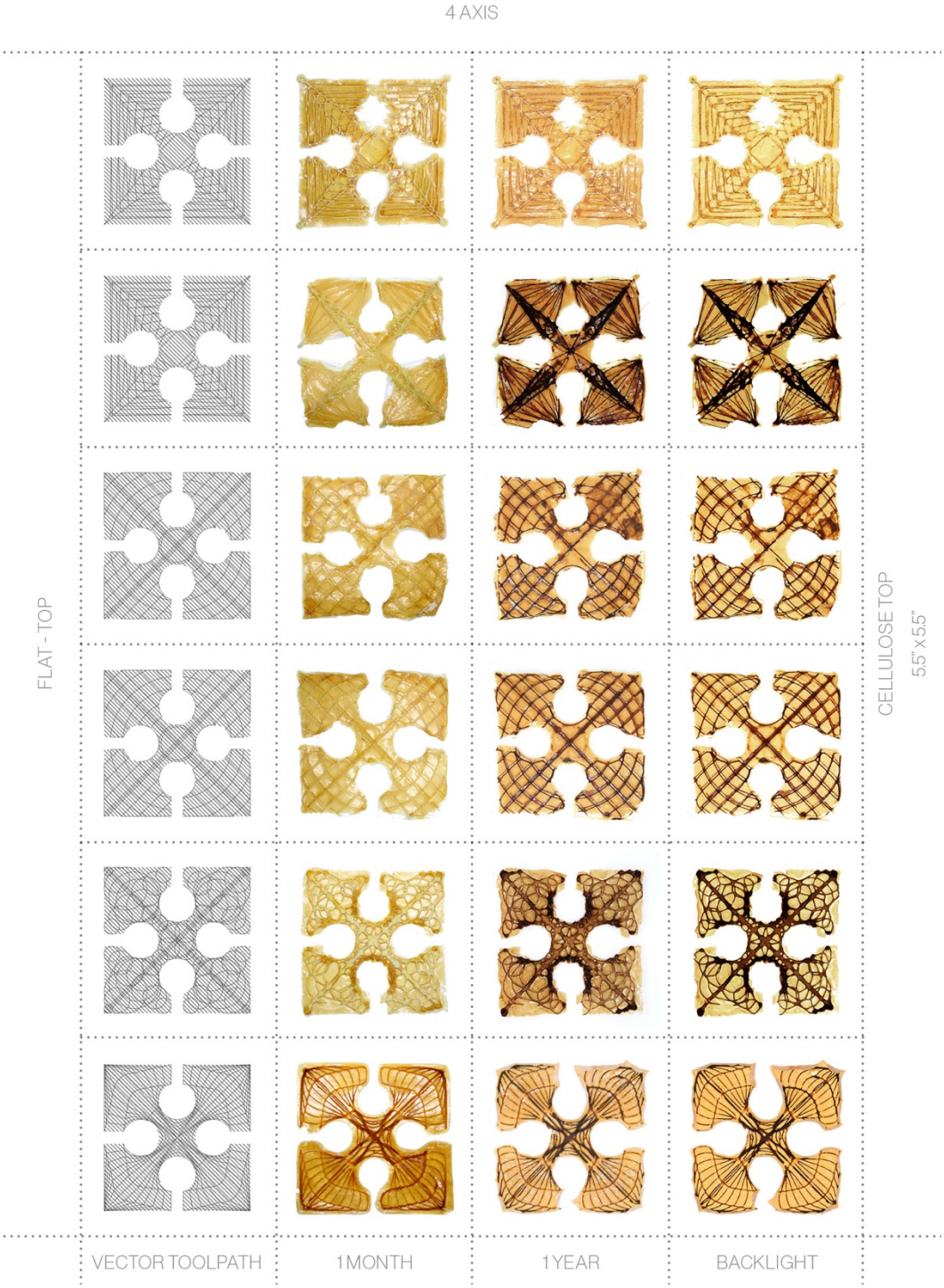

Figure 60: Matrix of X Swatch – Standard pectin and cellulose toolpaths comparing the color change and deformation of prints exposed to air over 1 year.

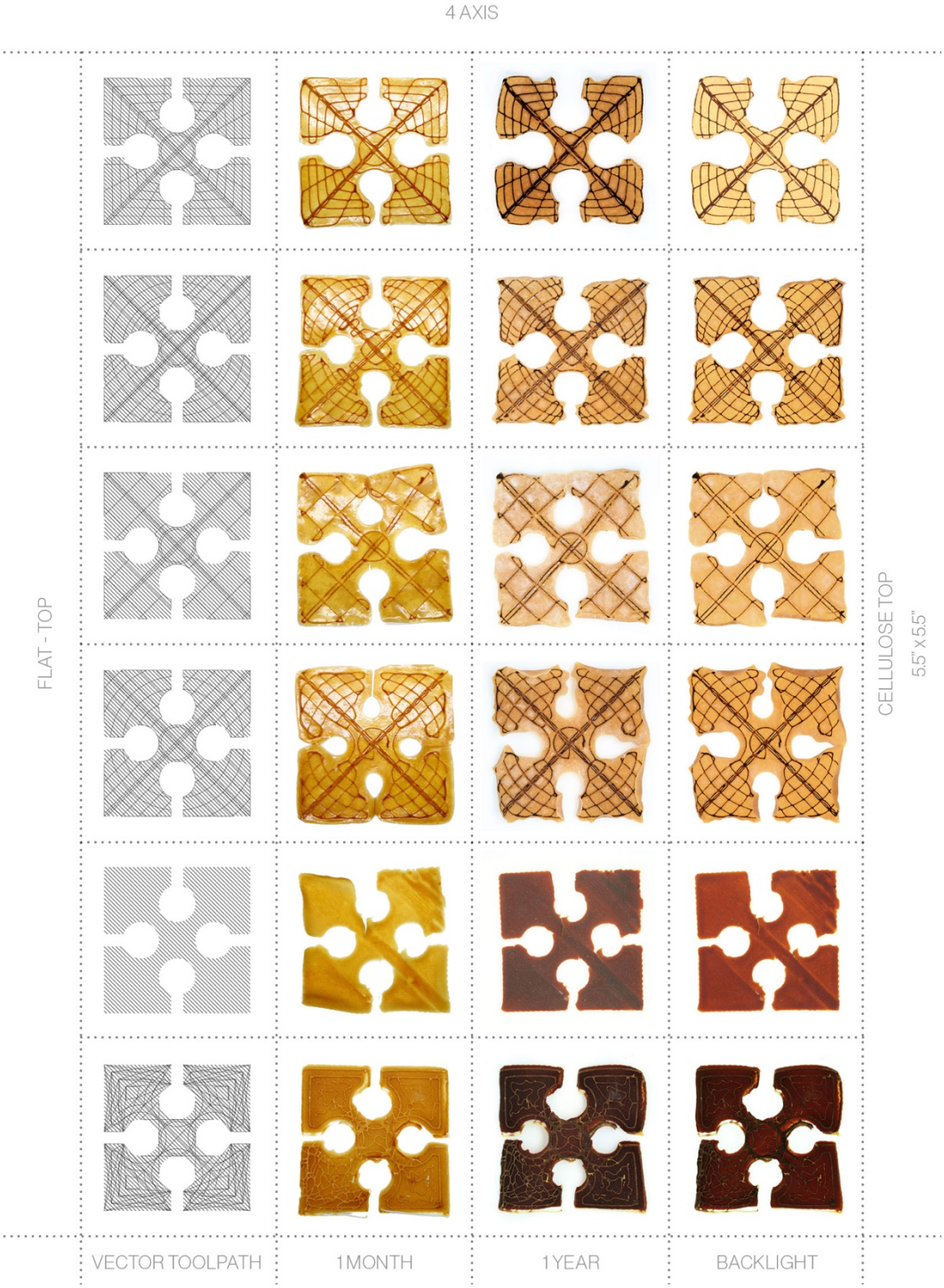

Figure 61: Matrix of X Swatch – Standard pectin and cellulose toolpaths comparing the color change and deformation of prints exposed to air over 1 year.

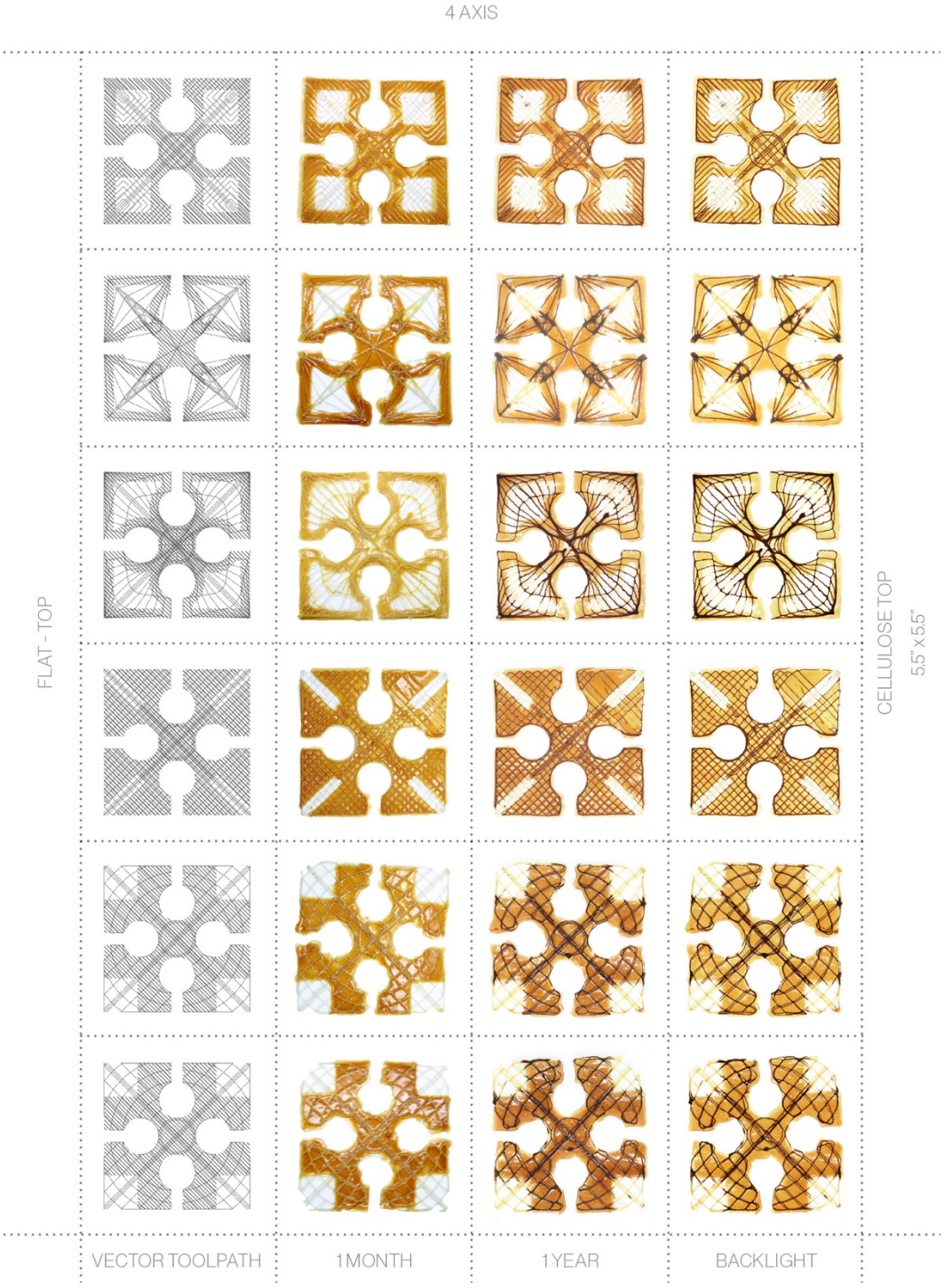

Figure 62: Matrix of X Swatch – Standard pectin and cellulose toolpath with internal voids comparing the color change and deformation of prints exposed to air over 1 year.

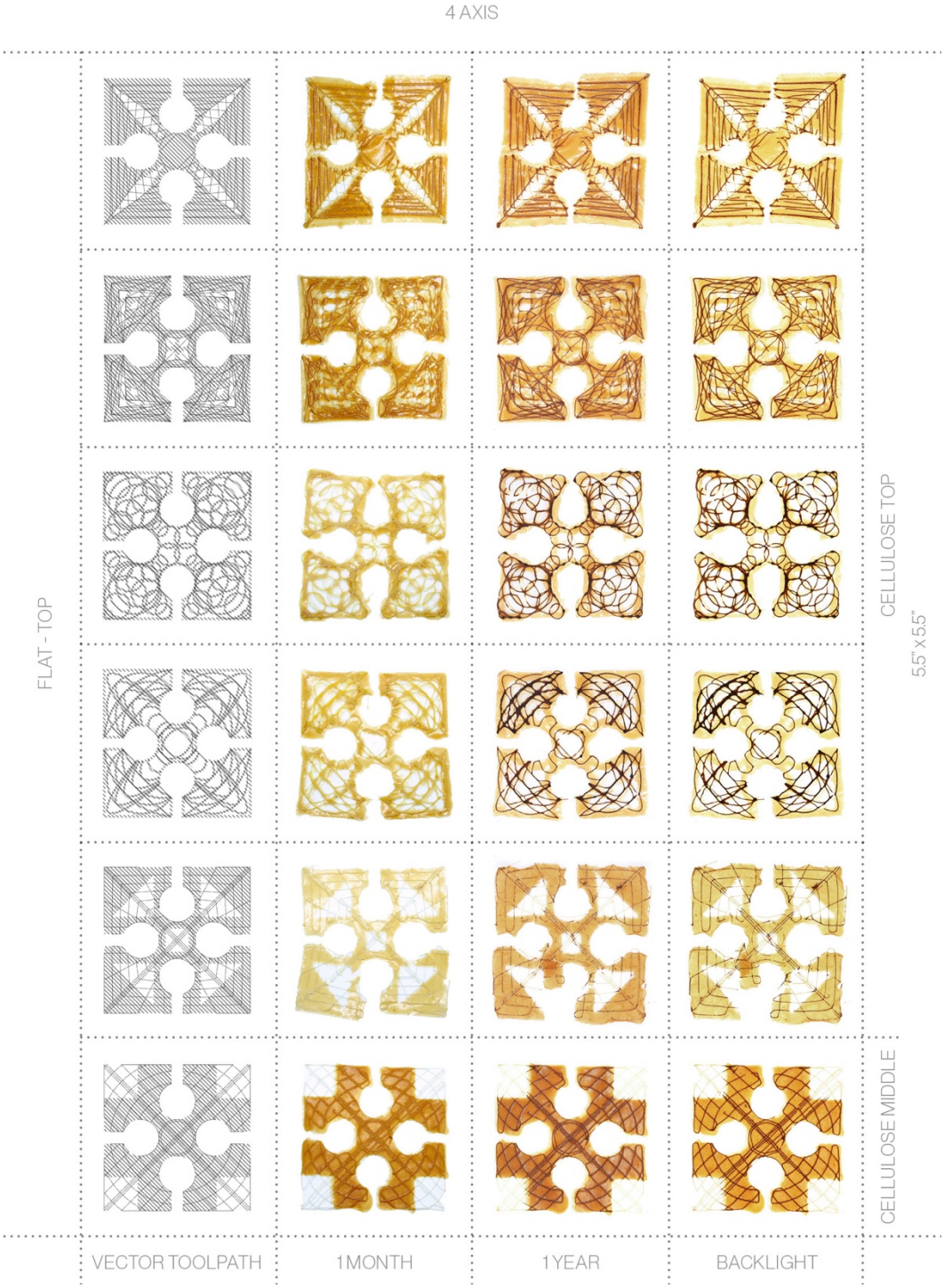

Figure 63: Matrix of X Swatch – Standard pectin and cellulose toolpaths with internal voids comparing the color change and deformation of prints exposed to air over 1 year.

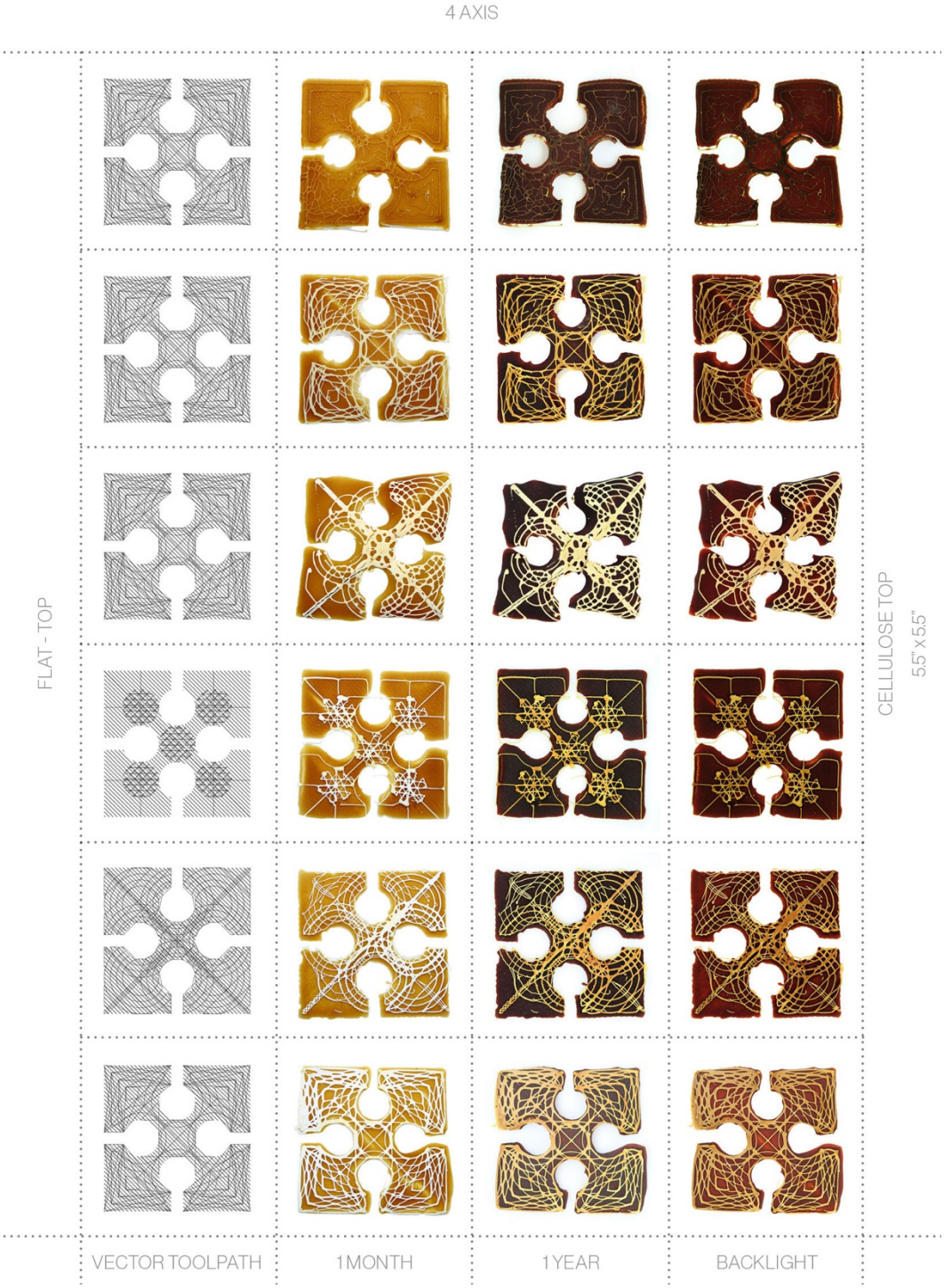

Figure 64: Matrix of X Swatch – Chitosan pectin and cellulose toolpaths comparing the color change and deformation of prints exposed to air over 1 year.

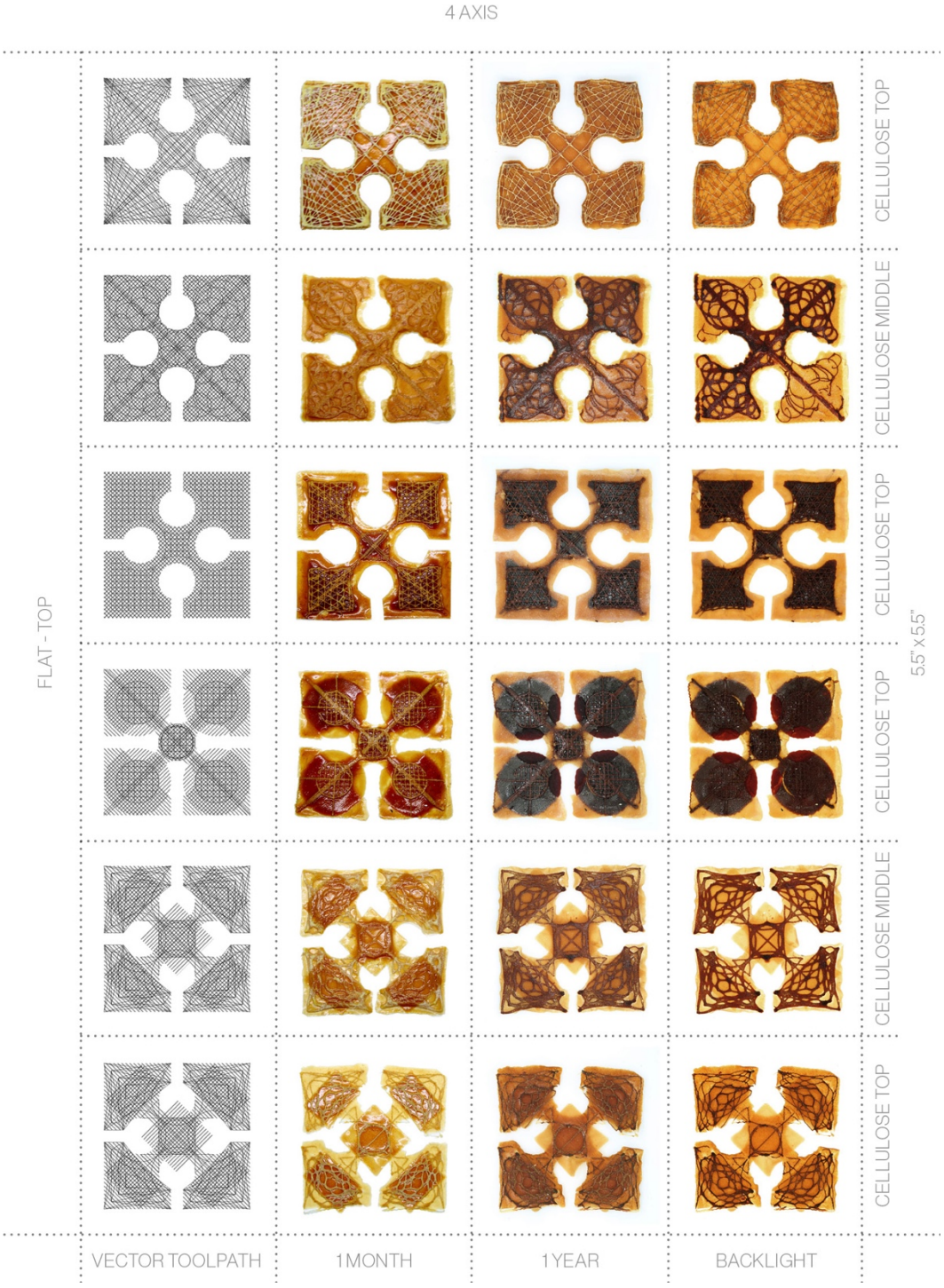

Figure 65: Matrix of X Swatch – Layered standard pectin and cellulose toolpaths comparing the color change and deformation of prints exposed to air over 1 year.

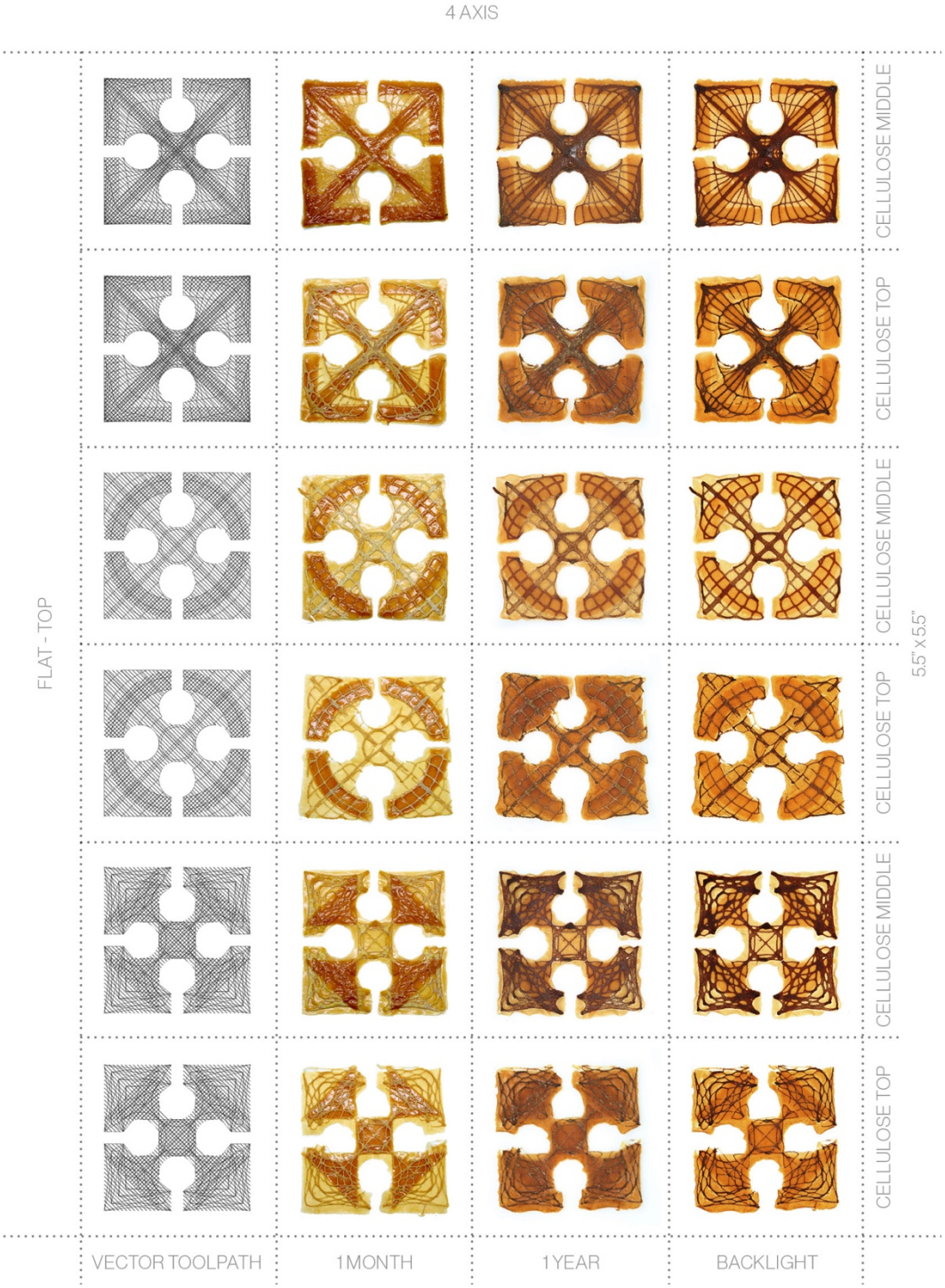

Figure 66: Matrix of X Swatch – Layered standard pectin and cellulose toolpaths comparing the color change and deformation of prints exposed to air over 1 year.

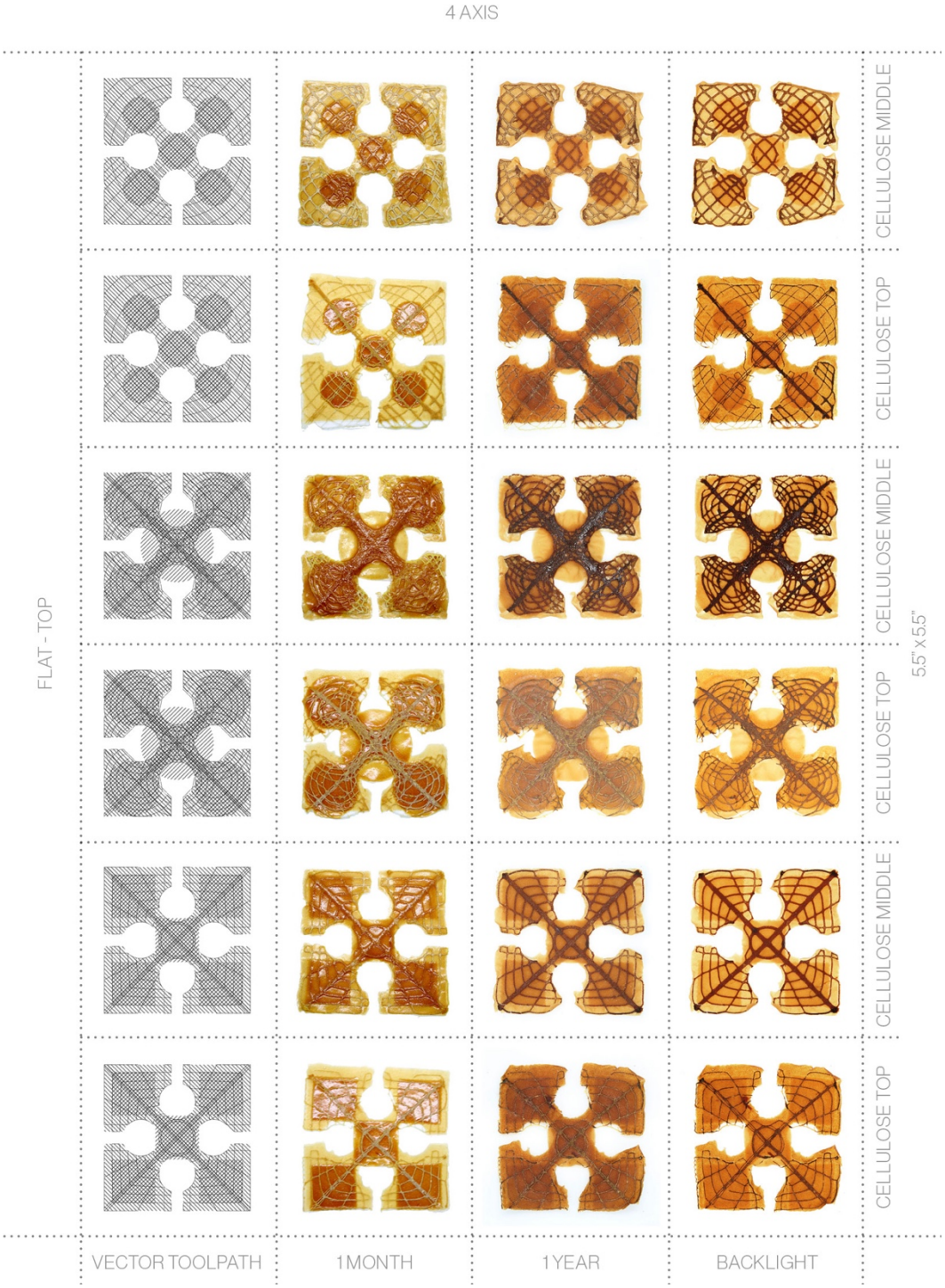

Figure 67: Matrix of X Swatch – Layered standard pectin and cellulose toolpaths comparing the color change and deformation of prints exposed to air over 1 year.

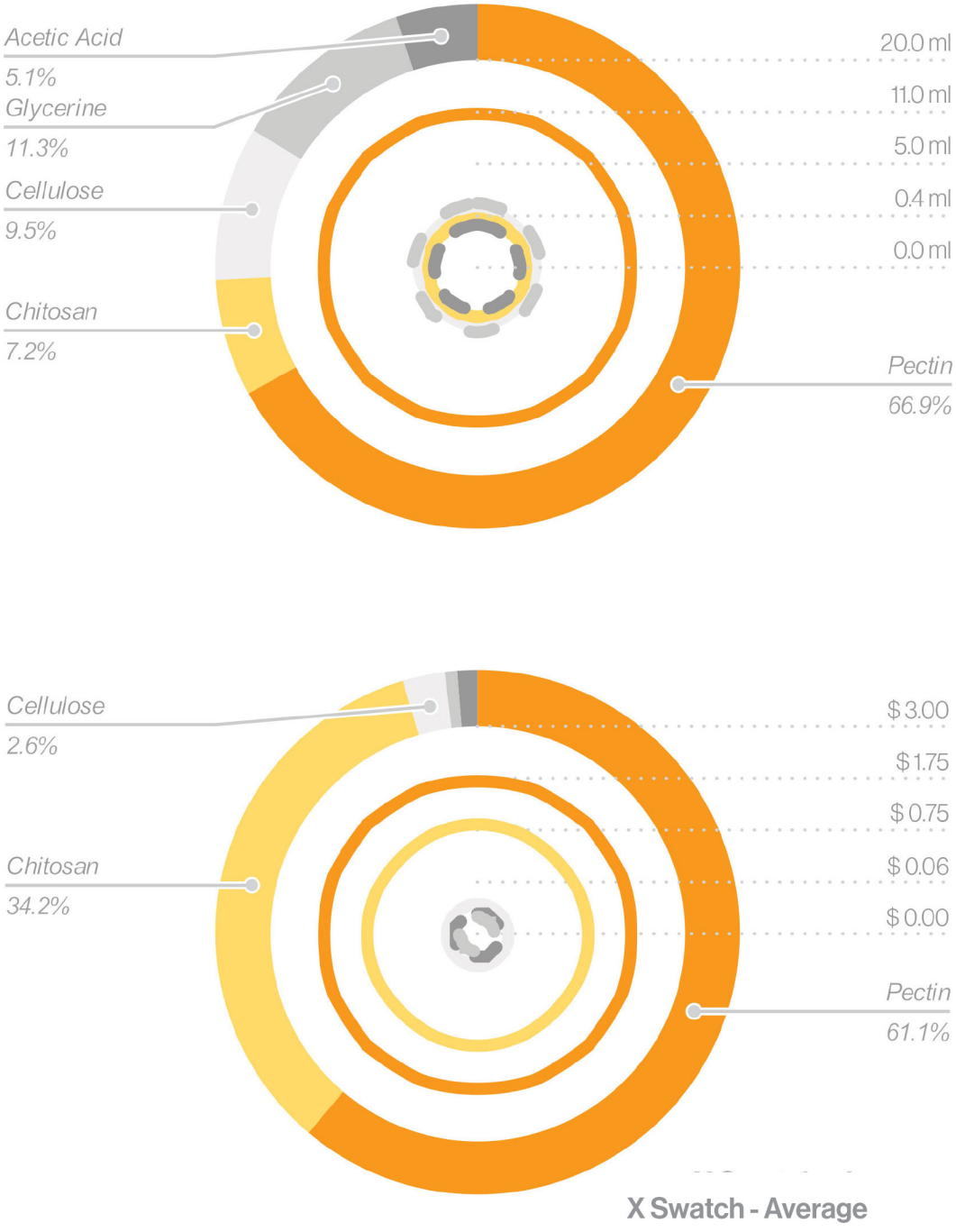

Figure 68: X Swatch – Average volume and cost of materials for each print in the series.

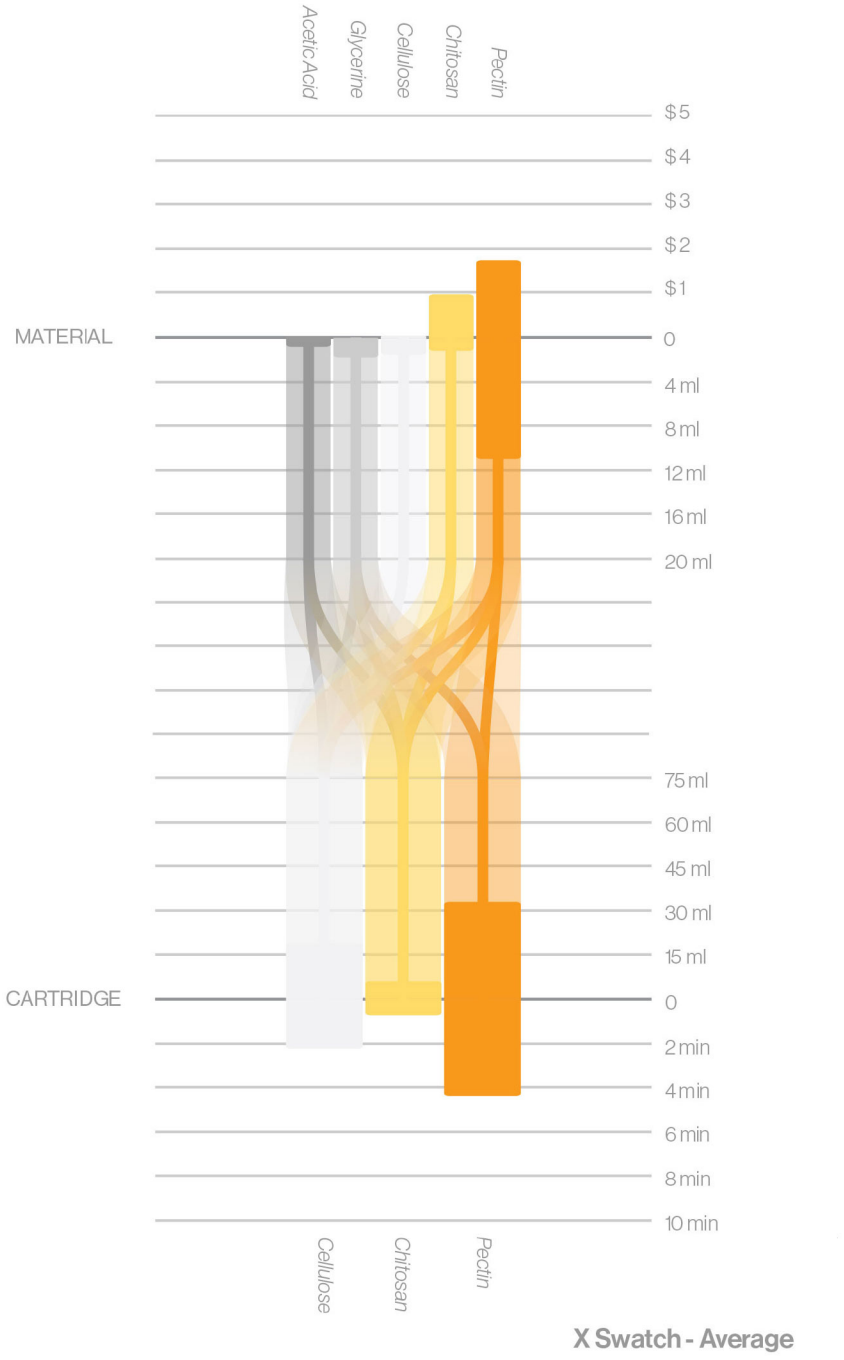

Figure 69: X Swatch – Average volume of material, print duration, and cost for different biopolymer formulas used in each print in the series.

9.3.3 X Flower

Figure 70: Matrix of X Flower – Multiple pectin formulas exposed to air over 1 year comparing color change and deformation of 3-dimensional form.

Figure 71: Matrix of X Flower – Multiple pectin formulas exposed to air over 1 year comparing color change and deformation of 3-dimensional form.

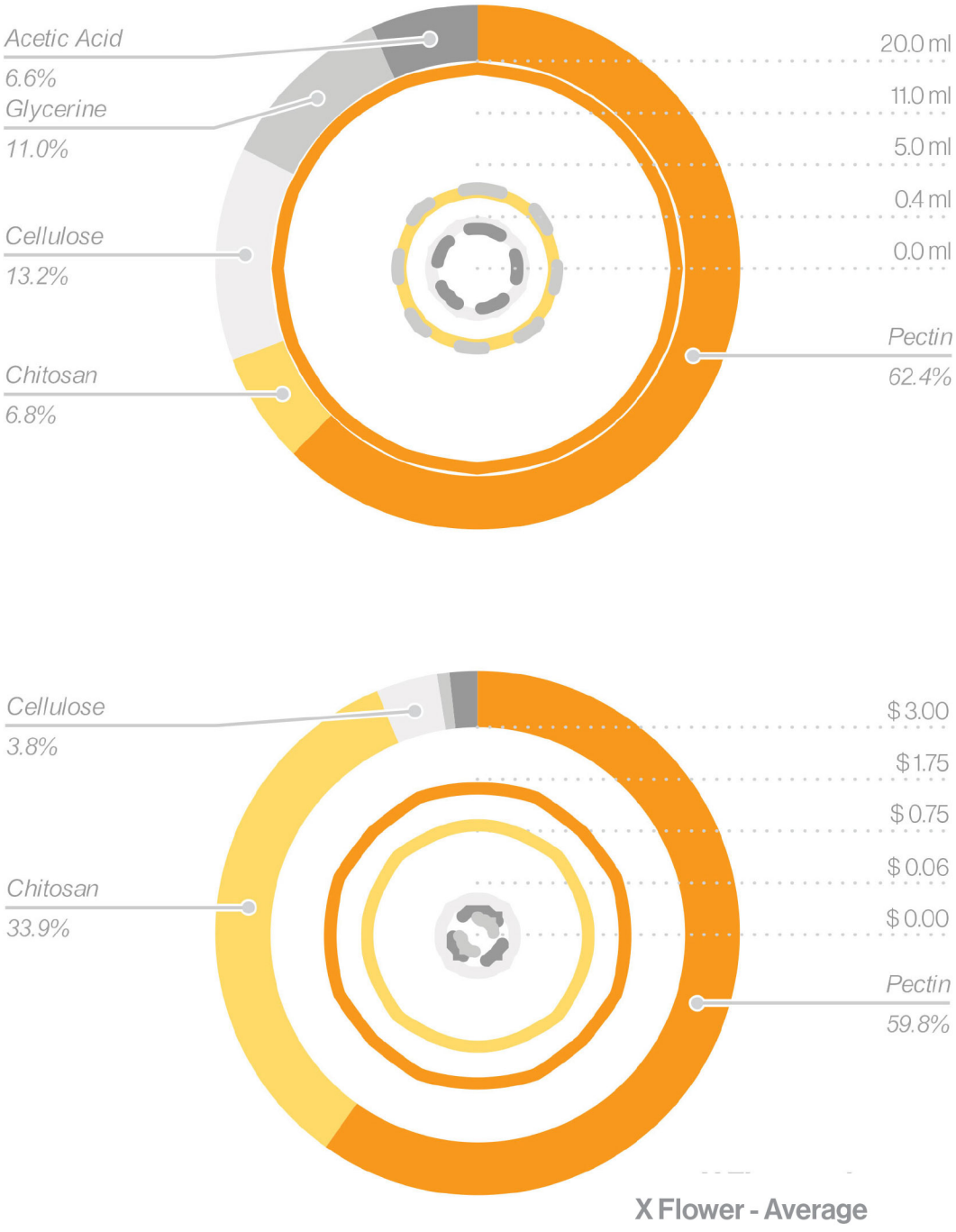

Figure 72: X Flower – Average volume and cost of materials for each print in the series.

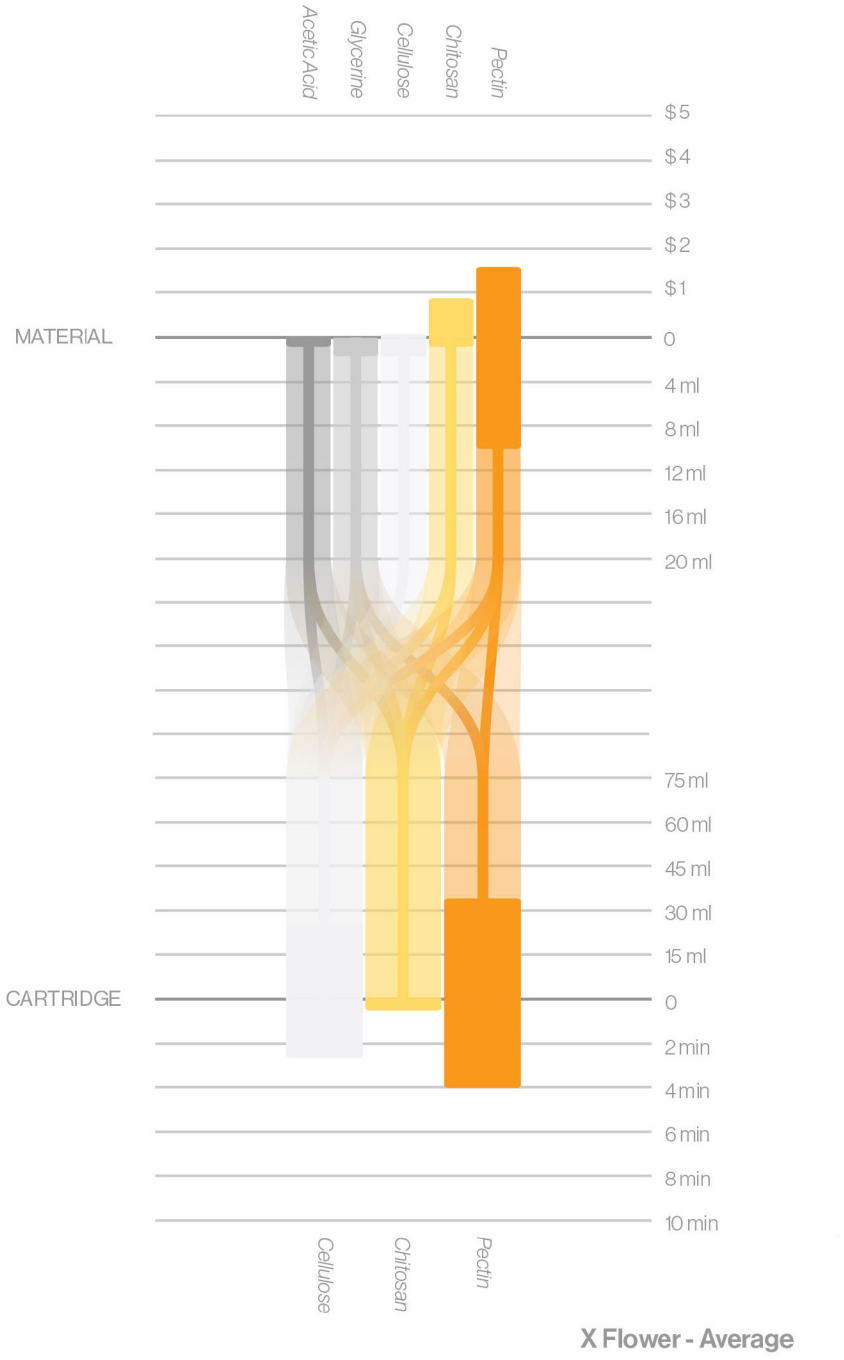

Figure 73: X Flower – Average volume of material, print duration, and cost for different biopolymer formulas used in each print in the series.

9.3.4 V Skull

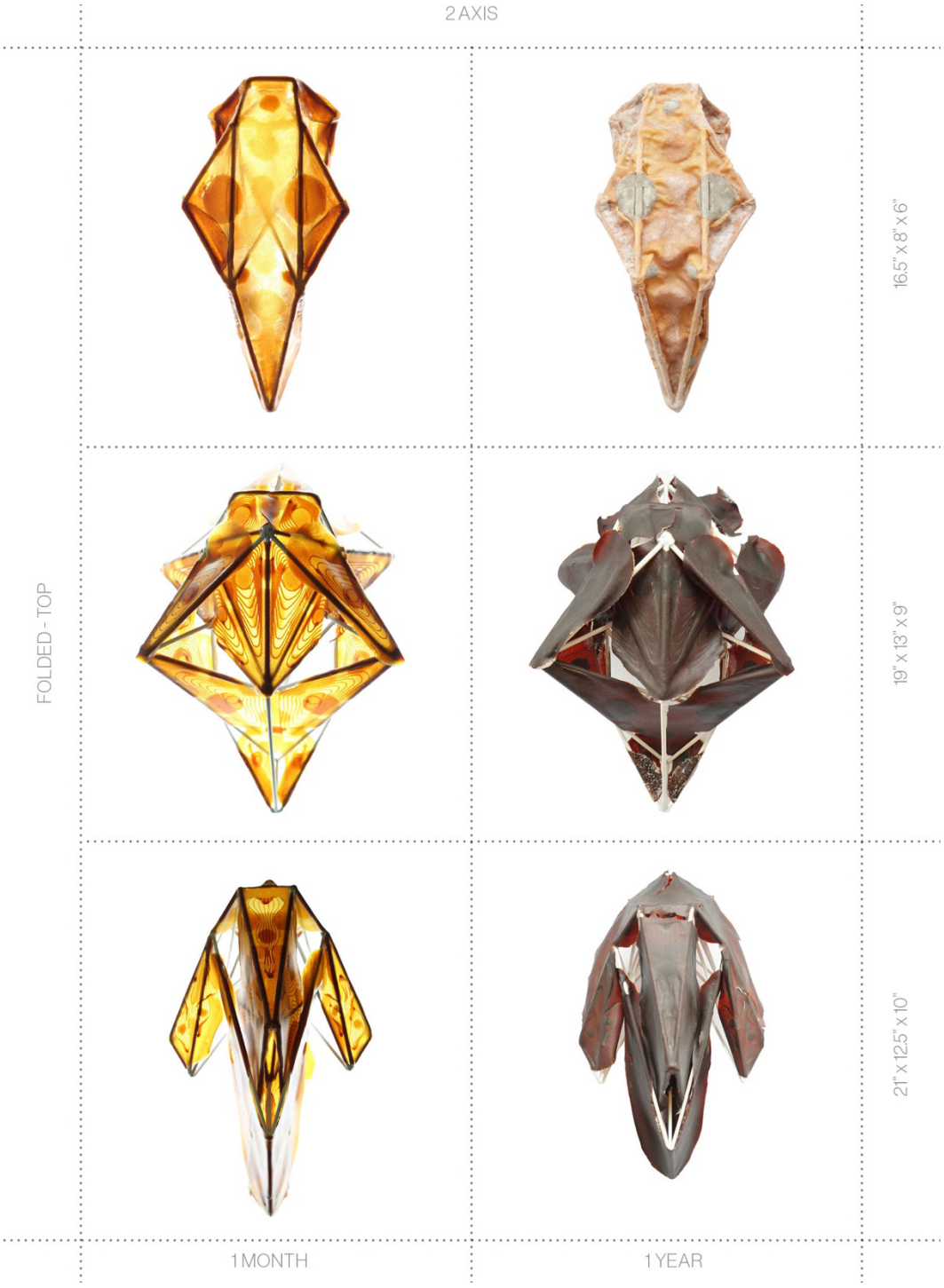

Figure 74: Matrix of V Skull – Multiple geometries exposed to air over 1 year comparing color change and deformation of 3-dimensional form.

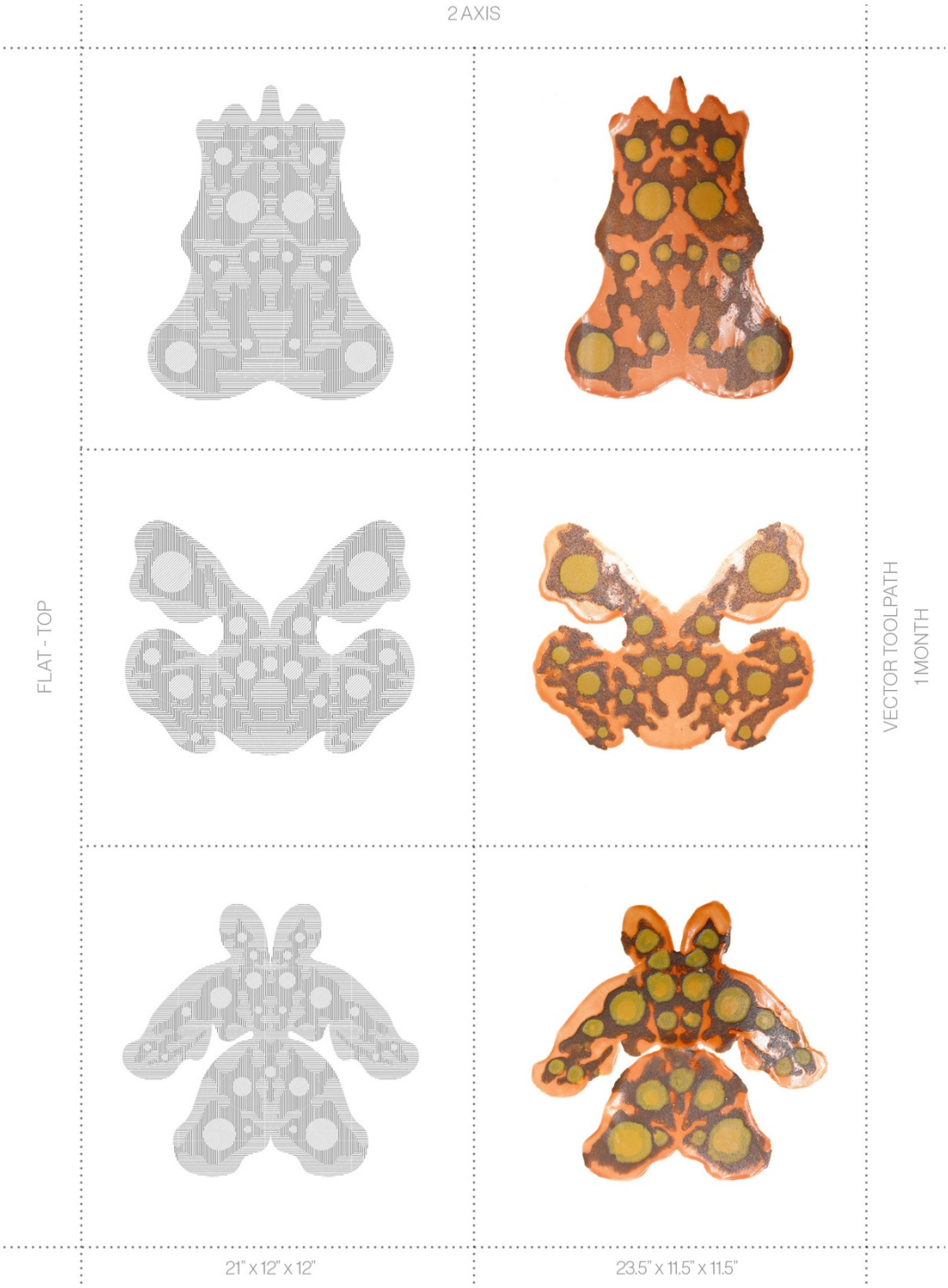

Figure 75: Matrix of V Skull – Multiple geometries comparing vector toolpaths to printed 2-dimensional forms.

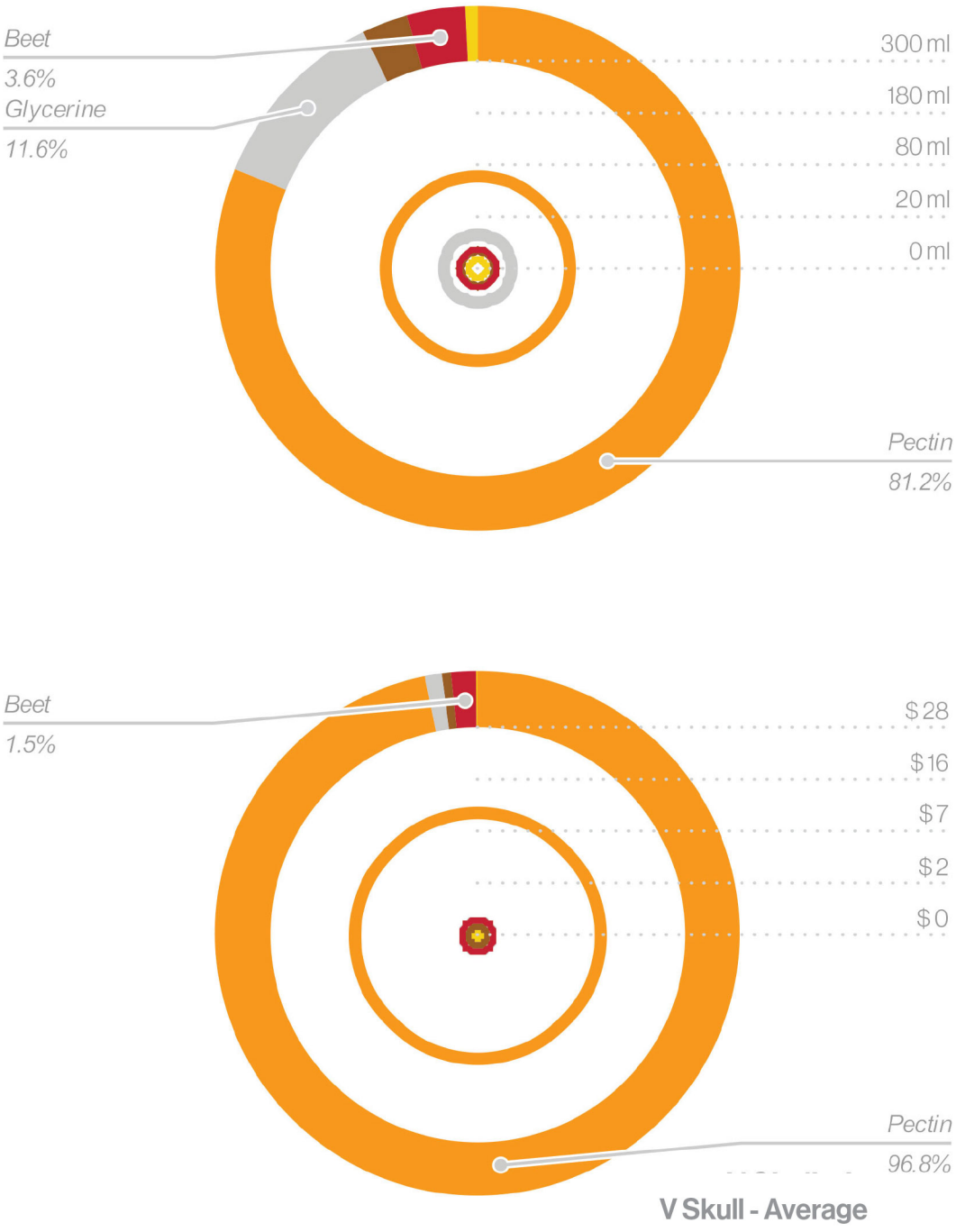

Figure 76: V Skull – Average volume and cost of materials for each print in the series.

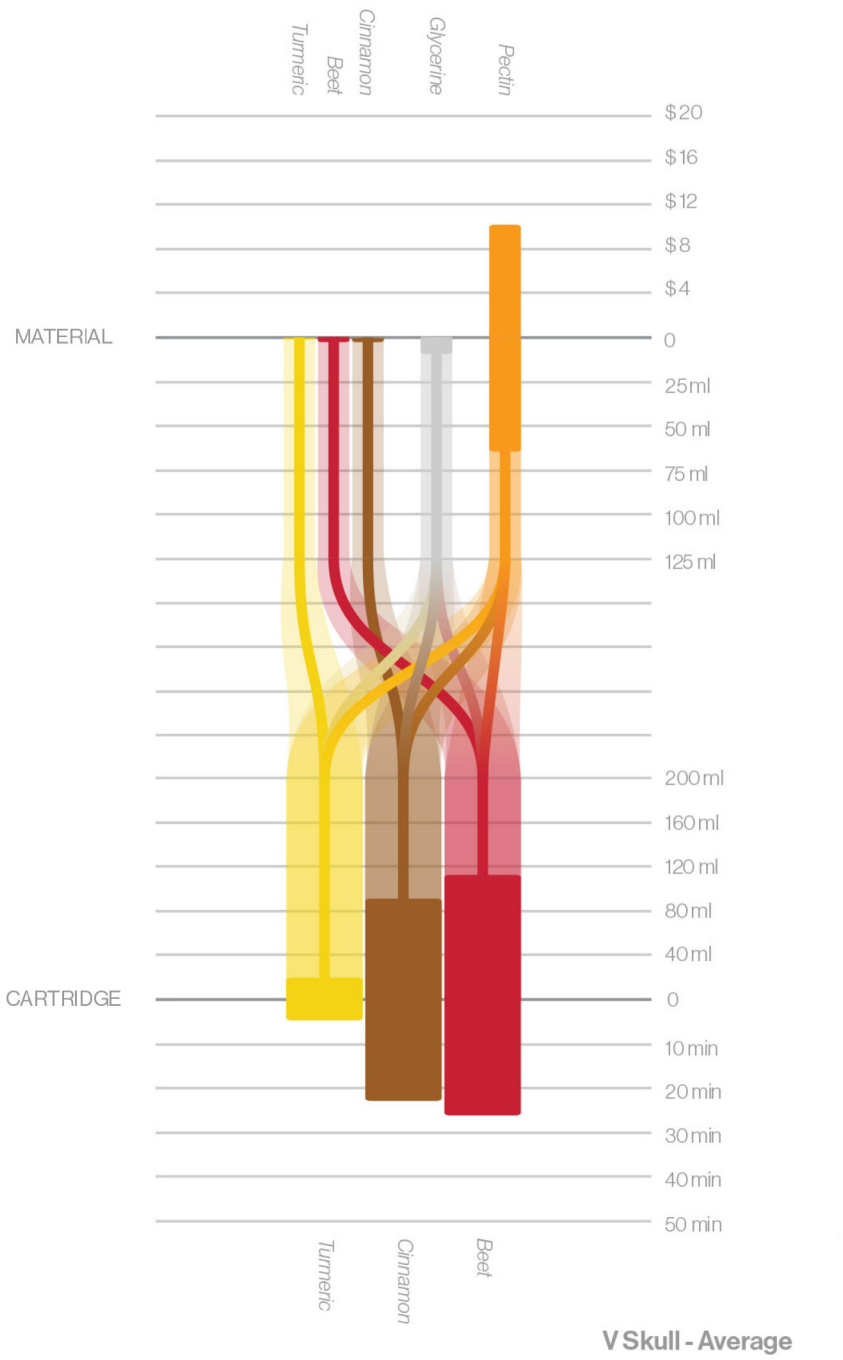

Figure 77: V Skull - Average volume of material, print duration, and cost for different biopolymer formulas used in each print in the series.

9.3.5 T Fold

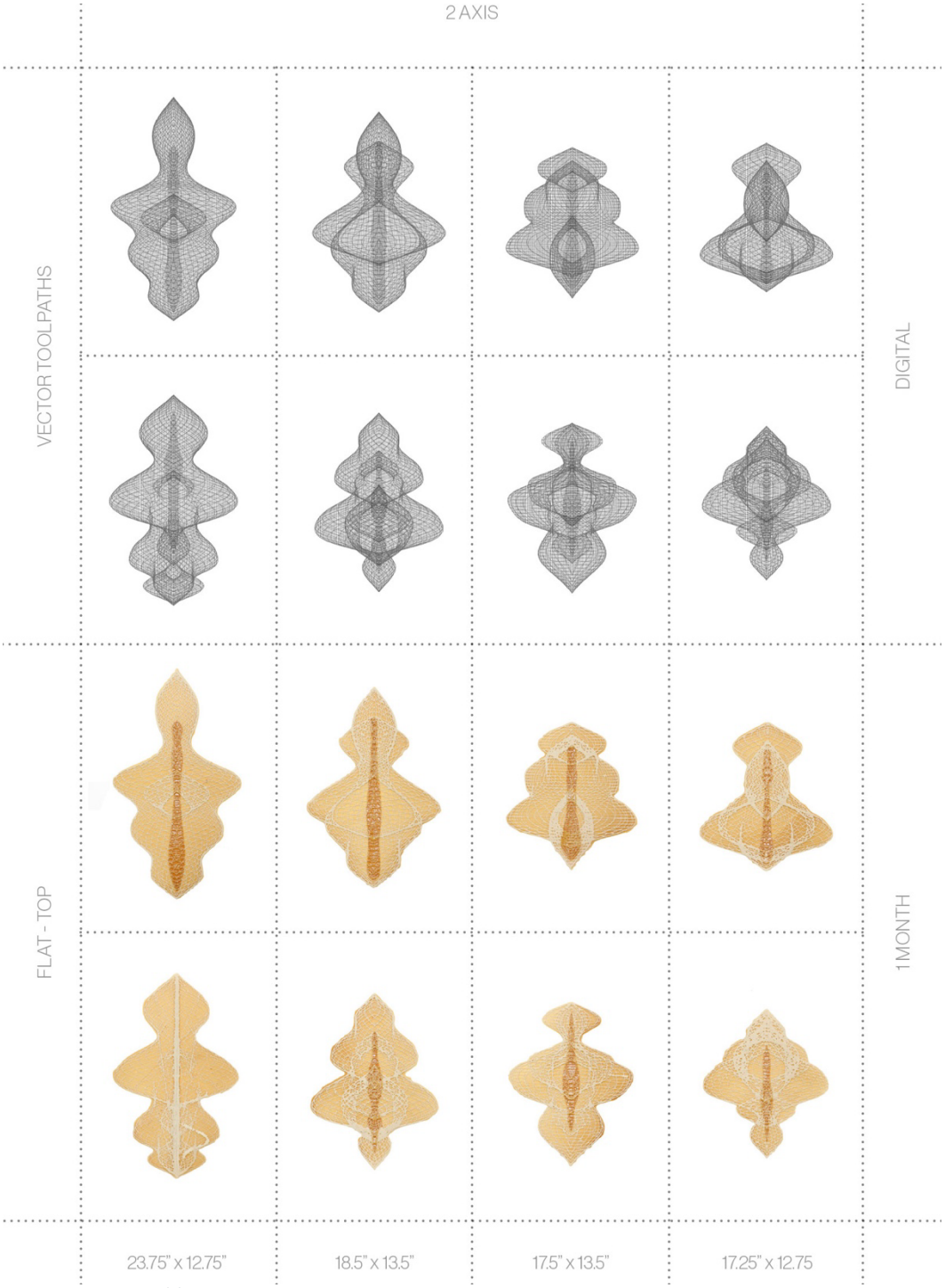

Figure 78: Matrix of T Fold – Multiple geometries comparing vector toolpaths to printed 2-dimensional forms.

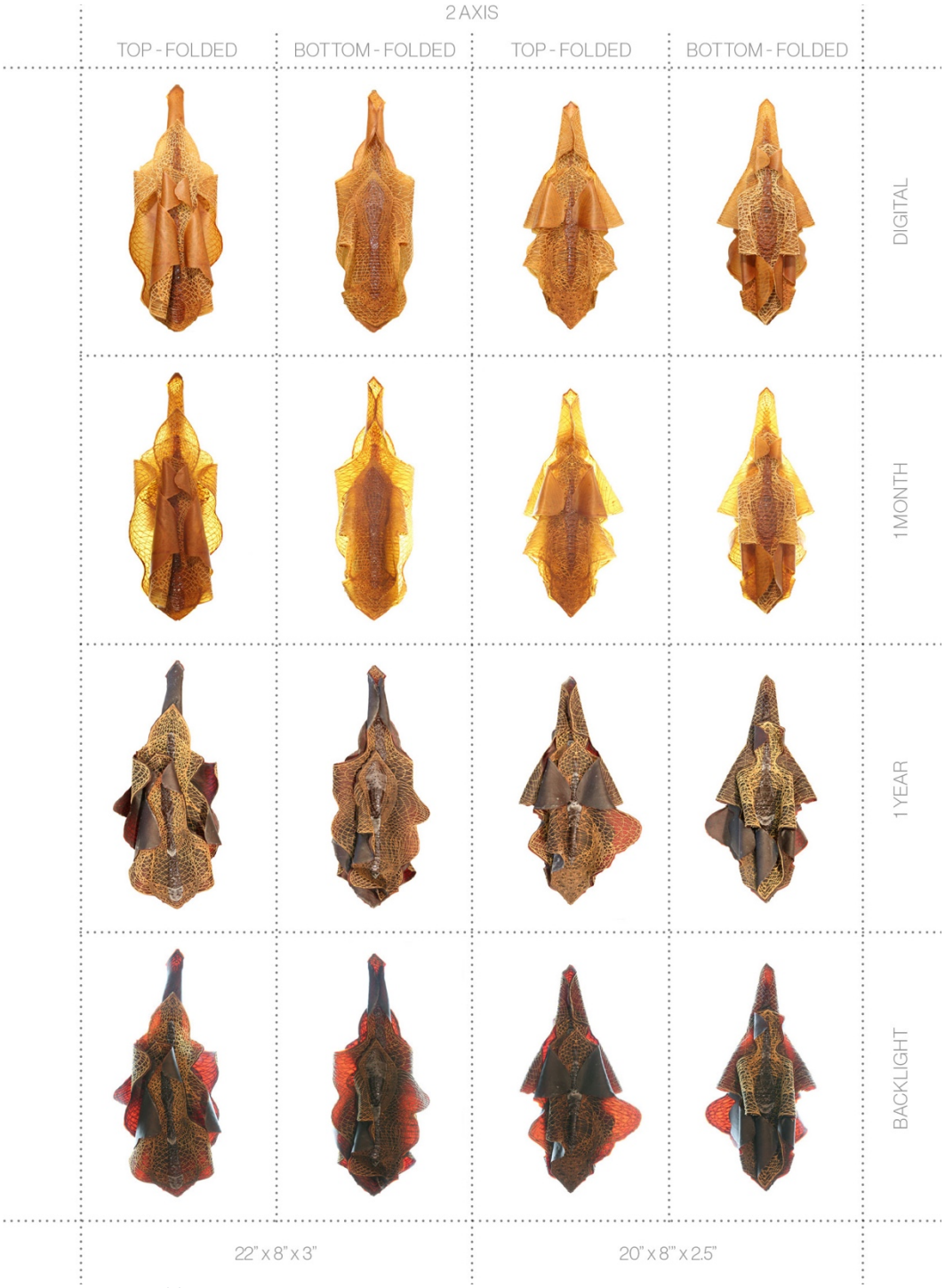

Figure 79: Matrix of T Fold – Multiple geometries comparing vector toolpaths to printed 3-dimensional forms.

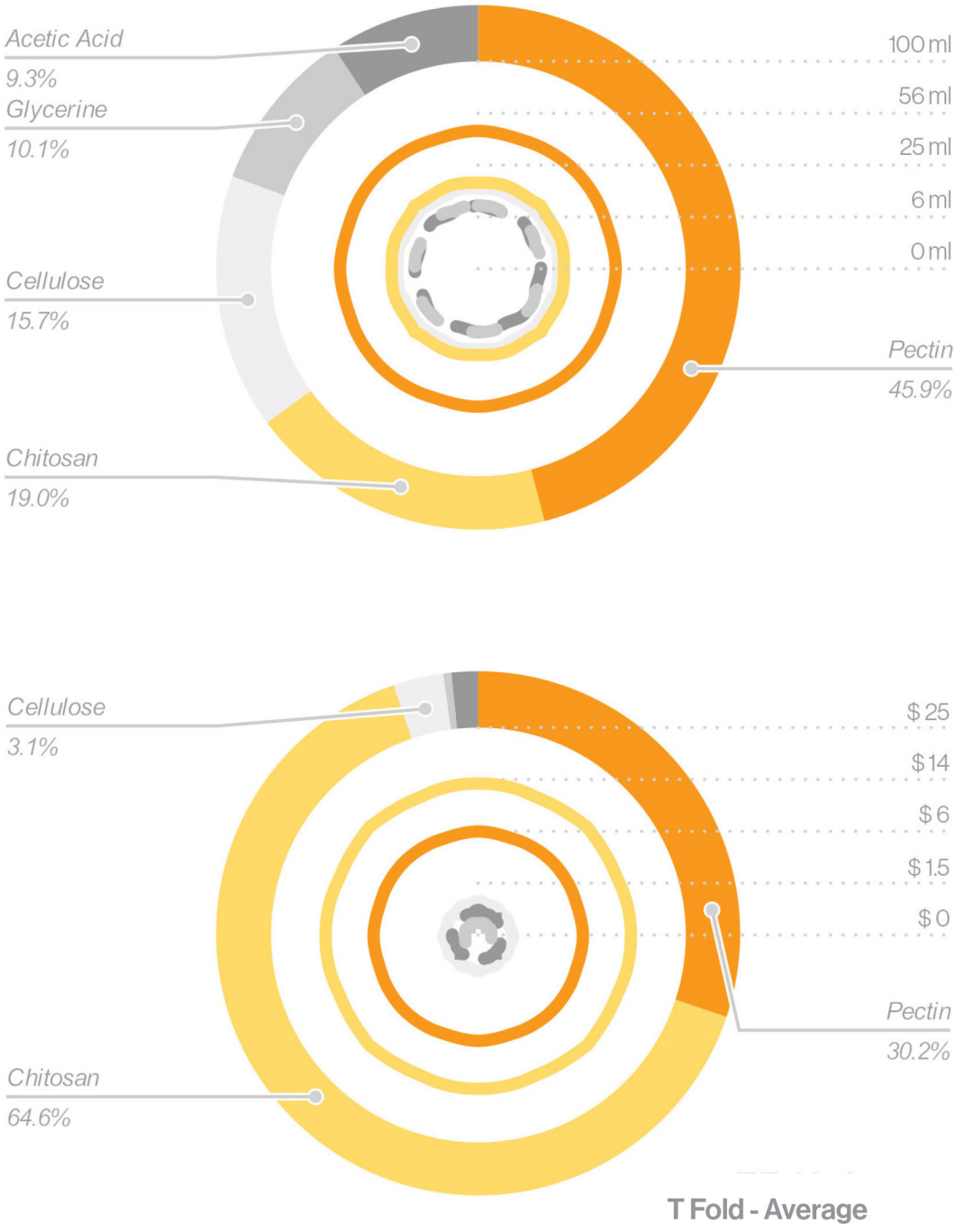

Figure 80: T Fold – Average volume and cost of materials for each print in the series.

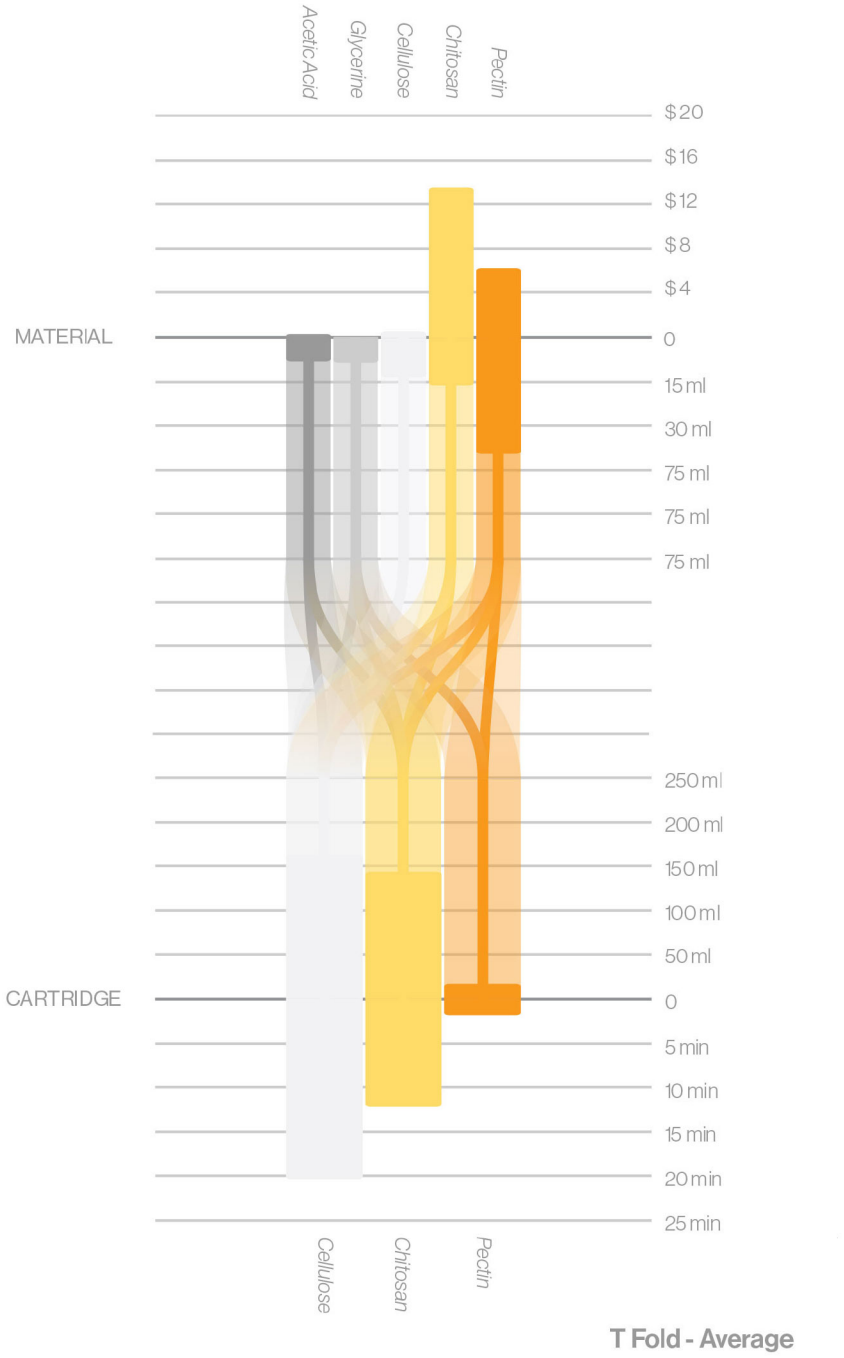

Figure 81: T Fold - Average volume of material, print duration, and cost for different biopolymer formulas used in each print in the series.

9.3.6 Y Fold

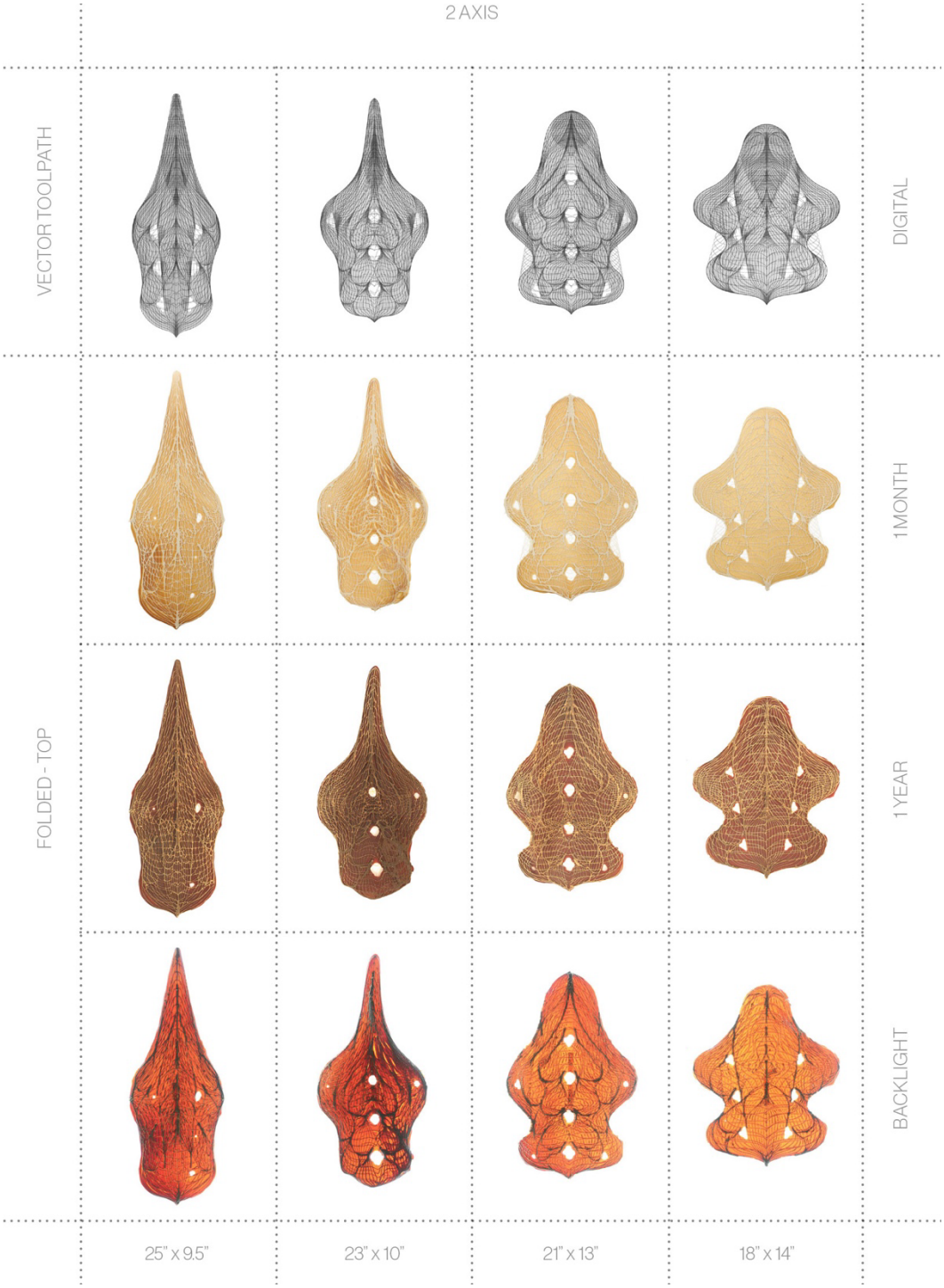

Figure 82: Matrix of Y Fold – Multiple geometries comparing vector toolpaths to the deformation and color change of printed 2-dimensional forms.

Figure 83: Matrix of Y Fold – Multiple geometries exposed to air over 1 year comparing color change and deformation of 3-dimensional form.

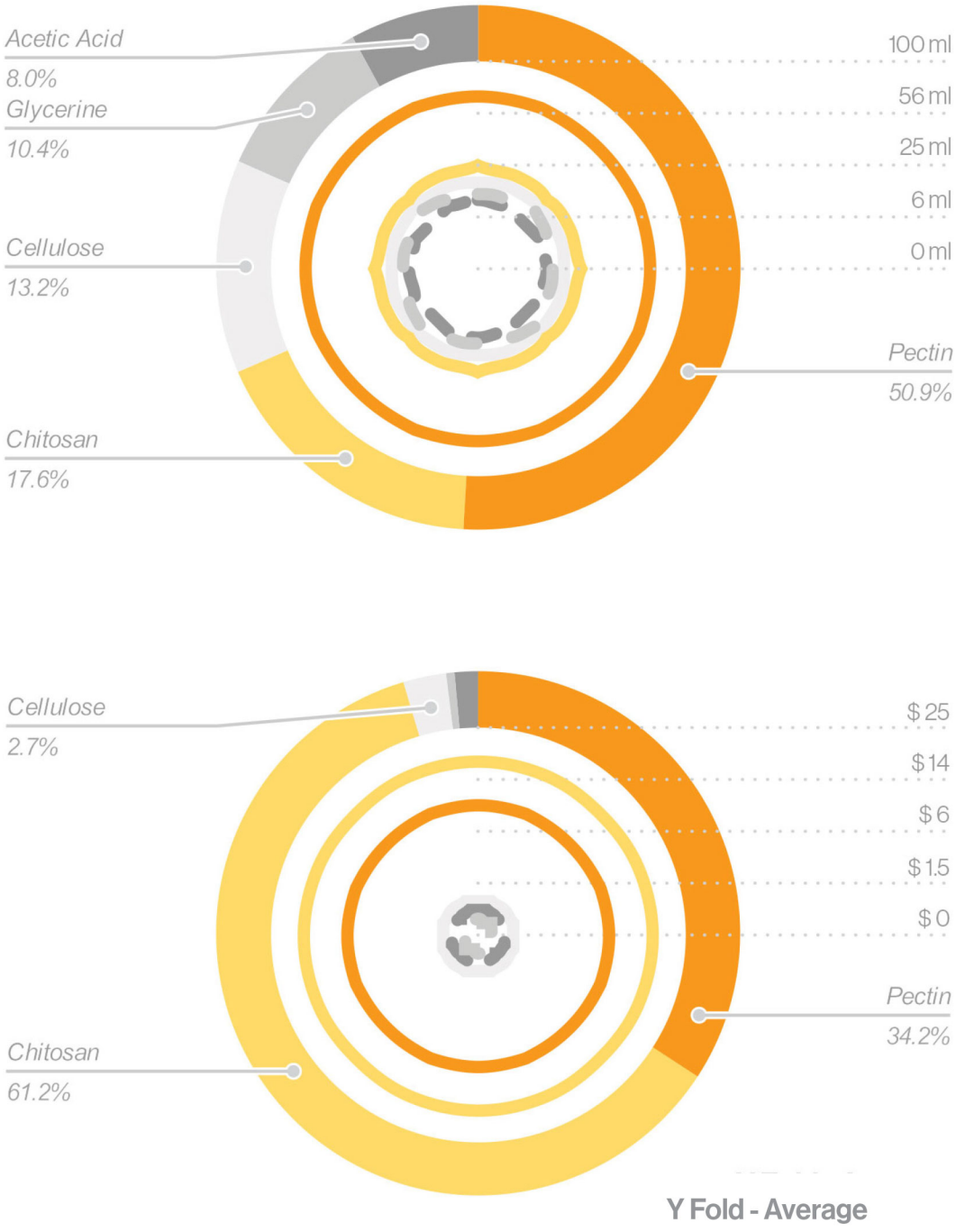

Figure 84: Y Fold – Average volume and cost of materials for each print in the series.

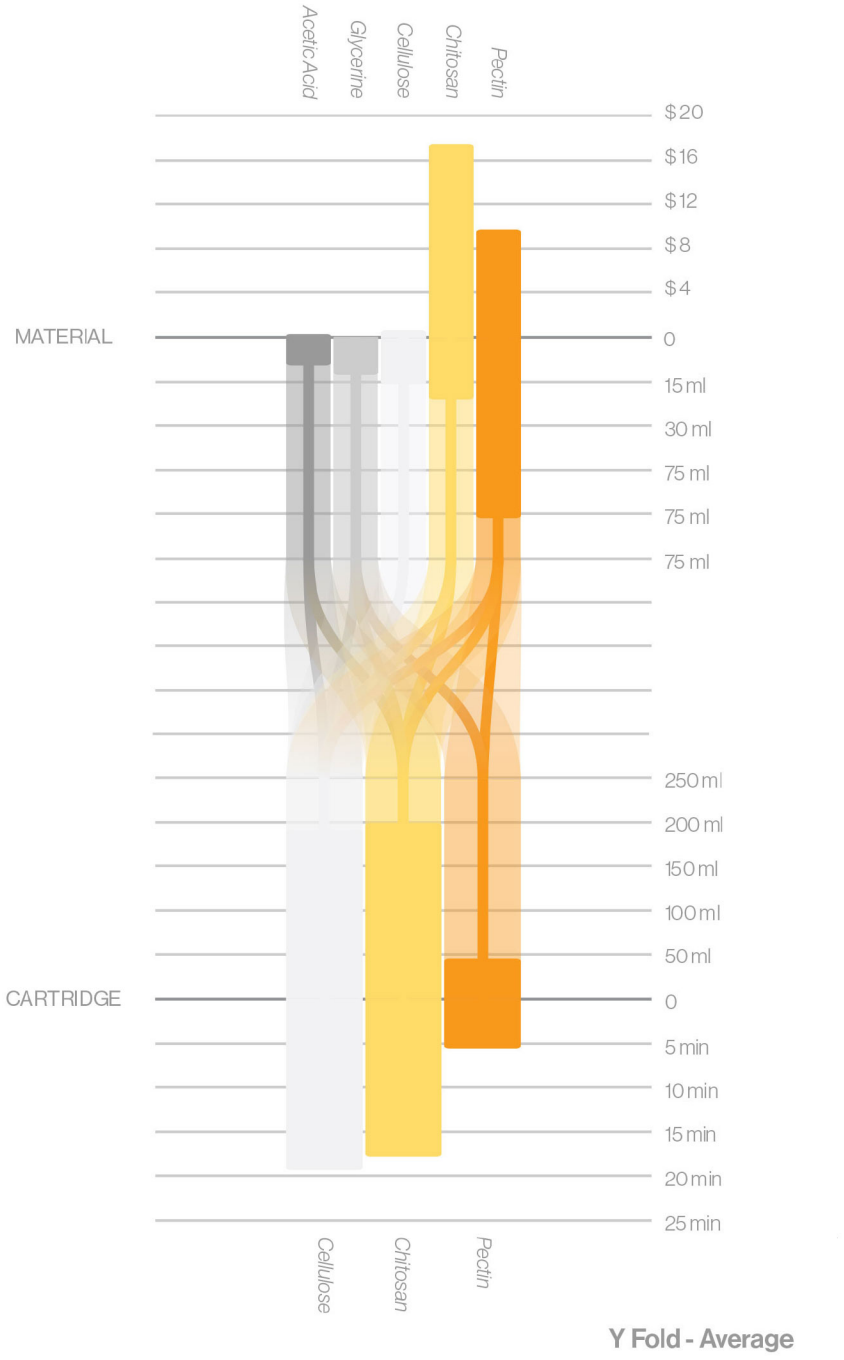

Figure 85: Y Fold - Average volume of material, print duration, and cost for different biopolymer formulas used in each print in the series.

9.3.7 I Crease

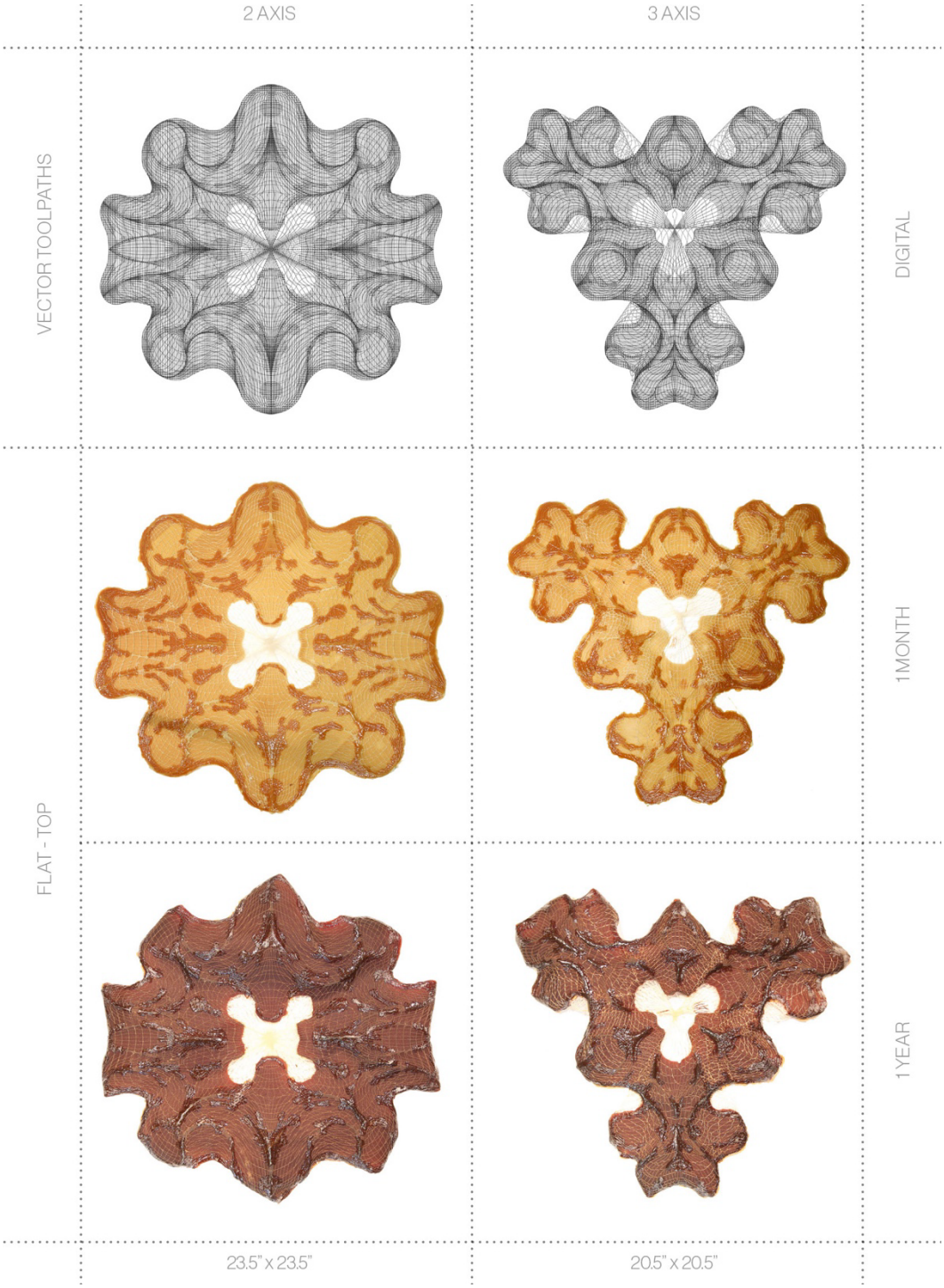

Figure 86: Matrix of + Crease – Multiple geometries comparing vector toolpaths to printed 2-D forms with deformation and color change over 1 year.

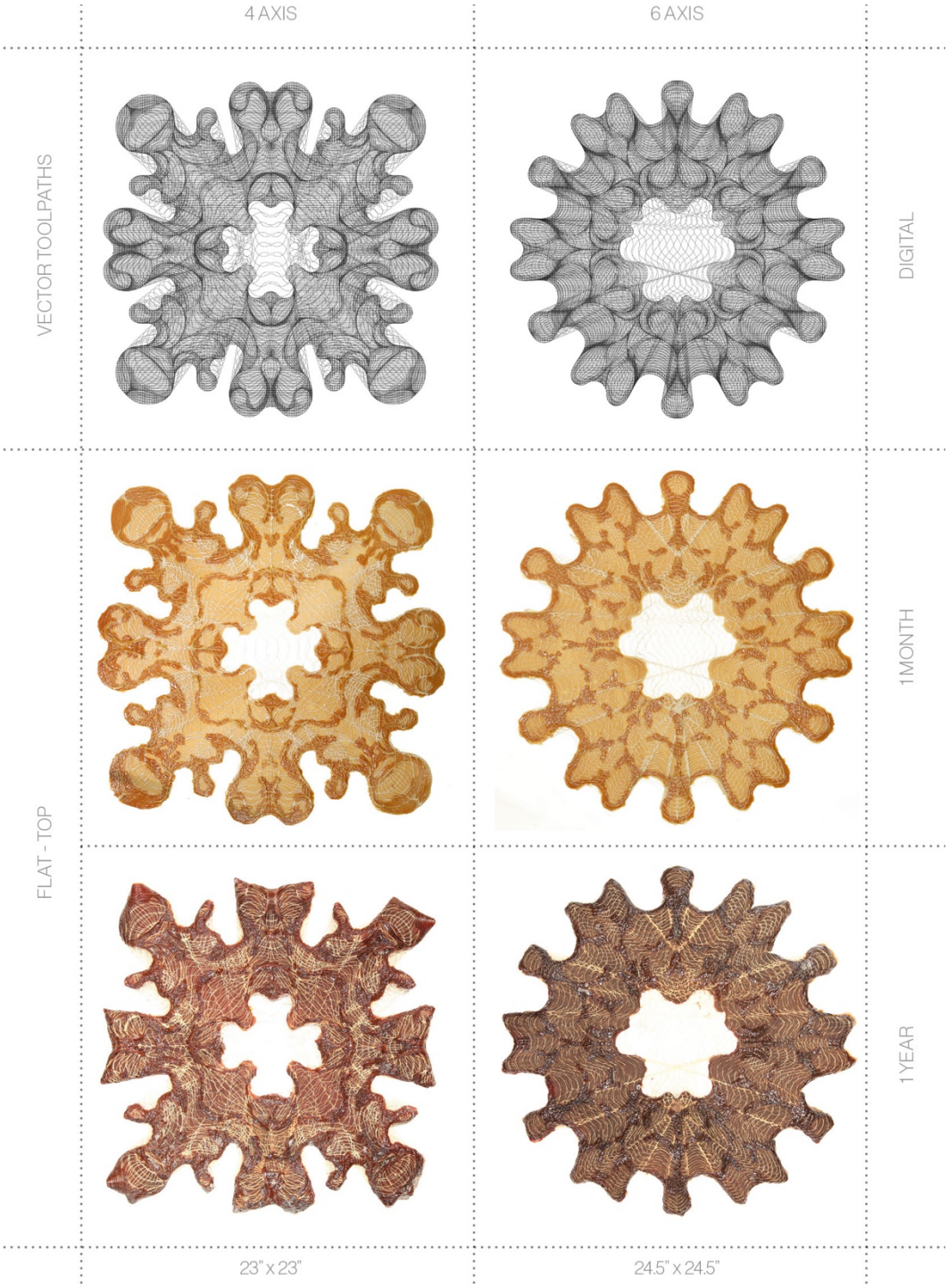

Figure 87: Matrix of + Crease – Multiple geometries comparing vector toolpaths to printed 2-dimensional forms with deformation and color change over 1 year.

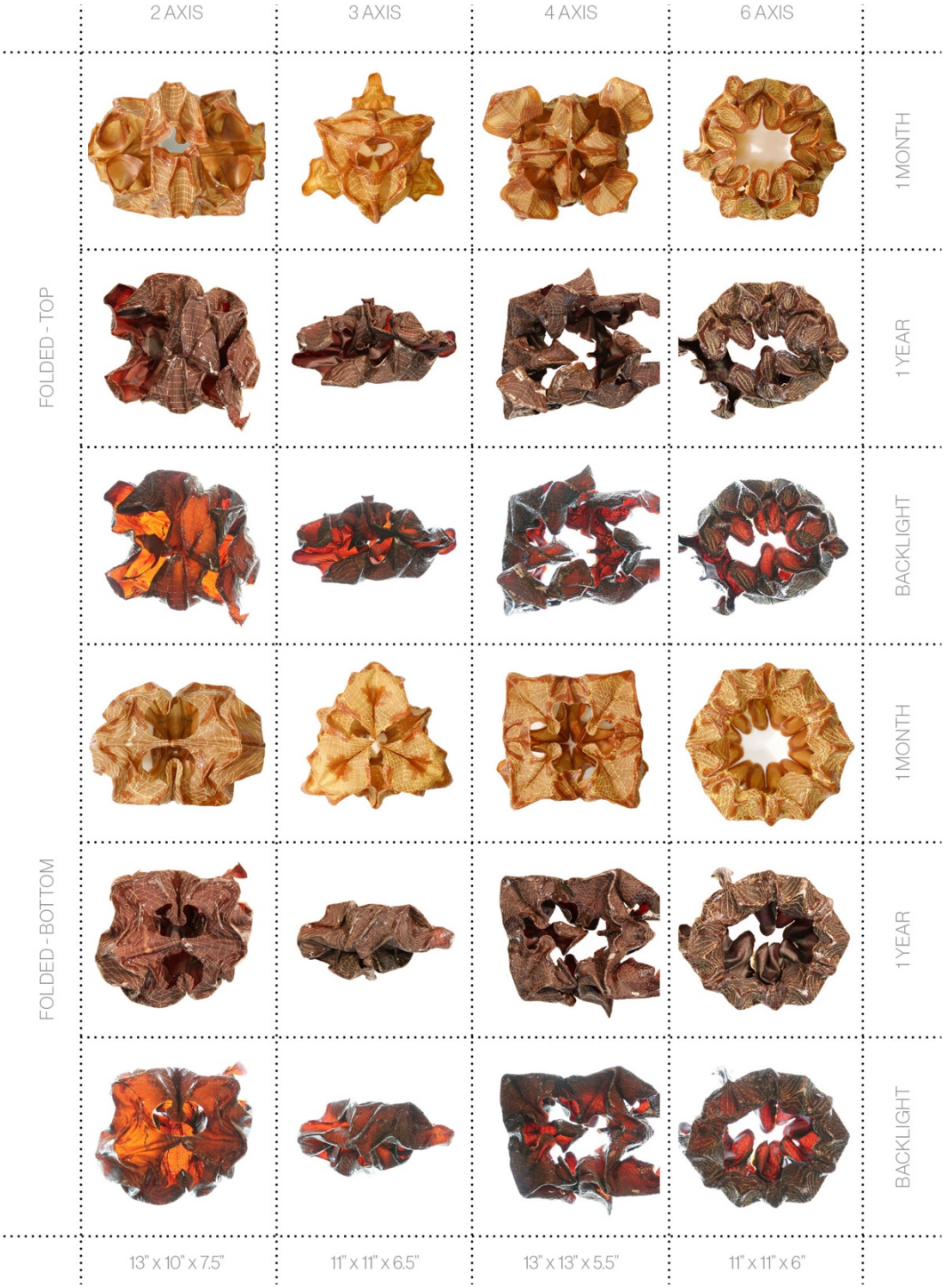

Figure 88: Matrix of + Crease – Multiple geometries comparing color change and deformation of 3-dimensional forms over 1 year.

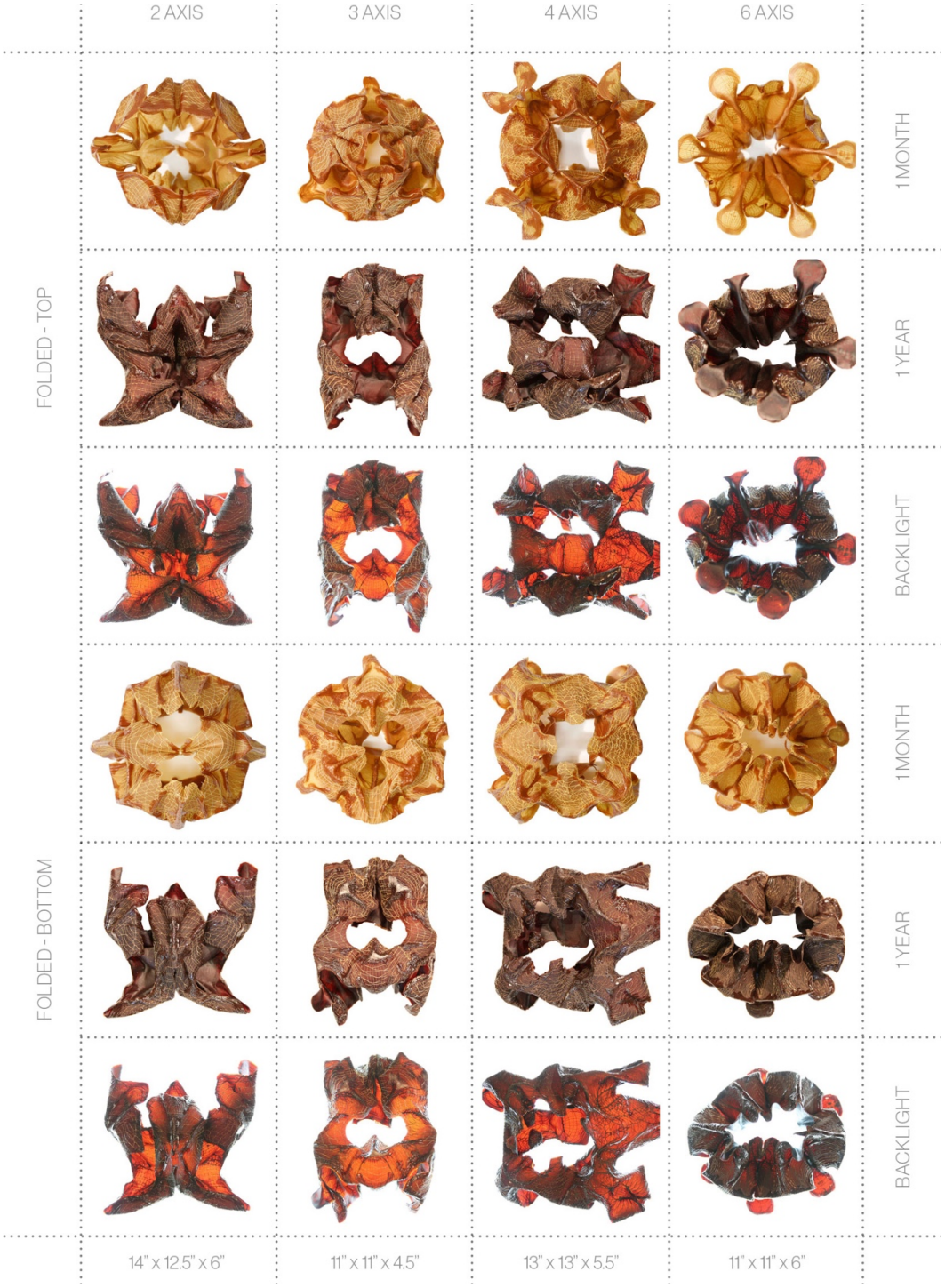

Figure 89: Matrix of + Crease – Multiple geometries comparing color change and deformation of 3-dimensional forms over 1 year.

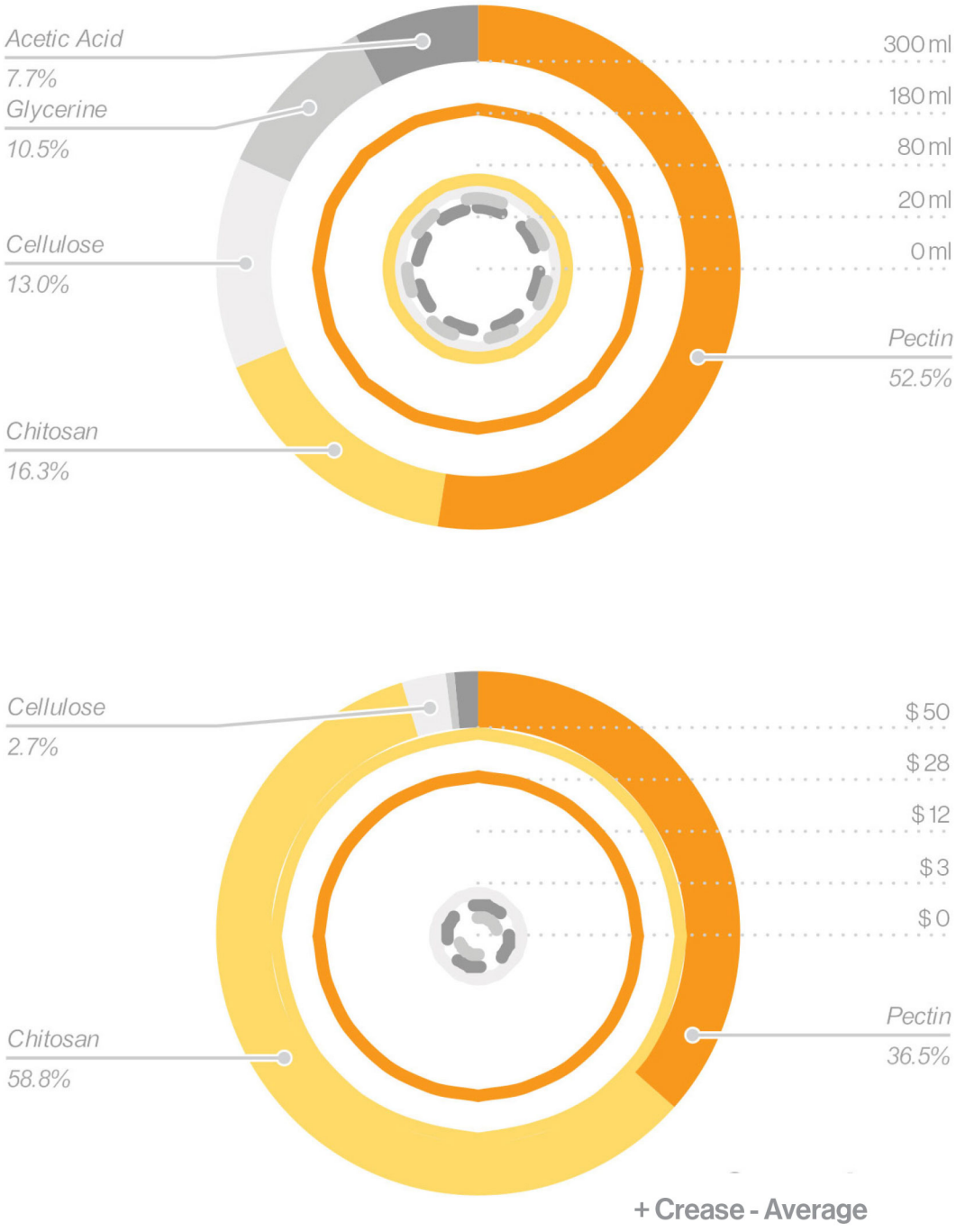

Figure 90: + Crease – Average volume and cost of materials for each print in the series.

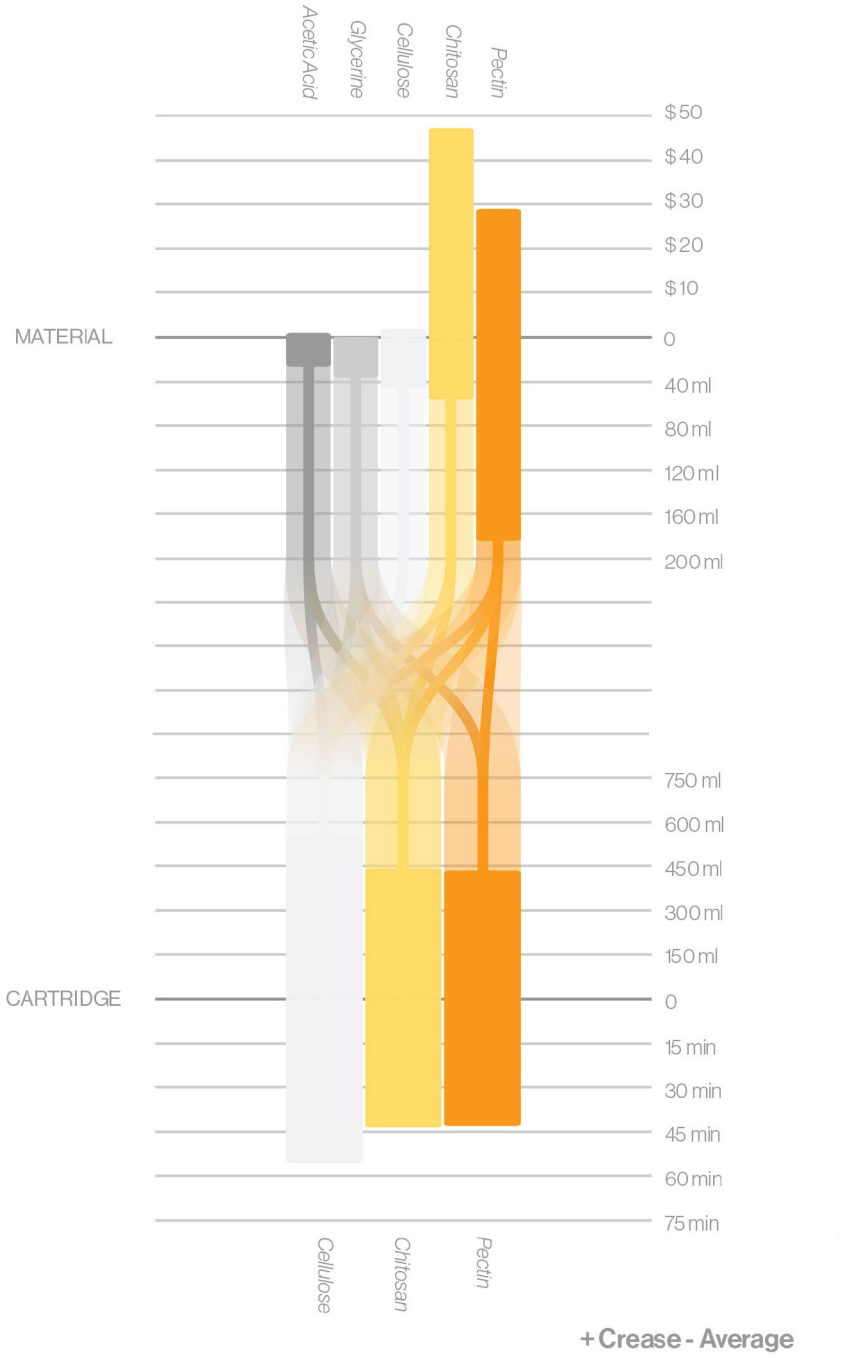

Figure 91: + Crease - Average volume of material, print duration, and cost for different biopolymer formulas used in each print in the series.

9.3.8 * Flat

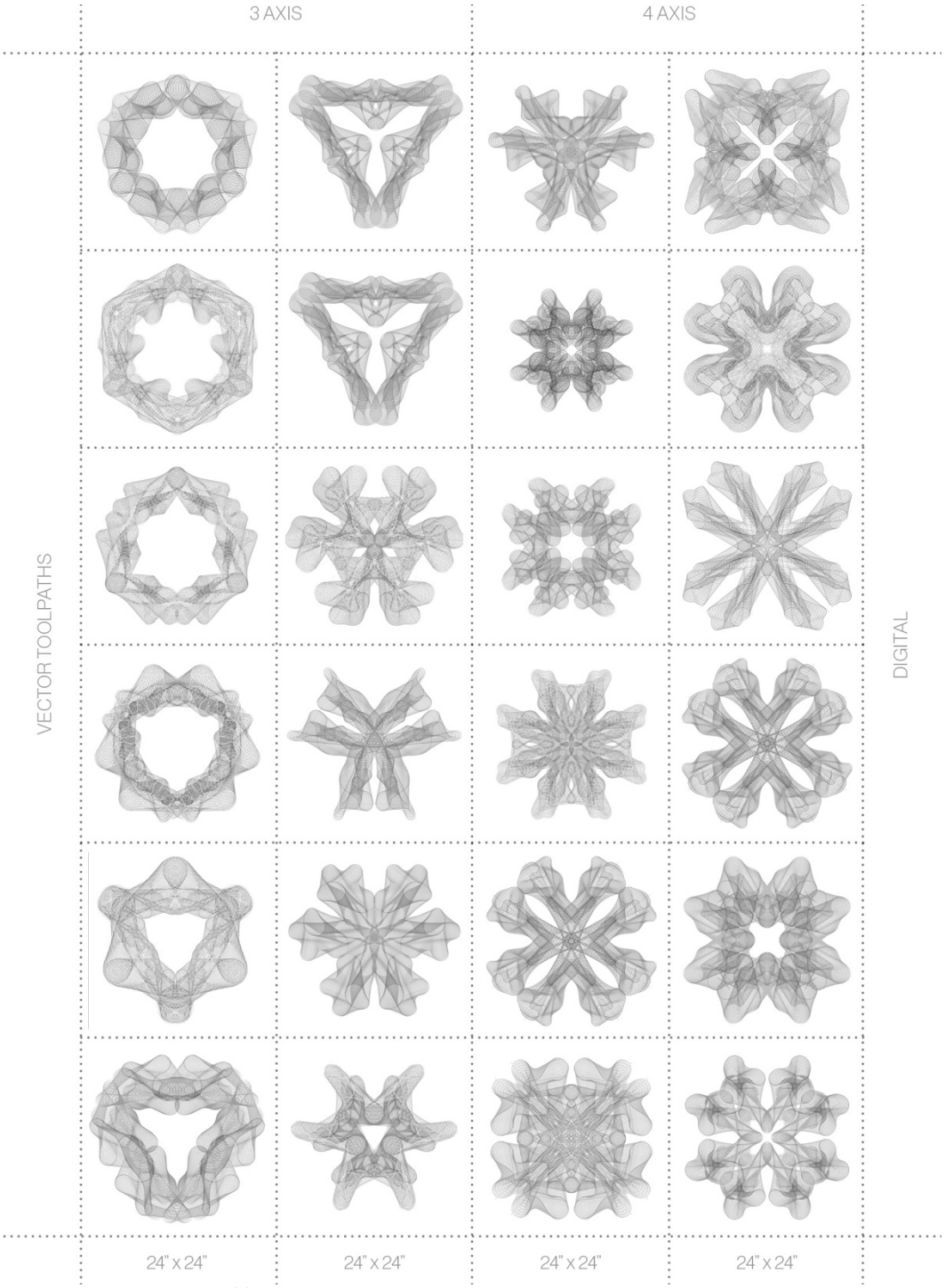

Figure 92: Matrix of * Flat – Toolpaths showing digitally generated variation in density and patterning.

Figure 93: Matrix of * Flat – Prints showing tunable variation in material color and composition.

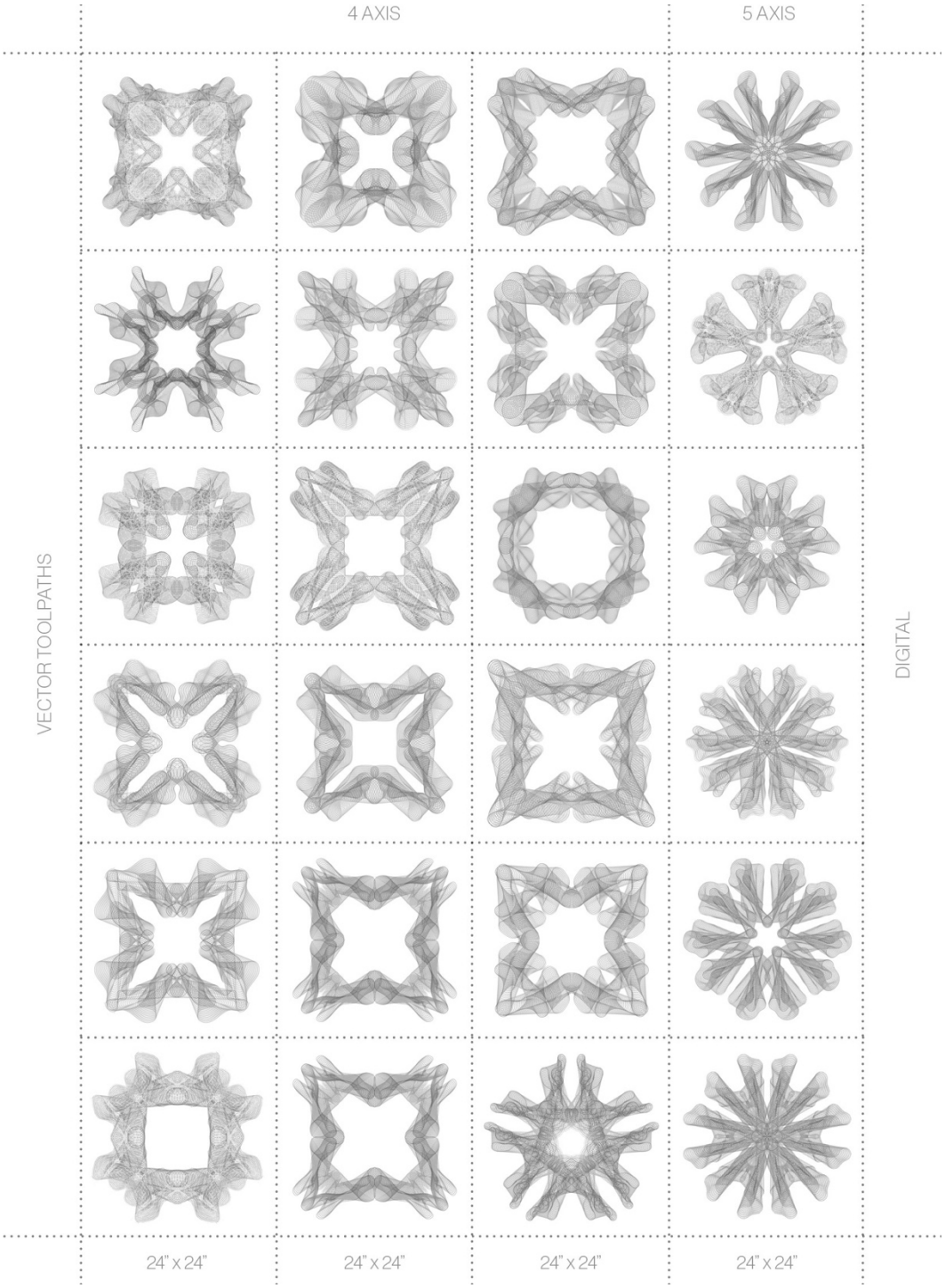

Figure 94: Matrix of * Flat – Toolpaths showing digitally generated variation in density and patterning.

Figure 95: Matrix of * Flat – Prints showing tunable variation in material color and composition.

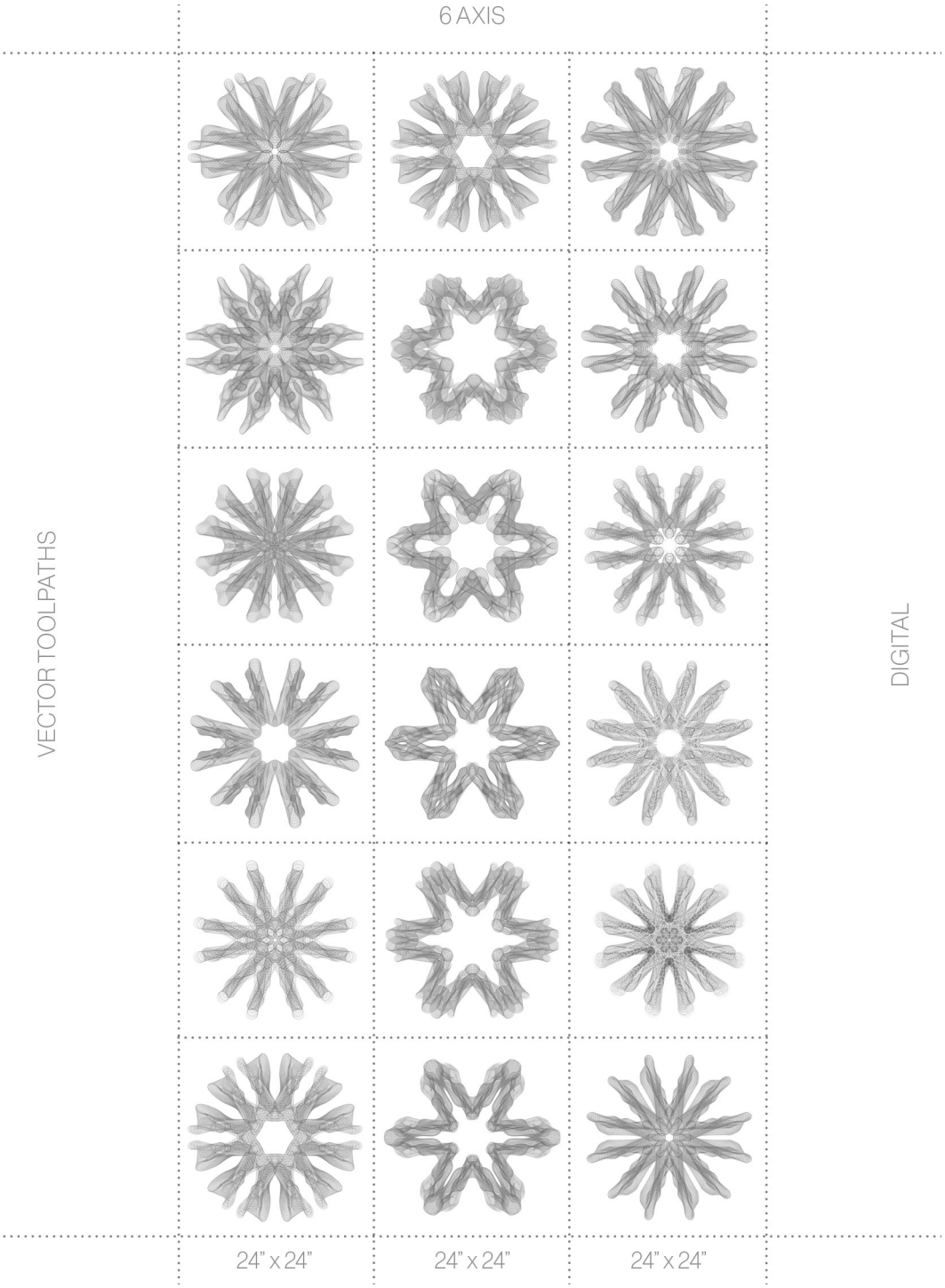

Figure 96: Matrix of * Flat – Toolpaths showing digitally generated variation in density and patterning.

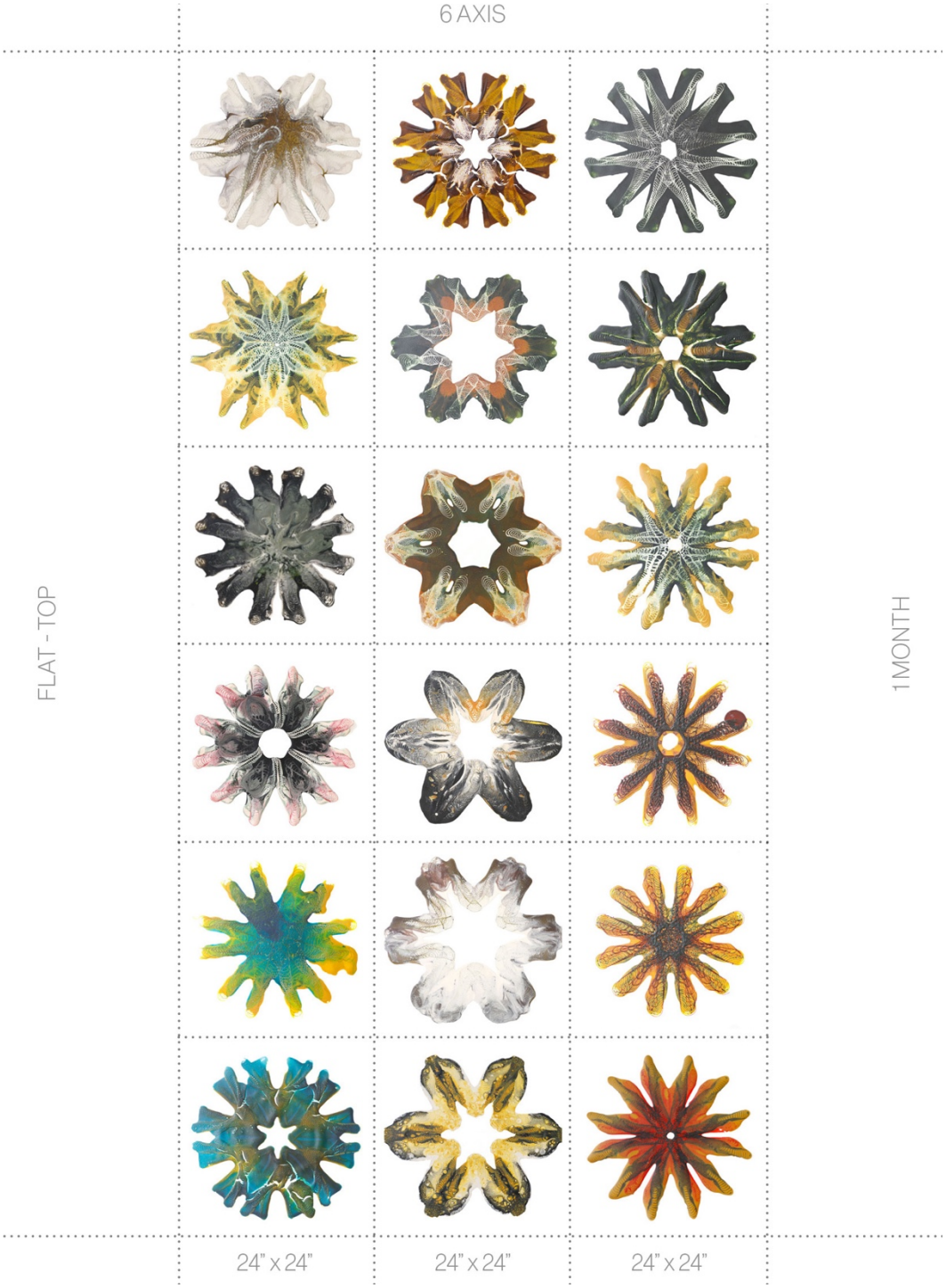

Figure 97: Matrix of * Flat – Prints showing tunable variation in material color and composition.

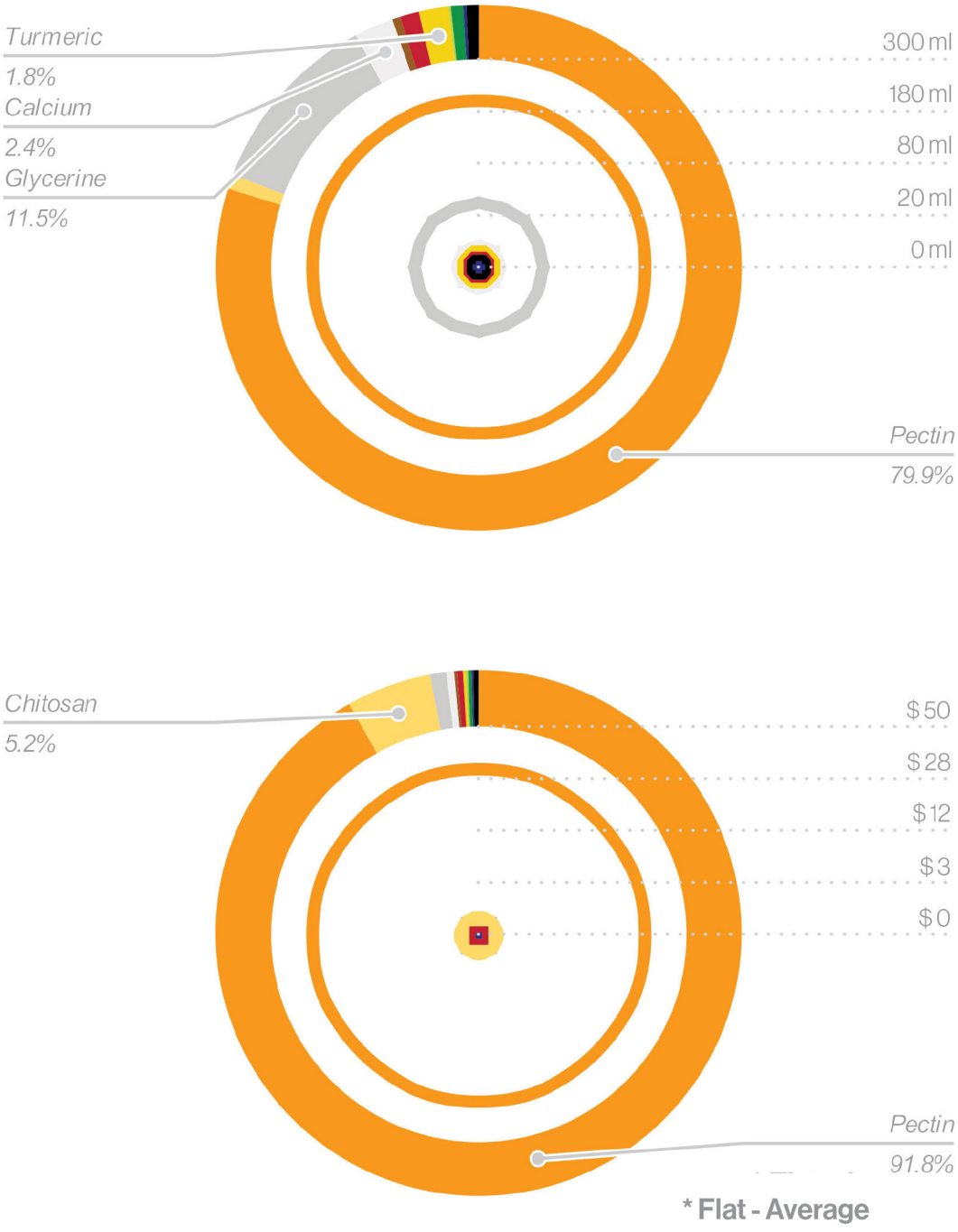

Figure 98: * Flat – Average volume and cost of materials for each print in the series.